

TALLINN UNIVERSITY OF TECHNOLOGY

SCHOOL OF ENGINEERING
Department of Electrical Power Engineering and Mechatronics

DESIGN AND OPTIMIZATION OF ULTRASONIC FLOW METER

ULTRAHELI VOOLUANDURI PROJEKTEERIMINE JA OPTIMERIMINE

MASTER THESIS

Student: Murat BAKKAL

Student Code: 165583MAHM

Mart Tamre – Program Director

Supervisor: (Mechatronics - English)

AUTHOR'S DECLARATION

Hereby I declare, that I have written this thesis independently.			
No academic degree has been applied for based on this material. All works, major			
viewpoints and data of the other authors used in this thesis have been referenced			
21.05.2020			
21.03.2020			
Author: Murat BAKKAL			
/signature – digitally signed document			
Thesis is in accordance with terms and requirements			
<i>""</i>			
Supervisor:			
·			
/signature/			
Accepted for defence			
<i>"</i> "20			
Chairman of theses defence commission:			

/name and signature/

Non-exclusive Licence for Publication and Reproduction of GraduationTthesis¹

I, Murat Bakkal (date of birth: 08.10.1986) hereby
1. grant Tallinn University of Technology (TalTech) a non-exclusive license for my thesis DESIGN AND OPTIMIZATION OF ULTRASONIC FLOW METER,
supervised by Mart Tamre,
1.1 reproduced for the purposes of preservation and electronic publication, incl. to be entered in the digital collection of TalTech library until expiry of the term of copyright;
1.2 published via the web of TalTech, incl. to be entered in the digital collection of TalTech library until expiry of the term of copyright.
$1.3\mathrm{I}$ am aware that the author also retains the rights specified in clause 1 of this license.
2. I confirm that granting the non-exclusive license does not infringe third persons' intellectual property rights, the rights arising from the Personal Data Protection Act or rights arising from other legislation.
¹ Non-exclusive Licence for Publication and Reproduction of Graduation Thesis is not valid during the validity period of restriction on access, except the university `s right to reproduce the thesis only for preservation purposes.
Digitally signed (signature)
21.05.2020 (date)

Department of Electrical Power Engineering and Mechatronics THESIS TASK

Student: Murat BAKKAL - 165583MAHM

Study programme, MSc. Mechatronics (code and title)

Supervisor(s): Professor Mart Tamre (Program Director - Mechatronics - English)

Thesis topic:

(in English) DESIGN AND OPTIMIZATION OF ULTRASONIC FLOW METER

(in Estonian) ULTRAHELI VOOLUANDURI PROJEKTEERIMINE JA OPTIMERIMINE

Thesis main objectives:

- 1. Constructing a mechanical model of an ultrasonic water flow meter for commercial purposes, as requested from the authors current employer company, Nordic Automation Systems OÜ in Tallinn Estonia.
- 2. Justification of design preferences that were made in the mechanical parts of the product. Explanation of preferences in the assembly methods of the components.
- 3. Providing simulations for the environmental and functional conditions that the device will be used in. Using computational tools to carry out stress analysis for industry requirement loads of temperature and pressure.
- 4. Simulation of water flow through the device in order to assess and help improve the accuracy of measurement, considering ultrasonic measuring technology methods in the industry. Analysis of the effect of construction geometry to this purpose.

Thesis tasks and time schedule:

No	Task description	Deadline
	Specification and documentation of technical requirements,	25.03.20
	standards and competition for the market that the device will be	
1.	used in. Providing an explanation for the build and features of the	
	model that has already been constructed by the author so far and	
	the reasons for improvement.	
	Finalizing the stress simulations for material thickness for the	08.04.20
2	enclosure. Documentation of the conditions that the device is	
2.	designed to operate in, such as maximum and minimum allowed	
	pressure and temperature.	
2	Simulation of water flow through the base model and final model	22.04.20
3.	in order to compare their performances according to ultrasonic	

measuring principles. Using this information to see if any	
improvements can be achieved by modification of the model.	
Providing information about simulated values that are relevant	
for the confirmity of the device to industry standards and will be	
needed for the hardware and software development process of	
the product also. These are values like pressure drop and	
allowable flow rates.	
Detailed documentation of the mechanical components of the	06.05.20
final design, assembly visuals and production related discussions.	

Language: English **Deadline for submission of thesis:** 22.05.2020

Student: Murat Bakkal	Digitally signed /signature/	21.05.2020
Supervisor: Mart Tamre	/signature/	""201a

Head of study programme:		"	 201.a
	/signature/		

Terms of thesis closed defence and/or restricted access conditions to be formulated on the reverse side

CONTENTS

PRI	EFACE	8
1.	INTRODUCTION	9
2.	REVIEW	.11
2.1	Ultrasonic flow metering	11
1.2	.1 Functioning principle	11
1.2	.2 Measurement inaccuracies	13
1.2	.3 Transducer positioning and beam path possibilities	13
1.2	.4 Transit time flow metering in literature	16
2.2	Mechanical construction	18
2.2	.1 Industrial standard	18
2.2	.2 Injection plastics design	19
2.2	.3 Employer specifications for the initial design	20
2.2	.4 Initial construction	22
2.3	Problems with the initial design	26
2.4	Definition of goals	27
3.	FEA SIMULATIONS	. 28
3.1	Material model	28
3.1	.1 Property inputs for custom material definition	29
3.2	Simulation methodology	33
3.2	.1 Model simplification	34
3.2	.2 Restriction of simulations based on worst-case conditions	34
3.3	Simulation setup parameters	35
	Simulation setup parameters	
3.3		35
3.3 3.3	.1 Fixtures	35
3.3 3.3 3.3	.1 Fixtures	35 35
3.3 3.3 3.3 3.4	.1 Fixtures .2 Loads .3 Mesh settings	35 35 37
3.3 3.3 3.3 3.4 3.5	.1 Fixtures .2 Loads .3 Mesh settings Simulation	35 35 37 38
3.3 3.3 3.4 3.5 3.6	.1 Fixtures	35 35 37 38 40

4.2 Components of the second revision	46
4.2.1 Main enclosure bottom part	46
4.2.2 Enclosure lid	48
4.2.3 Transducer assembly	48
4.2.4 PCB	50
4.2.5 Fixing part for the extension PCB	51
4.3 Assembly	51
4.4 Conclusions	52
5. FLOW SIMULATIONS	54
5.1 Definitions and motivation	54
5.1.1 Relation between flow regimes and Re number	56
5.2 Simulations	58
5.2.1 Initial simulation and velocity profile analysis	59
5.2.2 Parametric calculation of the Reynolds number for a range of	
variables	69
5.2.3 Pressure drop depending on total pressure and volume flow	73
5.3 Conclusions	75
6. SUMMARY	77
KOKKUVÕTE	79
I TST OF DEFEDENCES	Q 1

PREFACE

This thesis is submitted as a requirement to complete the master's degree education in

mechatronics engineering at Tallinn Technical University. It was carried out under the

supervision of the director of the study program, Professor Mart Tamre and the work

was done both at the employer company of the author, Nordic Automation Systems OÜ

in Tallinn - Estonia and the mechatronics laboratories at Tallinn Technical University.

The benefits of the results of specific simulations were verified by consulting the

manager and product developers in the company.

I would like to thank Professor Mart Tamre for his supervision and guidance throughout

the entire process and providing me with the needed tools and facilities at the

university. I would also like to express gratitude to my parents, Aydan and Turgay for

their love and support. They have been such strong believers in my ability to keep going

and a big part of my motivation to learn and achieve.

This thesis contains the documentation of the design and improvement of a transit time

ultrasonic water flow meter for measuring residential water consumption using

Solidworks CAD and simulation software. The work involves CAD construction of an

initial design that uses bought components and standard industry dimensions. Then the

second design is constructed to eliminate the need for a bought component and utilize

a different way of arranging the transducers. FEA analysis is made to validate that the

chosen material thickness is sufficient to withstand the determined operating

conditions. Fluid flow analysis and simulations are made to help improve the accuracy

of the product.

Keywords: Ultrasonic, flow metering, CAD, FEM, flow analysis, design.

8

1. INTRODUCTION

Ultrasonic transit-time flow metering is one of many ways of measuring the amount of fluid (liquid, gas or slurry) passing through a duct. This technology works by sending and receiving ultrasonic signals through the fluid between two transducers. A difference in the reception time of signals occur due to the movement of the fluid in one direction. This time difference is then used in deducting the velocity of the fluid that is passing through the duct.

This information is used in engineering applications such as process control or metrology [1], as well as commercial purposes like measuring the consumption of water in residential piping systems.

Transit-time UFMs (Ultrasonic Flow Meters) are highly accurate (can be calibrated to <0,1 % [2]), high precision and affordable flow measurement instruments [3]. They preserve accuracy in a wider flow range and can measure lower flow rates with less error, compared to widely used positive displacement meters [4, 5, 6, 7]. The absence of moving mechanical parts decrease the probability of malfunction due to wear and simplify maintenance [2, 8, 5]. Furthermore, they can measure bi-directional flow [2].

Ultrasonic flow meters have been in the industry for almost 60 years [8] and there are publications on the general principles of transit time flow measurement, ways to improve ultrasonic measurement results and calibration of ultrasonic devices. There are also tutorials on how the Solidworks simulation tools can be used and other specific technical information and help documents of the program. However, a guideline to how one can design and optimize a complete transit time ultrasonic flow meter product in Solidworks was not found. Since these devices are commercial products, detailed design guidelines and which aspects to consider are generally trade secrets. On this basis, it is the task of the author/constructor to find a way to provide output that contributes to the production and improvement of a transit-time UFM that complies with employer specifications and standards, using Solidworks software.

There is considerable increase in attention to IoT-based smart metering due to the recent development of information and communication technologies [4]. The author was assigned a task by the employer, of constructing the mechanical assembly of an ultrasonic transit time smart meter that can compete in the industry for the primary purpose of measuring domestic water consumption. Solidworks mechanical design and

simulation software was used in all construction and simulation tasks, because it was the program that is available at the company.

A review of the relevant technologies and scientific principles that can be utilized for this purpose are given in Chapter 2. The specifications from the employer and the relevant parts of the international standard for water metering devices is presented to set a basis for a guideline for the goals of the thesis. Furthermore, the design of the initial construction is presented and reasons to why it should be improved are stated.

In Chapter 3, FEA simulations for material thickness are carried out. This chapter focuses on FEA analysis of the pipe section of the device to obtain a minimum allowable wall thickness for the specified operating conditions and the chosen material. The chosen material thickness for the second revision is validated using the results of simulations.

The components of a second revision of the device are explained in Chapter 4. The new design is aimed to address the issues of reducing costs, conformity to standards and contributing to increasing measurement accuracy.

The flow simulation environment in Solidworks is presented and used in Chapter 5. Water flow through the improved construction is simulated. The reliability of the results is discussed for the chosen set-up parameters for the simulation. Furthermore, the Reynolds number for a range of temperature and flow rate values are calculated, which enable visualization and validation of the properties of flow, with the aim of improving the accuracy of the device. Finally, the pressure drop of the design is simulated with respect to varying pressure and flow rates which provides valuable information to contribute to the programming and calibration of the device and classification of the product according to standards.

2. REVIEW

2.1 Ultrasonic flow metering

1.2.1 Functioning principle

Ultrasonic water metering is used to measure the volumetric flow rate of gasses, liquids or slurries that are passing through ducts. There are two main approaches that use different physical principles: Doppler-Effect (Frequency-Shift) flow metering and transit-time flow metering [9, 6].

Doppler-Effect meters send ultrasonic sound into the fluid and compare the transmitted frequency to the frequency of the sound that is reflected from the particles or bubbles inside the fluid [10, 4]. Since the particles are moving, there will be a shift in the frequency of the reflected wave because of the Doppler effect. The velocity of the fluid is then deducted from this frequency difference and other known dimensions of the pipe. This method is used to measure the flow of fluids or slurries.

Transit time meters use two transducers that are placed upstream and downstream of the flow which can both send and receive sound signals to each other through the fluid (Figure 2.1).

If there is no flow, there will be no difference in the transmission time of the signal. When there is flow, the time of transmission that is going in the direction of flow is shorter than transmission that travels upstream. This difference in the time of flight of the sound is used to compute how fast the liquid is flowing.

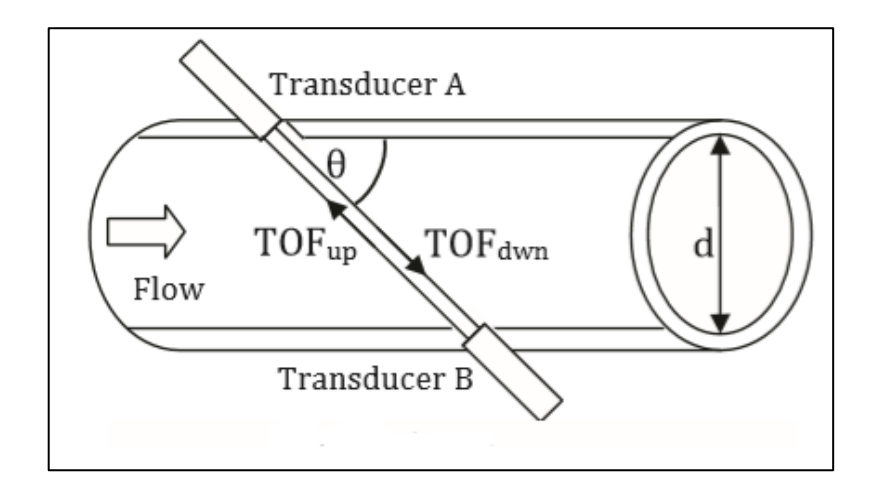


Figure 2.1 Transit-time ultrasonic flow measurement principle (image taken from [24])

t1 in equation 2.1 [1] is the time of flight of the signal from Transducer A to TransducerB in Figure 2.1 and t2 in equation 2.2 [1] is the time of flight from B to A.

$$t_1 = \frac{L}{c + v cos\theta} \tag{2.1}$$

$$t_2 = \frac{L}{c - v \cos \theta} \tag{2.2}$$

where L - the distance between transducers, m,

c - speed of sound in the medium, m/s,

 θ - angle between flow direction and the beam,

v - flow velocity of the liquid, m/s

These are simply time = distance/velocity equations for the sound beam from one transducer to the other where the angled component of the flow velocity is added to or subtracted from the ultrasound propagation velocity depending on which way the measurement is done.

The difference in the transmission times of the sound beams is given in equation 2.3

$$\Delta t = t_2 - t_1 = \frac{2.L.v.\cos\theta}{c^2 - v^2.\cos^2\theta}$$
 (2.3)

In the denominator of equation 2.3, the squared velocity of sound is much larger than the term $v^2.cos2\theta$. So $v^2.cos2\theta$ is neglected and the equation is solved for v in equation 2.4.

$$v = \frac{c^2 \, \Delta t}{2L \cos \theta} \tag{2.4}$$

Equation 2.4 is the solution for a uniform fluid velocity that depends on the "known values" of velocity of sound in the medium, the time of flight difference, the angle θ and distance between the transducers. Since the velocity of the fluid is now known, it can be multiplied with the cross-sectional area of the pipe to obtain the volumetric flow rate in equation 2.5.

$$Q = \frac{\pi}{4} d^2 \frac{c^2 \, \Delta t}{2L \cos \theta} \tag{2.5}$$

The calculation of equation 2.5 is taken from [4]. It was seen that the calculation steps of the flow rate vary significantly in other sources depending on the approach or the measurement method, but the operation principle is still measuring t_1 and t_2 and calculating the flow rate [3]. Examples of different approaches can be seen in [11, 2, 6, 12].

1.2.2 Measurement inaccuracies

The flow measurement shown in the obtained formula for the volume flow rate given in equation 2.5 is multiplied by a correction factor. This factor compensates for initial approximations [6] such as considering the velocity of the fluid as a mean value of the sum of all points. In reality, the flow is stationary where it touches the pipe walls and faster near the axis of the pipe and has velocity fluctuations [13]. The measurement accuracy also depends on the flow regime of the fluid. Different correction factors (called flow profile correction factors [14]) are applied when the flow is laminar, transitional or turbulent [11, 1, 15]. Furthermore, it is written in [16] that factors that affect the measurement accuracy are traceability, flow disturbances, Reynolds number, water chemistry [17], acoustics, zero-point [18] and meter body expansion. [1] sums up the causes of uncertainty in three main categories: the installation method of transducers; the measurement of transit time; velocity distribution across the pipe.

1.2.3 Transducer positioning and beam path possibilities

There are more ways of arranging the position of the transducers than what is shown in the generic set-up in figure 2.1. In this review, examples to what was found in literature about several transducer arrangements and examples from the industry are given.

Three types of transducer arrangements are shown in Figure 2.2 where A and B points are the transducers and the lines that connect them indicate the path of the beam. The difference between these is that the path of the beam is longer or shorter, which affects the detection time of the signal. This makes it possible to improve the accuracy of the measurement [1].

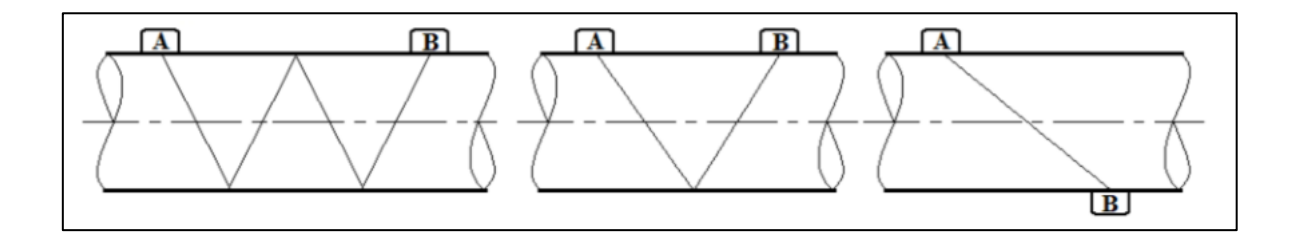


Figure 2.2 Some types of transducer arrangements (image taken from [1]). From left to right: W-type, V-type, Z-type meters.

Theoretical design and CFD simulations of a transducer arrangement that creates a 3D triangular path (figure 2.3) was seen from [19].

Furthermore, the transducers can be immersed in the fluid and face each other directly (figure 2.4). This is referred to as a "coaxial transducer flow meter" in [6]. In this publication, it is also stated that the benefits of this arrangement are "better transducer separation, the alignment of the ultrasonic beams to the principle direction of flow and the potential for a more complete understanding of the interaction of flow and ultrasound due to symmetry".

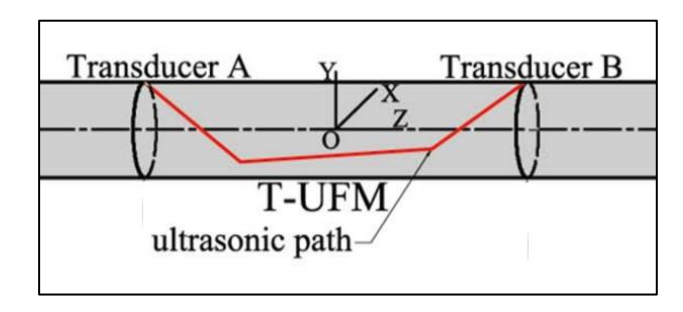


Figure 2.3 3D Isosceles trianglar ultrasonic path (image taken from [19])

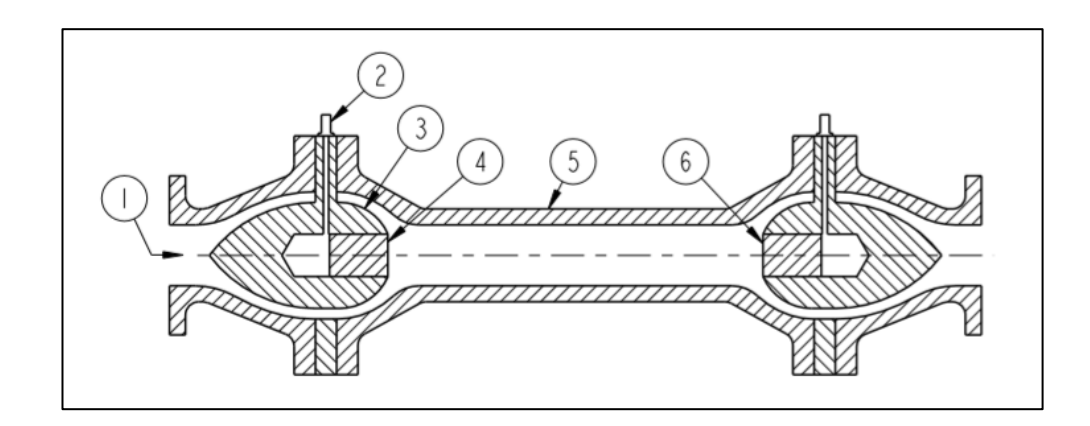


Figure 2.4 Coaxial transducer arrangement: (1) inlet, (2) cable connector, (3) transducer housing, (4) upstream transducer, (5) meter cell, (6) downstream transducer (image and explanation from [6])

An example to this arrangement can be seen in the image of a product in figure 2.5, where the transducer housings are inserted from both ends of the pipe separately and fastened with a screw from the top of the pipe. The threaded component has a hole through it to allow passage for the cables of the transducers to the inside of the device.



Figure 2.5 Example from the industry to coaxial transducers. With (right) and without (left) transducers

U-type meters use two reflectors that are positioned inside the pipe and with a 45° angle between the flow and the surface of the reflectors. These direct the beam into the direction of the flow [7] (figure 2.6). An example to the U-type meter is the Multical 21 by the company Kamstrup [20]. This product internally has piezo discs mounted on top of the pipe section that is closed off to the flow and has a bracket for the reflectors that is fitted inside the pipe section with rigid snaps. The reflector bracket and one of the piezo discs can be seen in figure 2.7.

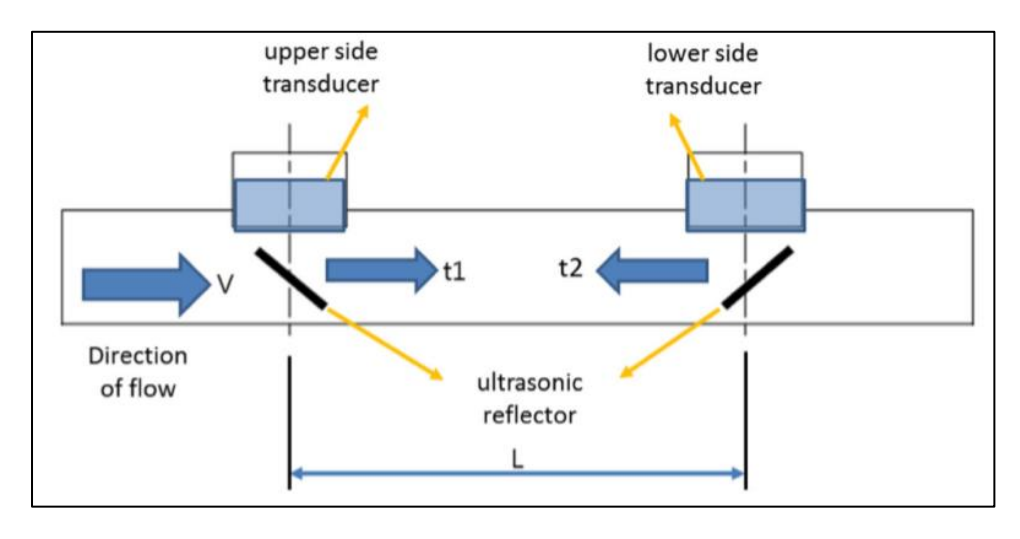


Figure 2.6 U-type transducer configuration (image taken from [7])



Figure 2.7 Kampstrup Multical 21 transducer and spool piece

Clamp-on devices can be attached to the outside of pipes. One advantage of this is that one does not need to disconnect the pipe of the flow at any section to mount the sensor [21]. This leads to ease of installation and maintenance costs [22]. Because they do not obstruct the flow, the measurement has no effect on the fluid state and there is no pressure drop [23]. However, this flexibility in installation leads to some disadvantages, compared to other options. The internal condition of the pipe, like surface roughness affects the measurement and is a source of uncertainty [22]. Due to additional sources of uncertainty like the positioning of the transducers during assembly, the material or the diameter of the pipe, the measurement accuracy and repeatability are significantly downgraded in comparison to devices that have their own pipe system and built-in transducers [21, 22].

1.2.4 Transit time flow metering in literature

Almost all the literature that were found in the subject of transit-time ultrasonic flow meters in the past five years are dealing with mitigating the effects of uncertainty and increasing the accuracy of measurement.

It is shown in [17] that the time difference measured by the device is affected by impurities in the water, because the ultrasonic wave attenuates differently in different concentrations of material in the fluid. It is shown that the error of measurement is

within allowable margins when the amount of calcium carbonate and yellow mud are below a threshold of 0.5%.

A 3D isosceles triangular ultrasonic path arrangement is proposed and simulated in [19] that increases accuracy depending on the length of the pipe.

In [24], dual transducers are used to increase the sampling period of the time difference which diminishes the probability of sudden change of flow velocity during the measuring period.

A differential time-of-flight (dToF) water meter is proposed in [4] which calculates the flow rate independently from the temperature of the water and is supposed to be more suitable for residential water meters that have small pipe diameters and low flow rates. This is proposed to account for some uncertainties because the dToF method is not dependent on the velocity of sound in the medium, which changes with respect to temperature.

In [18], the zero-flow error is demonstrated and minimized. Zero-flow error happens when there is no flow, but the measurement shows some flow. The effects of frequency characteristics of non-identical transducers are evaluated, and it is shown that this error can be minimized by optimizing the impedance of the circuits according to the impedance of the transducers.

A low-power differential time of flight ultrasonic water meter design is presented in [7] in order to achieve a battery life of minimum 10 years.

A new mathematical model to calculate the time difference is shown in [5]. It is based on the idea that the conventional model to calculate the transition times (equations 2.1 and 2.2) assumes that the ultrasonic beam travels straight from one transducer to the other. In this paper, the effect of the flow to the direction of the ultrasonic beam is modelled to add accuracy to the calculation.

In [22] uncertainties that occur as a result of the roughness of the inside of the pipe are explained. It is shown that the ultrasonic signal scatters when it collides with rough surfaces. Furthermore, it is concluded that for ultrasonic waves of 1 MHz and corroded pipe internal surfaces of 0,2 mm (RMS) systematic errors of 2 % can occur.

A design of an intelligent measurement technique to adapt to variations in pipe diameter, liquid density and temperature with a neural network is shown in [25].

Flow profile correction factors for laminar and turbulent flow for transit-time UFMs, that can be used to calibrate the measured flow rate are presented in [1]

The procedure to optimize the shape of the transducers in a coaxial transit-time UFM design is given in [6].

2.2 Mechanical construction

2.2.1 Industrial standard

The standard in the industry is OIML R 49-1 which is the first part of the 2013 international recommendation for the metrological and technical requirements for water meters for cold potable water and hot water. The technical requirements by this standard concerning the mechanical construction are:

- i. A water meter shall be manufactured from materials of adequate strength and durability for the purpose for which the it is to be used.
- ii. A water meter shall be manufactured from materials which shall not be adversely affected by the water temperature variations, within the working temperature range.
- iii. All parts of a water meter in contact with the water flowing through it shall be manufactured from materials which are conventionally known to be non-toxic, noncontaminating, and biologically inert. Attention is drawn to national regulations.
- iv. The complete water meter shall be manufactured from materials which are resistant to internal and external corrosion or which are protected by a suitable surface treatment.
- v. A water meter indicating device shall be protected by a transparent window. A cover of a suitable type may also be provided as additional protection.

- vi. Where there is a risk of condensation forming on the underside of the window of a water meter indicating device, the water meter shall incorporate devices for prevention or elimination of condensation.
- vii. A water meter shall be of such design, composition, and construction that it does not facilitate the perpetration of fraud.
- viii. A water meter shall be fitted with a metrologically controlled display. The display shall be readily accessible to the customer, without requiring the use of a tool.
- ix. A water meter shall be of such design, composition, and construction that it does not exploit the MPE or favour any party.

Furthermore, some rated operating conditions (in Section 6.4 of the standard) specify physical properties that can be taken as reference values.

- Nominal diameter of the pipe. This is shown by the DN designation of size for components of a pipework system. This class was determined by the employer to be DN20, which corresponds to 26,7 mm outer diameter in ASME and 26,9 mm outer diameter in ISO 6708 and DIN EN 10255 standards.
- The meter should have a pressure rating on it that indicates the pressure range that the device is able to operate at. It is mentioned that the upper value should be at least 1 MPa.
- The water temperature range should be specified in the range that the meter is able to operate at. This is affected by the physical properties of the used materials.
- Minimum and maximum flow rates that the device can measure within permissible errors need to be specified. Although the measurement results depend on the electronics design of the device and are not in the scope of this study, the flow rate classes mentioned in the standard provide a reference to what the mechanical conditions should be.

2.2.2 Injection plastics design

Injection moulded plastics are widely used in many components of electronic devices due to the possibility of gathering detailed small features in limited spaces, their mechanical properties and various surface finish options. The enclosure of the design and other small parts in the assembly are made from injection moulded plastic. It is important that the design is feasible and can be manufactured without defects.

The most important rules for designing plastic injection parts are [26]:

- The constructor should have a scenario of how the mould will split and a split line should be determined.
- The material thickness should be as uniform as possible, to avoid sink marks and loss of mechanical strength due to non-uniform cooling of the plastic.
- The material should have drafts in the mould pull direction, fillets and rounded corners so that friction between part and mould is minimized. This friction causes wear of the mould over time and makes it difficult to pull the part out of the mould without damaging it.

2.2.3 Employer specifications for the initial design

The initial design was constructed using reference components that were provided by the employer. These components are parts of a bought assembly. The assembled product is a U-type flow meter enclosure that consists of a pipe component that has sockets for transducers and sensors (figure 2.8 - right), an internal bracket (spool piece) that holds the beam reflectors (figure 2.8 - left), two circular transducers and a temperature probe (dimensions of diameter shown in figure 2.9). The rest of the design task is to construct a compact enclosure -instead of the pipe component- that contains a main PCB and other components that are determined by the hardware and software design divisions of the company. The components that occupy space and determine the shape of the enclosure are:

- C-cell battery (maximum outer dimensions: DIA 26,2 mm x 51 mm x1
- A-cell battery (maximum outer dimensions DIA 17 mm x 51 mm x1
- Super capacitor with outer dimensions DIA 15 x 20 mm x1
- Display x1
- Flexible antenna that is used for NFC (Near Field Communication) with smart phones or any other device that can read it. x1
- PCB antenna for LoRaWAN communication. x1
- The bracket for the mirrors of the transducers
- Ultrasonic transducer x2
- Temperature probe x1
- Pressure probe x1



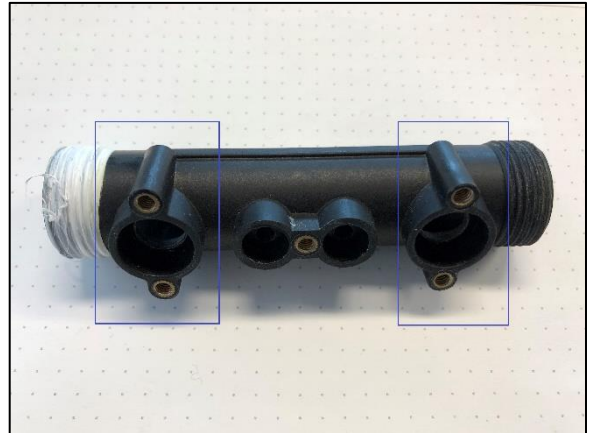


Figure 2.8 Reference spool piece for the initial construction (left) and enclosure pipe for transducers and sensors (right). Transducer sockets are shown with blue rectangles

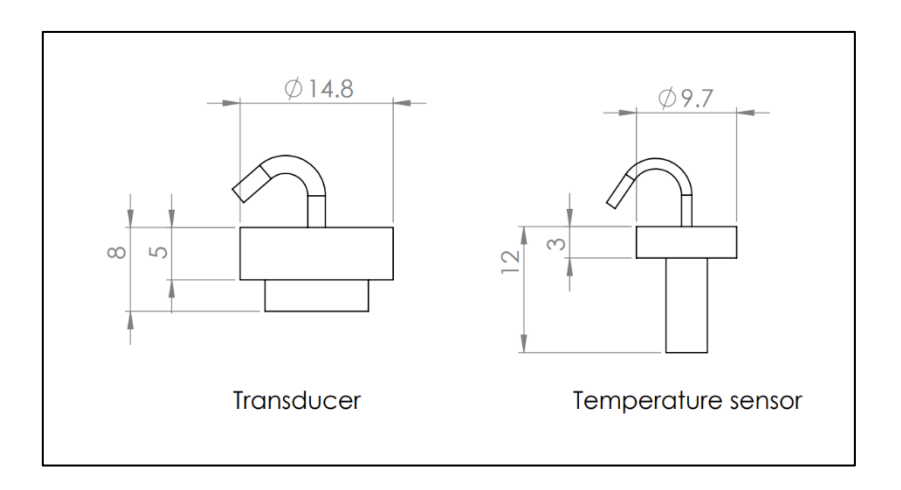


Figure 2.9 Transducer and temperature probe dimensions

The design was done according to the following restrictions that were set by the employer:

- It is important to consider minimizing empty space inside the device while keeping a tidy and appealing look, making it easier to promote in the market.
- The device should have ingress protection, specifically dust and water.
- It should have the possibility of disassembly.
- The transducers should be flushed with the inside surface of the pipe to touch the water but not restrict its flow.
- There are two additional openings on the mirror bracket part, that are for the temperature/pressure probes that also lock the spool piece in its place, so it does not rotate or slide inside the pipe. One opening will be used for a pressure sensor that needs to be a surface mount (SMD) component on a PCB. The other opening

is there for further development possibilities and at least so that it has a locking function.

2.2.4 Initial construction

An exploded view of the components of the resulting device construction is shown in figure 2.10.

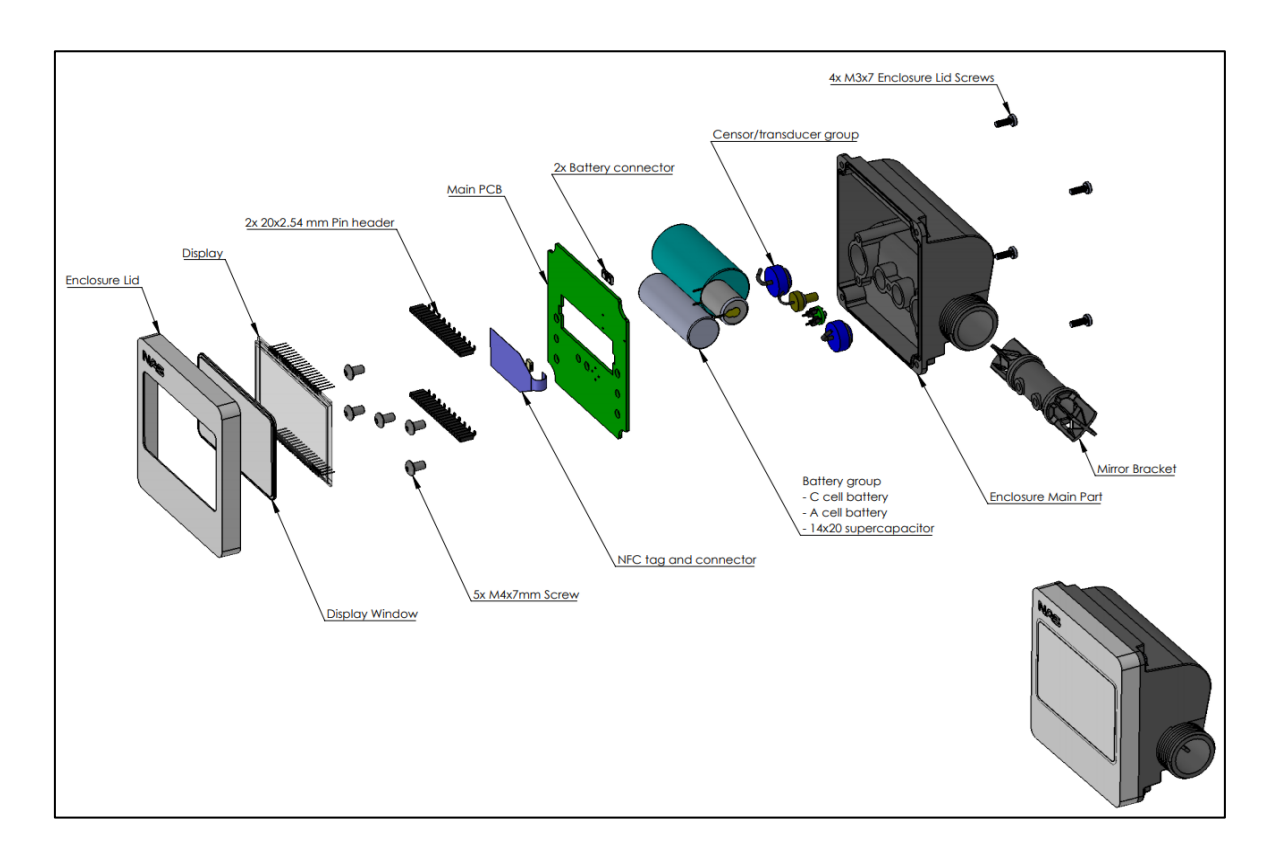


Figure 2.10 Components of the initial construction

The design process started with the idea that the transducers with the shown measured dimensions in figure 2.9 can be fixed in the pipe sockets by utilizing the PCB as a mechanical component to press down on them with screws.

This should save material costs since the PCB is doing something extra. Otherwise there would be a need for some other mechanical component to fix them in place, which not only would cause extra material costs but also an increase in enclosure height because the transducer heights are a constraint and everything that is fixed on top of them need to expand upwards. Furthermore, less parts generally mean less assembly time and assembly errors in production. The construction cross section is shown in figure 2.11.

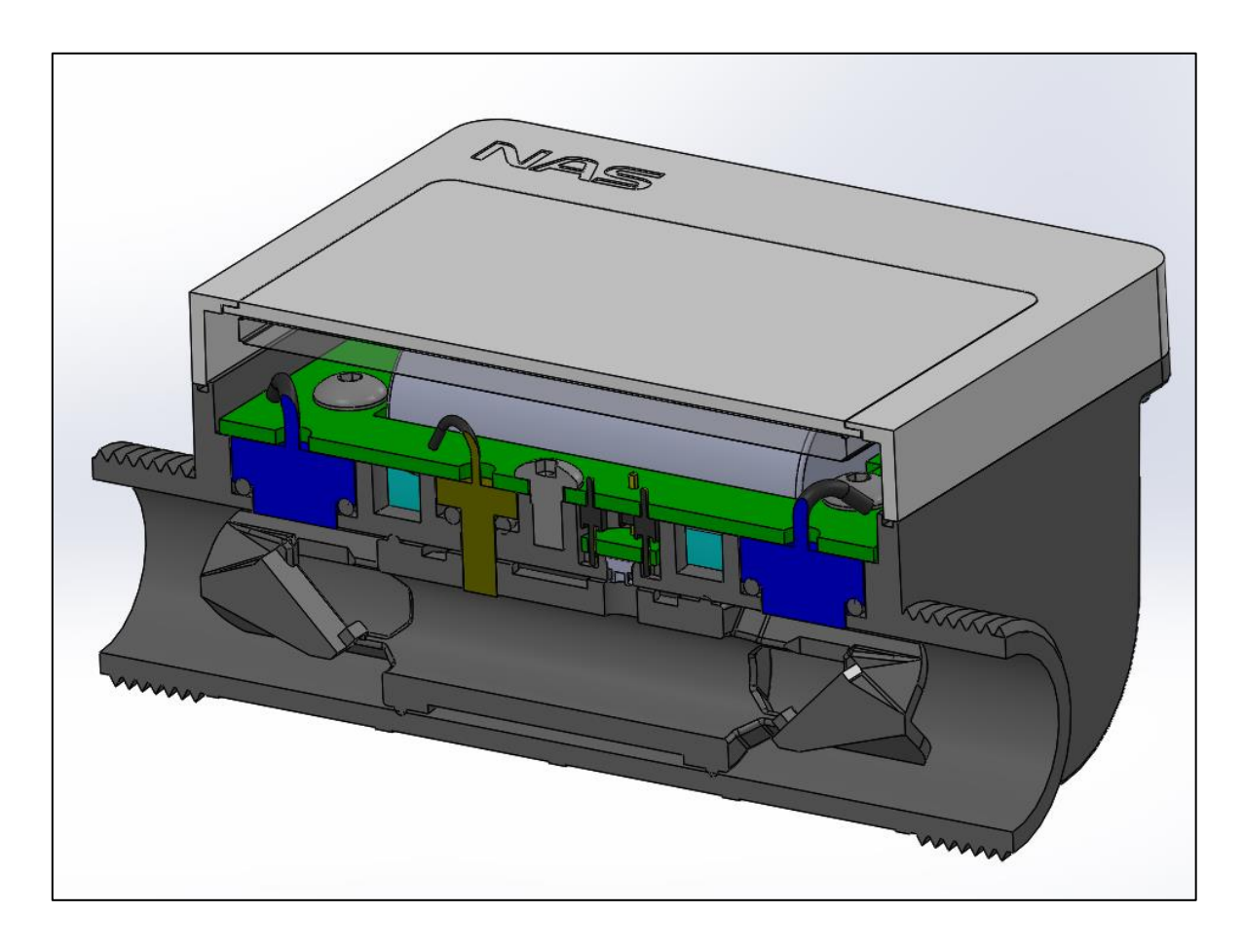


Figure 2.11 Cross section of the initial assembly

For the hole diameter and depth dimensions for of the transducer sockets of the enclosure, the dimensions of the reference transducer housing were used. The diameters of the holes were determined as a 0,2 mm offset from the transducer diameter. The transducers are fixed with two M4 screws each. The screw ports are as close to the openings as possible to minimize flexing of the PCB and benefit from the direct force of the screw as much as possible. One M4 screw holds both middle smaller holes, since they have smaller diameter and would require less force and because there are already four screws holding the PCB. A break-off PCB is used to immerse the pressure probe TE Connectivity MS5837-30BA (figure 2.12) into the pipe as much as possible. This can also be seen in figure 2.11. MS5837-30BA is a surface mount component that has four inputs and outputs. These ports were directed to the main PCB via four pin headers on the break-off PCB where the censor is soldered. To make room for the through-hole pins of this break-off PCB, there are closed bores at the bottom of the socket for the pressure sensor on the main enclosure pipe section.



Figure 2.12 TE Connectivity MS5837-30BA

The other hole was just made to fit the example temperature probe which is also visible in figure 2.11. This hole was modelled to have the same measurements with the example component that was provided (figure 2.8)

After constructing the pipe section, the batteries which take the most space were placed in the assembly and as close to the pipe as possible and the enclosure walls were constructed to wrap around the electronic components. The size of the battery side of the device depends primarily on the space of the batteries and the horizontal extension seen on the right-hand side of figure 2.14. This feature not only provides a resting area for the PCB but also is a result of the dimensions of the screw ports for the lid. The other side (left-hand side of figure 2.14) of the pipe is determined by the size of the other components that are on the PCB and their positioning. These components are the display, SMD female pin headers for the display, and the NFC tag shown in image figure 2.13.

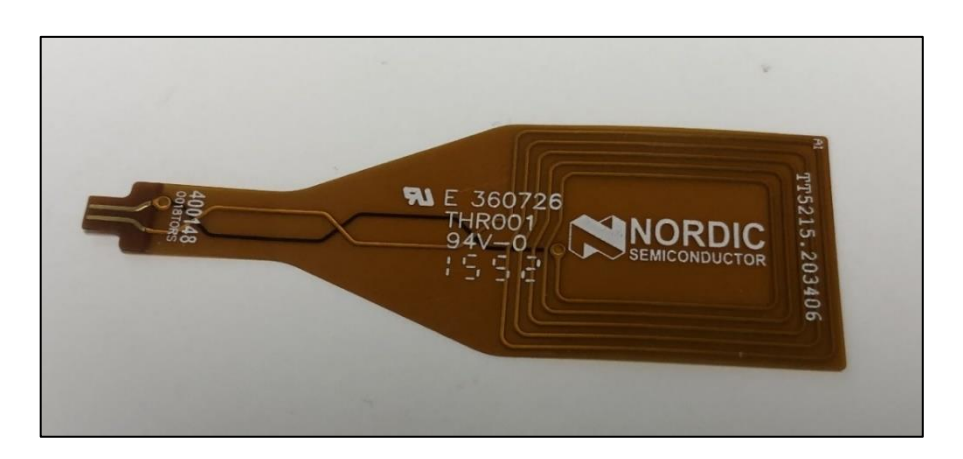


Figure 2.13 Flexible NFC tag

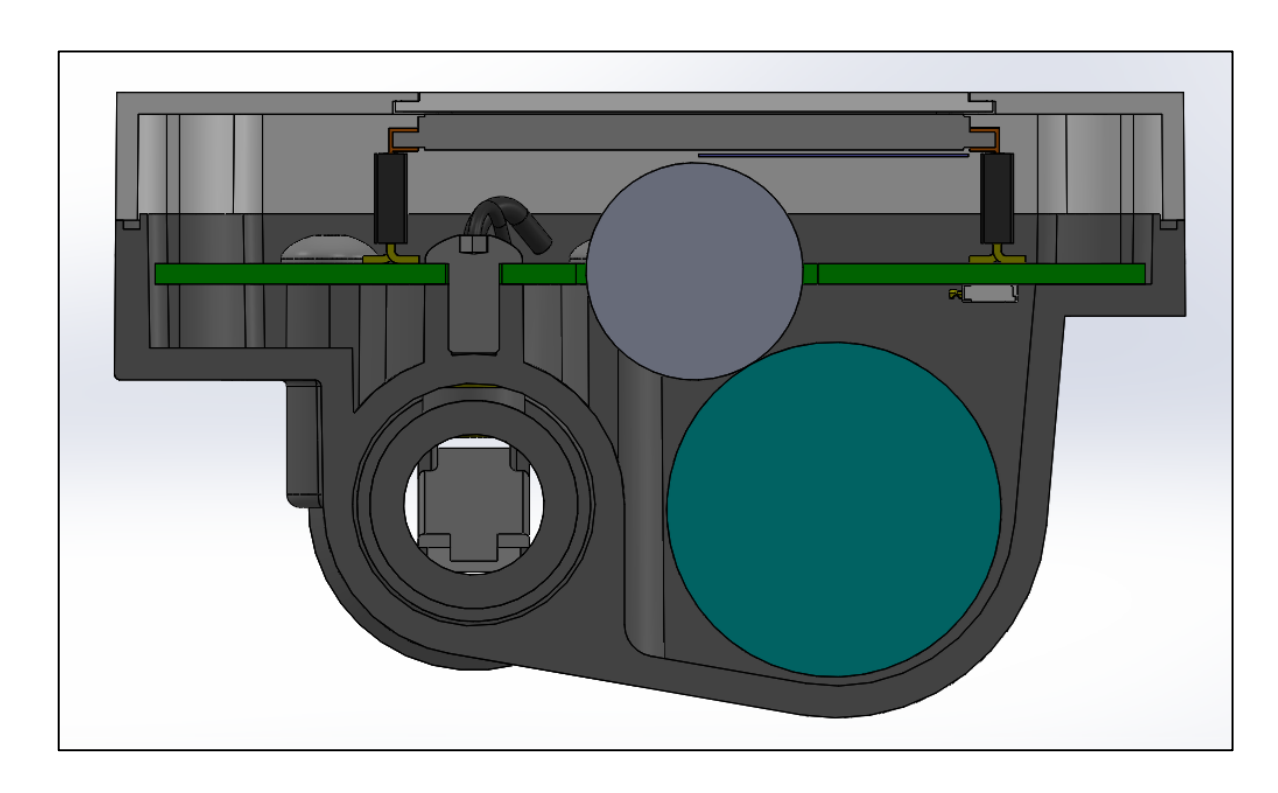


Figure 2.14 Side view cross-section of the initial assembly

The depth of the enclosure below the PCB on this side was made to be lower than the actual resting level of the PCB to make room for possible components on the bottom surface of the PCB. There is a possibility that the device could be modified to function as a heat meter in future revisions, which might need this kind of space for cable connectors, cable outlet features on the enclosure or censors to measure ambient conditions.

The LoRaWAN frequency antenna is a PCB antenna that is also used in the other products of the company and has a certain shape that can be placed on top of the PCB model by pasting it as a sketch (figure 2.15).

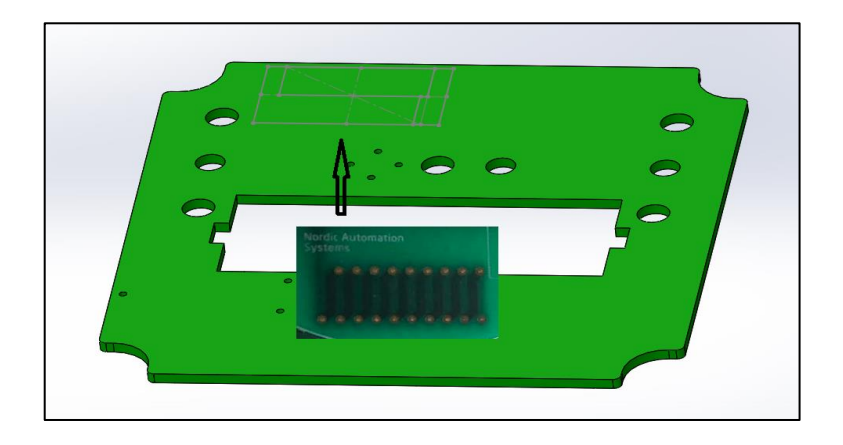


Figure 2.15 LoraWAN antena placement on the PCB

The criteria for this place are that the antenna should be as far away from the batteries as much as possible and it occupies a rectangular space on the PCB with minimum dimensions of $14 \text{ mm} \times 25 \text{ mm}$.

The enclosure lid was constructed last, along with the display window. These two components will be bonded to each other by ultrasonic welding to prevent ingress. In the initial stages of the development process, they will be bonded with adhesive materials until the provider for the ultrasonic welding process is certain. In both cases, it is better to have the window and the lid in the same material [27]. It was assumed that the upper part (lid and window) of the device is not affected by any criteria that is determined by the physical properties of the flowing medium, because the pipe is already sealed by the PCB. ABS plastic was chosen for the material of these parts, simply because of its strength and cost benefits. The only difference is that the window part is transparent ABS.

The sealing groove on the bottom part that leaves the screw connections on the outside provides ingress protection. An elastic sealing material is placed inside this groove which is compressed by the lid and the screws.

The material thickness of the main plastic enclosure was chosen to be 2,5 mm, by measuring the wall thickness of the example thickness of one of the competitors (figure 2.7) and the rest of the bottom part was designed to have a mean wall thickness of 2,5 mm. This means that the material thickness can be +-25% of 2.5 mm, depending on the draft and other geometric conditions. The draft was chosen to be minimum 0.5 degrees because that draft angle was also used in other parts that were ordered from the manufacturer and they worked. Further discussion on the final draft angles and split lines of the mould are discussed in chapter 4.

2.3 Problems with the initial design

After receiving the initial batch of produced samples of the enclosure and testing, it was seen that some revisions are needed.

- The internal mirror bracket is about 7 times more expensive than what would be paid if it was designed in-house and injection moulded along with the other plastic parts.
- ii. The housings of the bought transducers are for general industrial use and their dimensions are not tailored to the design of the meter. The plan is to buy only

the piezo ceramic discs that are the actual working element in these transducers and integrate them into the enclosure. The current design is not suitable for this.

- iii. It can be seen in figure 12 that the SMD pressure and temperature sensor surface is not flushed with the fluid flow because of the material thickness of the spool piece. According to the datasheet of this sensor, this will compromise the accuracy of the component.
- iv. The mechanical performance and functionality of the product is based on dimensions from reference products in the industry and a basis for the rating of the meter according to industry standards does not exist. For example, it should be able to withstand a total pressure of 16 bar (PN16 pressure rating, taken as a reference point from Multical 21) and there is no validation of this performance in the design stage.
- v. Feedback was received from the testing of the device and it is working with a measurement error of as high as %10 which can be mitigated with calibration, but the amount of initial error should still be reduced in order to reduce accumulated error as much as possible.

2.4 Definition of goals

The goals of this thesis were set to address the problems presented in 1.3, using Solidworks. These goals are:

- Justifying the choice of material and the material thickness of the enclosure.
- Designing a new enclosure that encapsulates solutions to the conformity standards and addresses all of the stated problems.
- Providing work to contribute to the improvement of the measurement accuracy.

In chapters 3, 4 and 5, these goals are addressed in the light of available technologies, principles and standards given in the review. Conclusions of the works and simulations are presented by referencing the corresponding problems that were solved at the end of each chapter.

3. FEA SIMULATIONS

3.1 Material model

The material of the bottom part of the enclosure that includes the pipe was chosen as polyphenylene sulphide with %40 glass fibre reinforcement (PPS-GF40). PPS is a high-performance semi-crystalline thermoplastic that has almost zero moisture absorption and is known for its chemical resistance properties in higher temperatures which make it a suitable material to be used for a device that will measure residential water flow that can contain chemicals which would otherwise be harmful to other plastics.

In order to simulate these conditions in Solidworks, the material properties of PPS-GF40 were created as a custom material in the materials database of the program. Since the current manufacturer of the enclosure is not able to provide a detailed datasheet for the material, these values were gathered from datasheets of other commercial brands of PPS-GF40 in order to provide the computational tool with values that are at least close to reality and can be modified when a more accurate description of the behaviour of this company's own product is known. This approach would cause some inaccuracies in simulation results because the products of every company are slightly different. It was assumed that it would at least provide a basis for the simulation to take place and the error would not be so large that it would even surpass the safety factor margin that will be used in the construction.

It was seen in several datasheets and design manuals that this material is anisotropic, meaning that the mechanical properties of the material vary depending on which way the force is being applied. This is due to the self-orientation of glass fibres in the part that occur during the moulding process. The mechanical properties in the flow direction of a part are greater than those in the transverse direction [28]. It was noted that the available model type selection "Linear Elastic Orthotropic" could have provided a better representation of the material since it is anisotropic (orthotropic), but data that was needed to define this material type, such as mechanical property values in three dimensions in space was unavailable and information on the flow behaviour of the current model is unknown. The material was introduced to the library as a "linear elastic isotropic" model in order to make it possible to provide as much information from datasheets as possible. This anisotropic property is accounted for in the section 3.5.

3.1.1 Property inputs for custom material definition

The material properties that can be specified for a custom linear elastic isotropic model type material in Solidworks and the source of these values are as follows:

Elastic modulus (Young's modulus) is defined by Hooke's law with the equation

$$E = \frac{\sigma}{\varepsilon} \tag{3.1}$$

where E - elasticity modulus, Pa,

 σ - the stress, *Pa*

 ε – ratio of elongation to initial length.

It describes the relation between stress that is applied to a material and how much that material elongates as a result of that stress. This value is constant for a linear-elastic material [29] before plastic deformation occurs (the material is not able to take the same shape as it was before the application of the stress). It was seen in [28] that the elastic modulus of PPS-GF40 is temperature-dependent (figure 3.1).

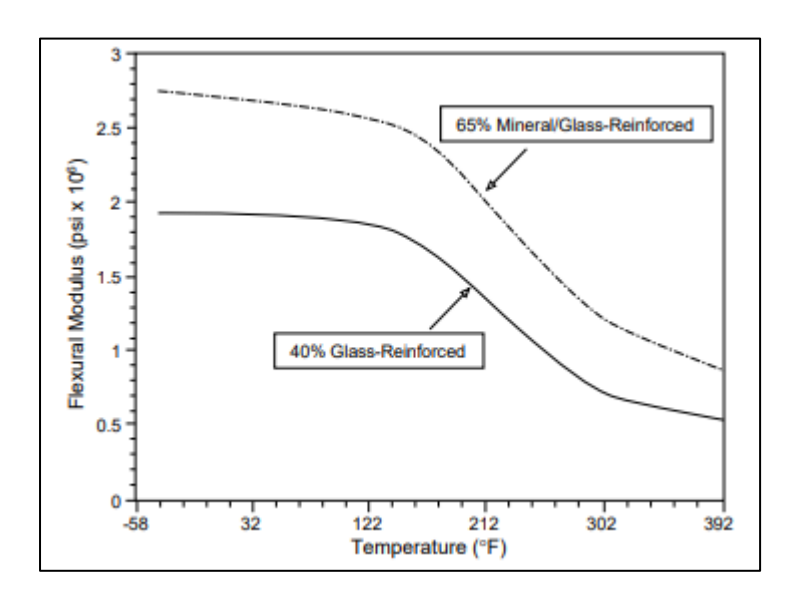


Figure 3.1 Effect of temperature to elastic modulus for PPS-GF40. Image taken from [28]

A cleaned -of unnecessary information like comparison curves with other materials-screenshot image of the curve from the .pdf document [28] was uploaded to www.graphreader.com and instructions on the website were followed. This website tool generates a curve and outputs comma separated values for the number of user defined

points. These values can then be processed in Excel and imported to Solidworks as custom material properties.

When a value of a property is set as "Temperature Dependent" in the properties tab, the user is directed to the "Tables & Curves" tab where the .csv file can be imported by browsing directories (figure 3.2), using the "File" button shown in the image. It is important to note that technical difficulties (seemingly random changes in values in the imported values) were experienced when changing the units in "Table data" area to match the .csv file units. It was seen in the help forum of Solidworks [30] that this is a situation that is experienced by other users as well who want to import values in .csv format and there seems to be no solution to it accept converting the .csv file values to whatever default unit is set in the "Table data" section. In this case, all values in the .csv file were converted to "K for temperature and MPa for pressure. To sum up, playing with the "Units:" drop-down menus in this section at any time (before or after the import) affects the reliability of the data negatively in this version of Solidworks (version 2019, SP5.0).

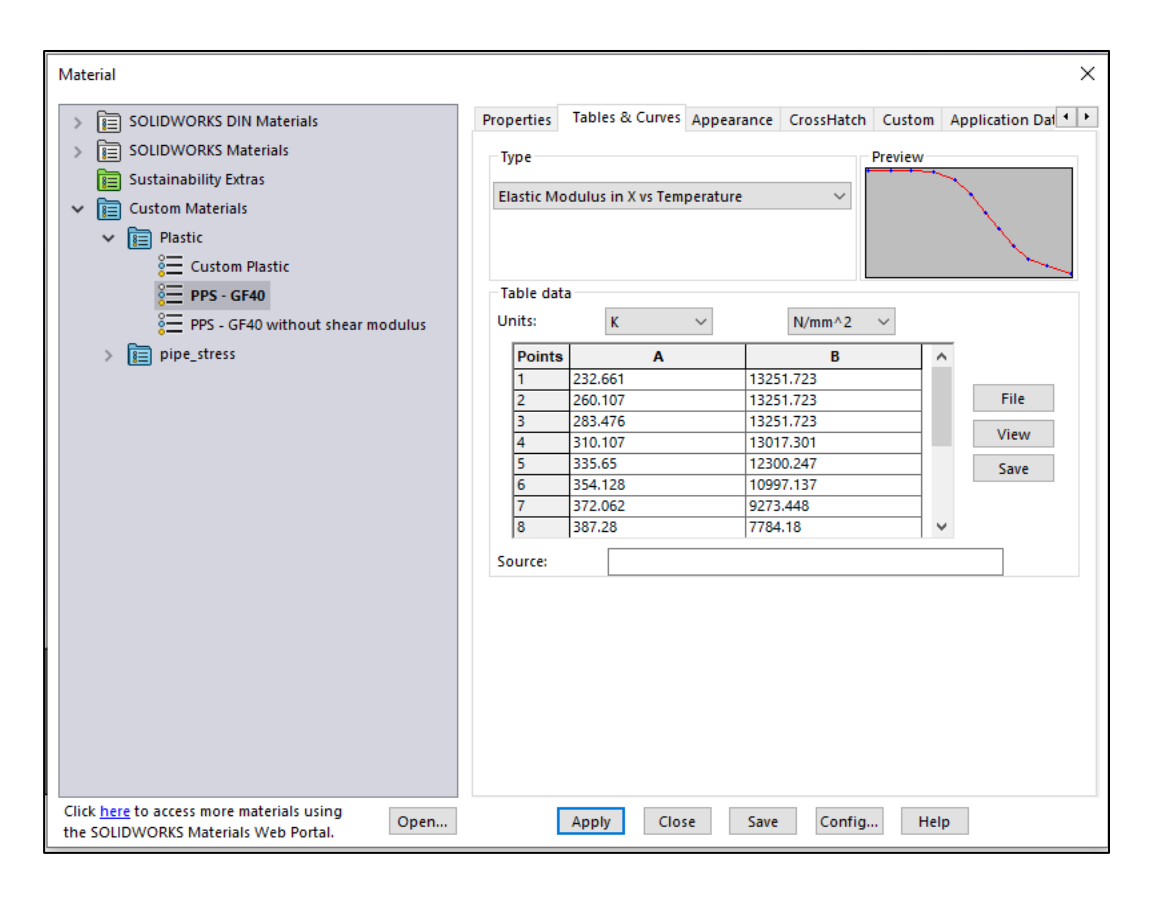


Figure 3.2 Importing temperature dependent properties to define a custom material

Poisson's ratio is the ratio of the lateral strain to longitudinal strain and was taken as a constant value of 0,35 from [28].

Shear modulus describes the materials dimensional response to shear stress. The temperature-dependent values (figure 3.3) of it were taken from [31], but it was seen that the simulation failed to complete unless the shear modulus was left blank. It was assumed that the source of the problem could be that the shear stress-strain behavior was calculated by the program using the poisson's ratio and elastic modulus which were already given, and these did not exactly match the values that were manually acquired from an image of a graph.

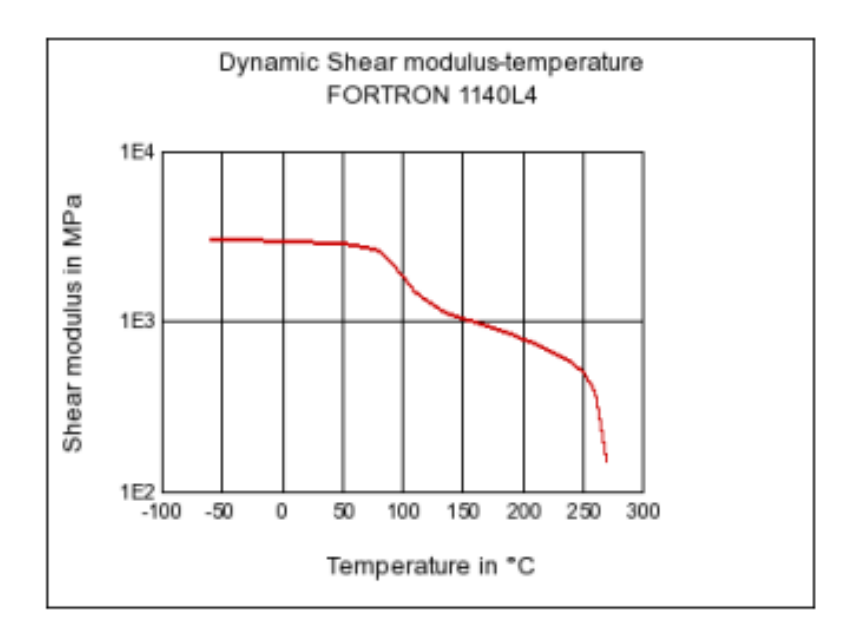


Figure 3.3 Effect of temperature to shear modulus for PPS-GF40. Image taken from [31]

Mass density was taken from [31] as 1650 kg/m³.

Compressive strength value was taken from [32] for their PPS-GF40 product as 250 MPa as a minimum value.

Yield strength is the amount of stress where the material starts plastic deformation. This is the limit value which is used as a constraint in the simulations because no plastic deformations should be allowed in this design task.

As mentioned, PPS-GF40 is a semi-crystalline polymer, meaning it consists of amorphous regions where molecular chains are entangled; and crystalline regions where they are neatly packed. Semi-crystalline materials have a property called glass transition temperature. If the temperature of the material is under this specific value, the amorphous regions in the material stop moving as much and are referred to as a

glassy state. This makes the material rigid and brittle [28][29]. The glass transition temperature for this material is 90 $^{\circ}$ C, which was taken as an average number from multiple datasheets.

Figure 3.4 shows the stress-strain graph of the product of [32], for their version of PPS-GF40 at different temperatures.

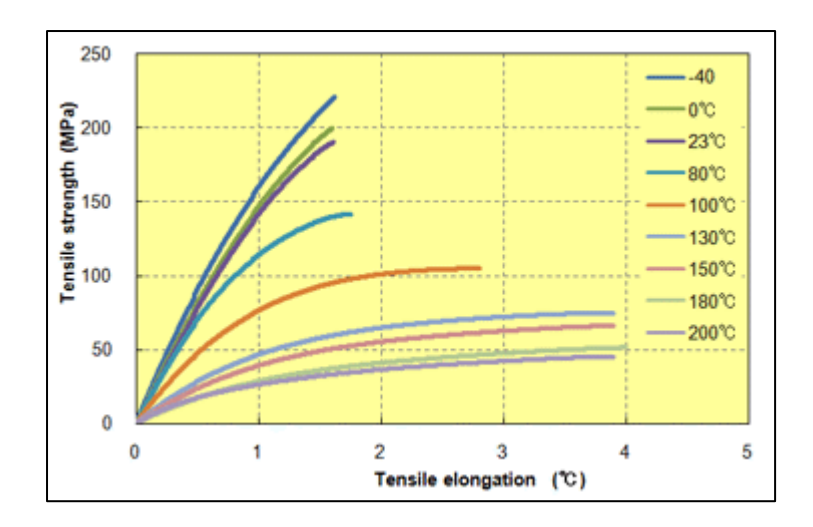


Figure 3.4 Stress-strain curves of PPS-GF40 for different temperatures, taken from [32]

The difference of behaviour around the glass transition temperature can be seen by observing that below 90 °C, the material exhibits a more brittle behaviour. Since the analysis will only be made up to 70 °C, the same .csv file that was used for the tensile strength of the material was also used for the yield strength as a temperature dependent value. This is because the yield point of brittle materials is close to the value of their tensile strength since there is very little room for plastic deformation before break.

Thermal expansion coefficient was taken from [32] as 0.00003 1/ °K

Thermal conductivity was taken from [28] as 0.2 W/(m $^{\circ}$ K) that is the value of 40% glass and between 25 and 125 $^{\circ}$ C.

Specific heat was taken from [28] as 1.5 J/g °C which converts to 1500 J/kg °K

Tensile strength is the stress value when the material breaks. This value was also temperature dependent and can be observed from figure 3.5. It was acquired and imported to Solidworks the same way as was done for the elastic modulus.

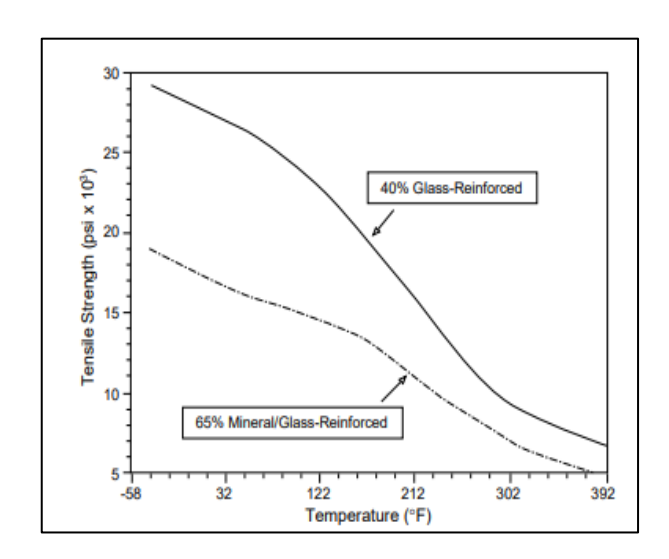


Figure 3.5 Effect of temperature to tensile strength for PPS-GF40 (image taken from [28])

3.2 Simulation methodology

The aim of the FEA simulation is to determine a minimum allowable wall thickness for an enclosure that is made of this specific material and assess the material thickness that is already being used in the product. Since the pipe that the water flows through is a part of the enclosure, the thickness of the pipe material will directly affect the wall thickness of the enclosure. This is because an injection moulded part should have uniform material thickness.

Mechanical constraints that should affect the stresses acting on the device:

- Geometry. The device is initially designed according to the pipe size standard DN20 (Diameter Nominal), which corresponds to an outer diameter of 26,9 mm.
- The device should be able to withstand an internal pressure of 16 bar = 1600000 Pa, which is determined by the pressure rating PN16 (Pressure Nominal).
- The flow temperatures range from 0,1 °C to 70 °C, which is a chosen temperature class (T70) from the international recommendation document published by the International Organization of Legal Metrology (OIML R49).
- From the same standard, the ambient temperature should range from 5 $^{\circ}\text{C}$ to 55 $^{\circ}\text{C}$.

The material thickness was determined according to pressure that is applied to the inside of the pipe at the maximum cross-sectional diameter. In the revised model, there is a reduction in the middle section of the pipe diameter (Chapter 4). Pressure in the reduced part of the diameter would be less than the pressure in the simulation diameter because of the Bernoulli equation for incompressible flow (equation 3.2).

$$\frac{p}{\rho} + \frac{v^2}{2} + gz = constant \tag{3.2}$$

Where p - pressure, Pa,

 ρ - density, kg/m³,

v - velocity, m/s,

g - gravitational acceleration, m/s²

z - height difference, m

In the case of the horizontal pipe, the term gz is zero because there is no height difference between inlet and outlet. The velocity increases in the reduced pipe section because of equation 4.3, and pressure decreases to satisfy a constant sum.

3.2.1 Model simplification

Although there are irregular geometries and fillets inside the pipe, the geometry was taken as circular for the FEA analysis. This is a simulation of the minimum conditions and it is assumed that the pipe section of the device will be stronger in reality. The actual plastic part has walls and additional features that provide mechanical support to the pipe.

Since the pipe is circular, the pipe was modelled as a quarter-section using simplification due to symmetry.

Furthermore, the simulation study was chosen to be on a thin-section model because only the radial stress (hoop stress) is present. Longitudinal and shear-bending stresses are ignored [34][35].

3.2.2 Restriction of simulations based on worst-case conditions

The yield strength of the material decreases with increasing temperature. Consequently, the material performs the worst when both inside and outside temperatures are chosen to be the highest. This case was chosen to be the worst case, so that in any other

temperature condition within the determined constraints, the material would perform better.

3.3 Simulation setup parameters

3.3.1 Fixtures

Two fixture constraints were applied to the quarter section. Two edges of the quarter section were allowed no movement in the perpendicular direction to that specific edge. This allows the simulation to model movement so that these chosen edges always coincide with the central axis of the pipe, conserving symmetry. Movements along these edges are allowed since it imitates the expansion of the pipe. Selection of one of these fixtures is shown in figure 3.6 where movement along the *y* axis is not allowed. The other fixture is applied to the bottom edge where movement in the *x* axis is not allowed.

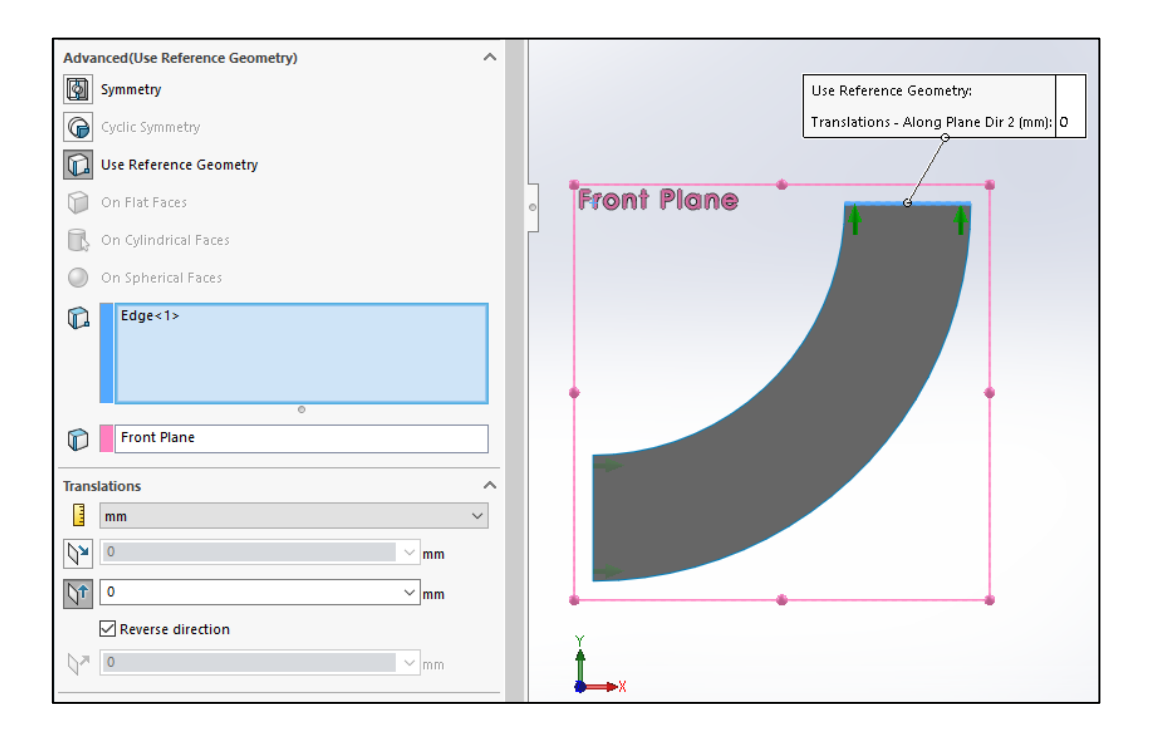


Figure 3.6 Fixture definition

3.3.2 Loads

The loads acting on the model are: Internal pressure of 1,6 MPa, external pressure of 1 atm = 101325 Pa, internal temperature of 70 °C and external temperature of 55 °C. The screenshots of the chosen settings and where the external loads are applied are given in figures 3.7 to 3.10.

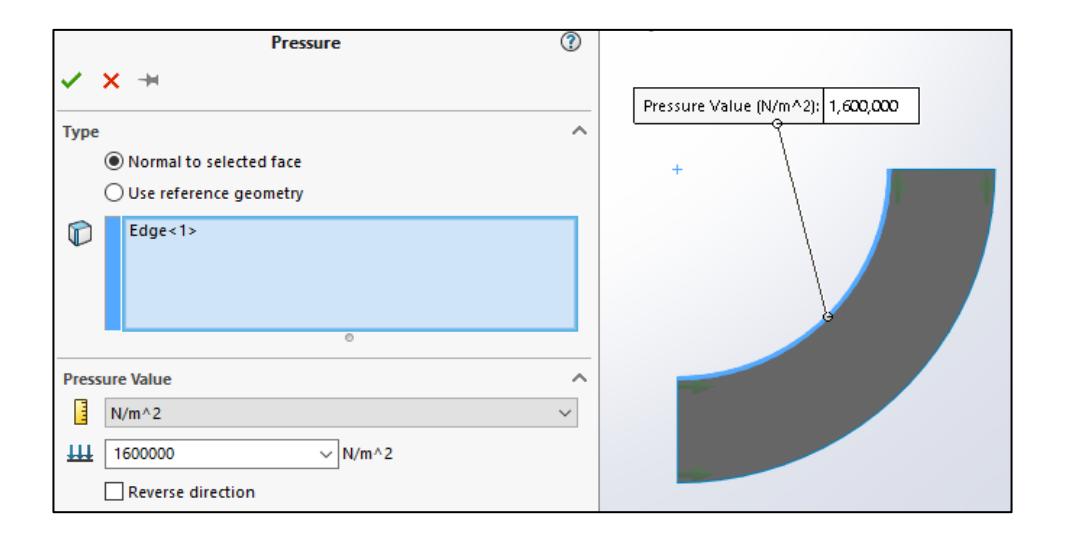


Figure 3.7 Pressure load applied to internal face

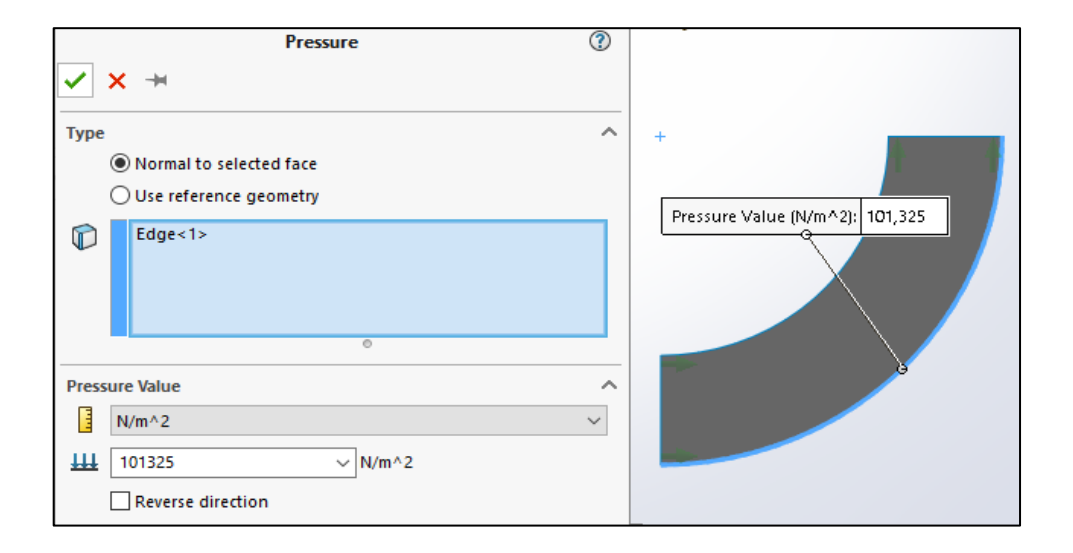


Figure 3.8 Atmosphere pressure load applied to outer surface

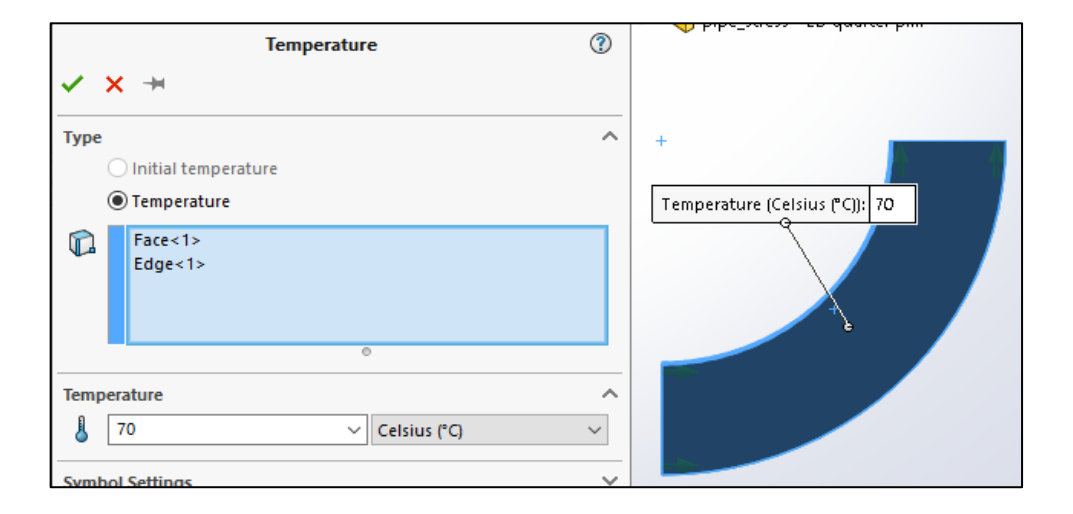


Figure 3.9 Temperature applied to inner surface and material

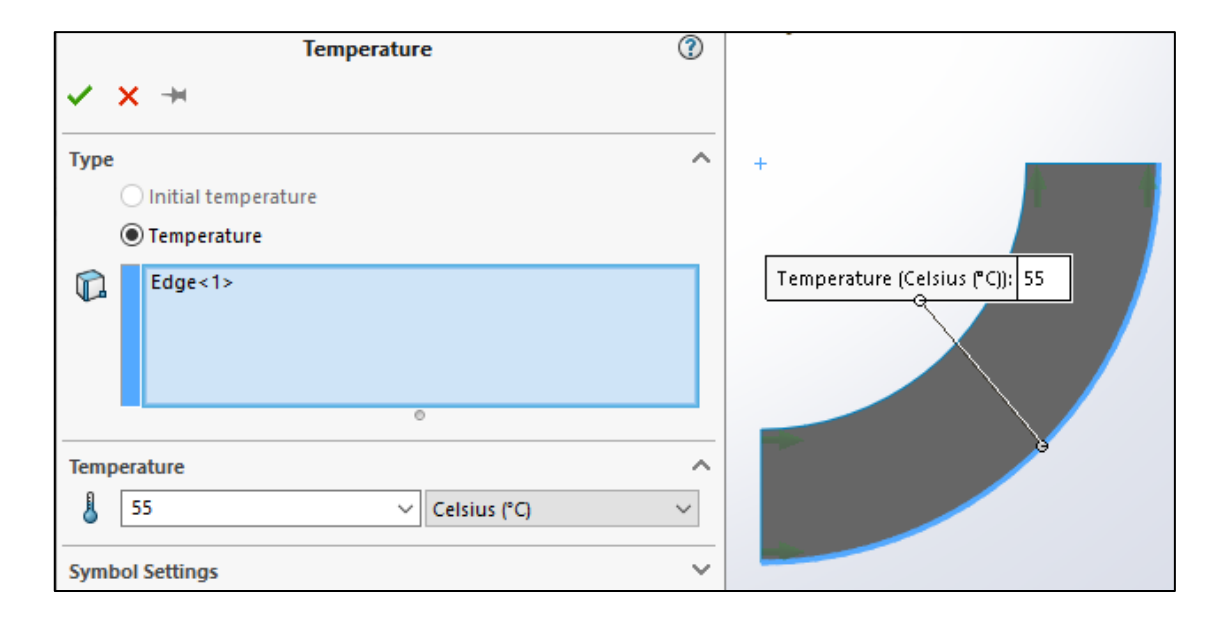


Figure 3.10 temperature applied to outer surface

3.3.3 Mesh settings

It was seen that a standard mesh selection produced more asymmetrical results in the simulation with some ripples of colours that should not be there (figure 3.11-a). It was assumed that the distribution of the stress should be as homogeneous and symmetric as possible because the pressure and temperature are applied homogeneously, and the geometry is circular. Curvature based mesh selection produced more symmetrical looking results in the simulation, but there were spikes in the rings (figure 3.11-b). The blended curvature-based mesh selection produced the most symmetrical rings (figure 3.10-c), which is the reason that the final simulations were made with this setting. All comparisons were made with medium mesh size. Changing the mesh size did not seem to have a significant effect on anything.

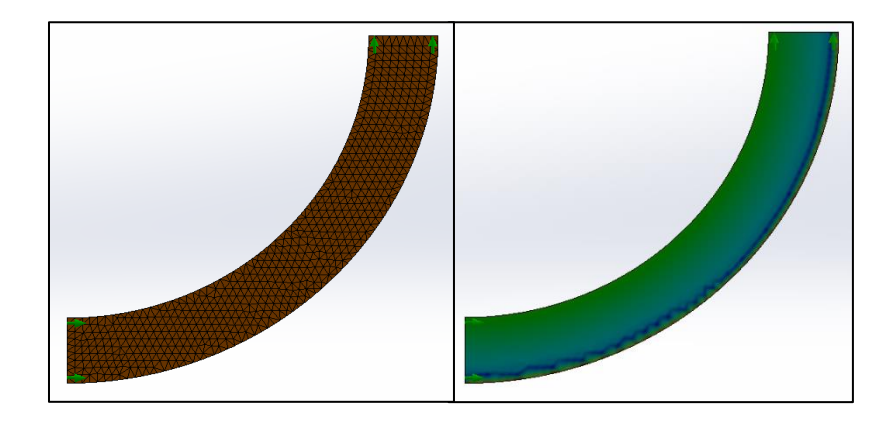


Figure 3.11-a Standard mesh results

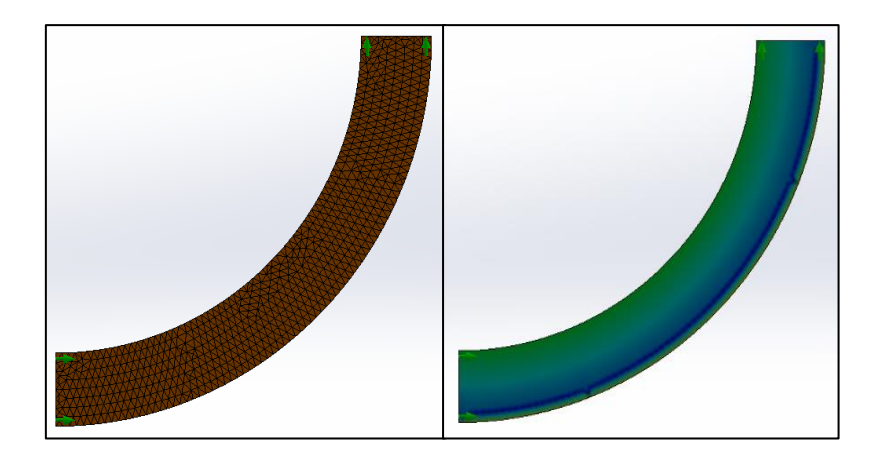


Figure 3.11-b Curvature-based mesh results

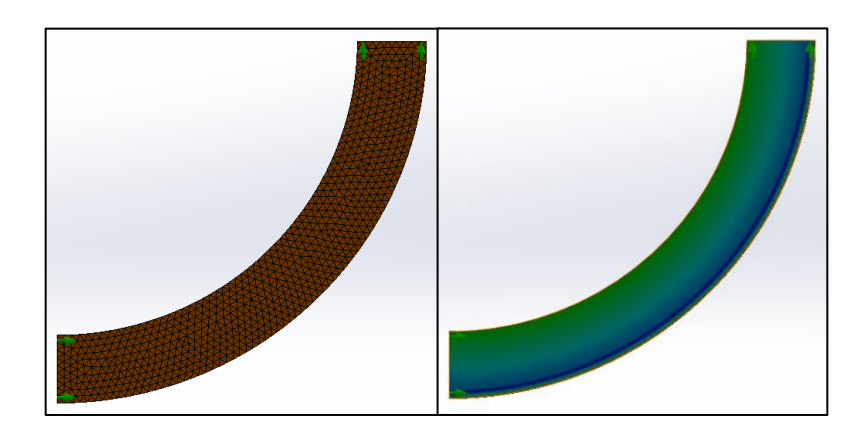


Figure 3.11-c Blended curvature-based mesh results

3.4 Simulation

The minimum wall thickness was determined by trial and error until the minimum factor of safety of 1 was obtained, meaning the Von Mises stress at that point is equal to the yield strength of the material at that specific temperature and pressure conditions. The factor of safety result chart was used instead of a stress plot because the reference value for the yield strength does not show on the plot when it is temperature dependent.

Figures 3.12 and 3.13 show two simulations where every setting is the same, accept that the internal temperature is additionally applied to the material face as well in the second one. The minimum material thickness was determined according to the latter, since it gave weaker results and is intuitively a more accurate representation of the conditions of constant operation where the effects of the internal fluid temperature is conducted to the entire material of the pipe wall.

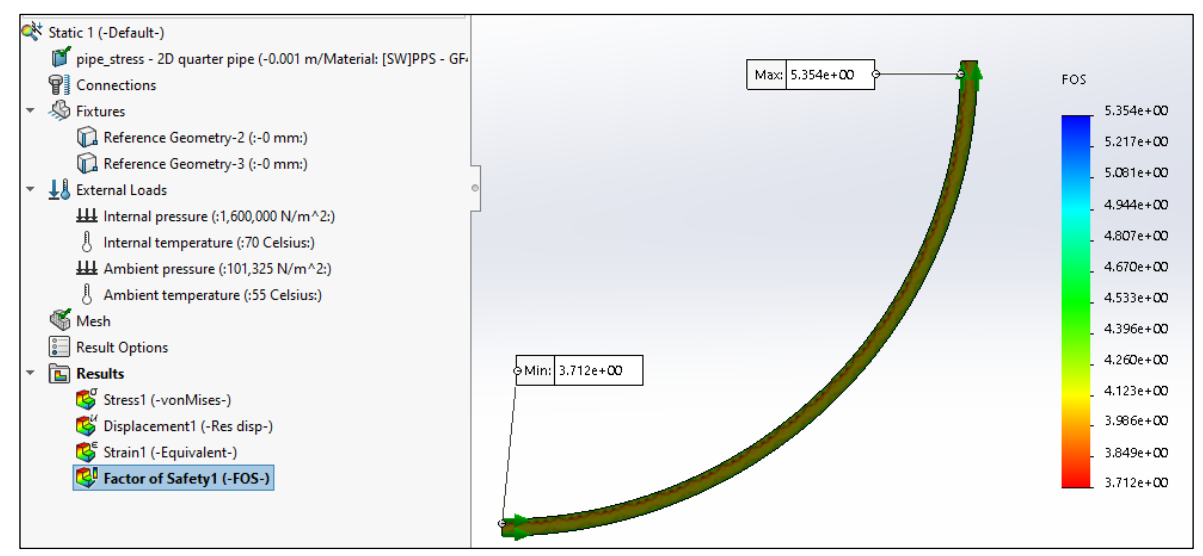


Figure 3.12 Factor of safety plot for temperature applied to edge only

It was seen that in the extreme conditions, the factor of safety is just above 1 (Figure 3.13) when the material thickness is 0,47 mm. It was concluded that any wall thickness greater than this value should have a safety factor greater than 1 in the scope of the predetermined operating conditions. A material thickness of 3,5 mm was used in the design. For the condition where the internal temperature is assigned to the entire material face, a factor of safety and stress plot is given in figures 3.14 and 3.15 where the maximum and minimum values of the stress distribution and FOS can be seen.

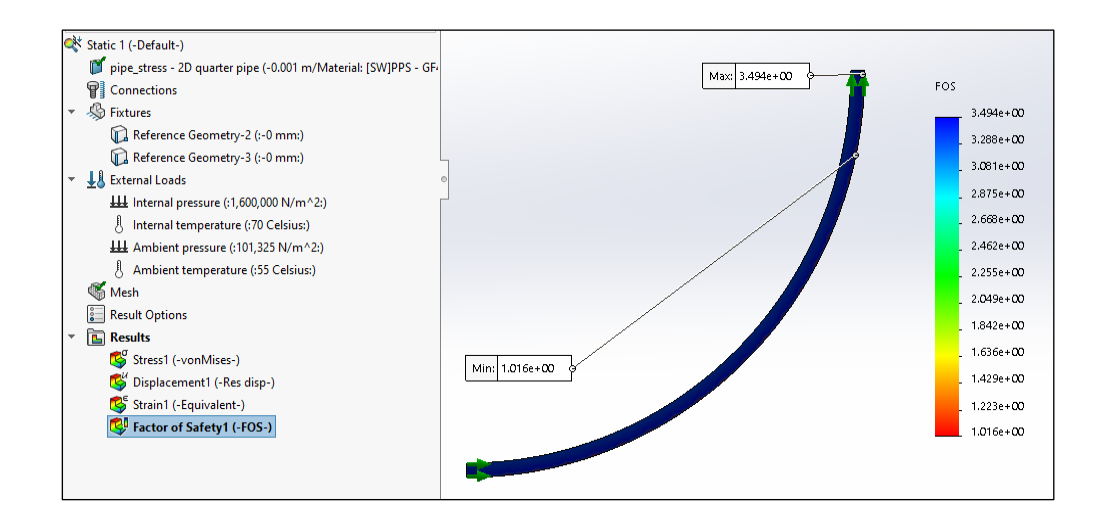


Figure 3.13 Factor of safety plot for temperature applied to both edge and face

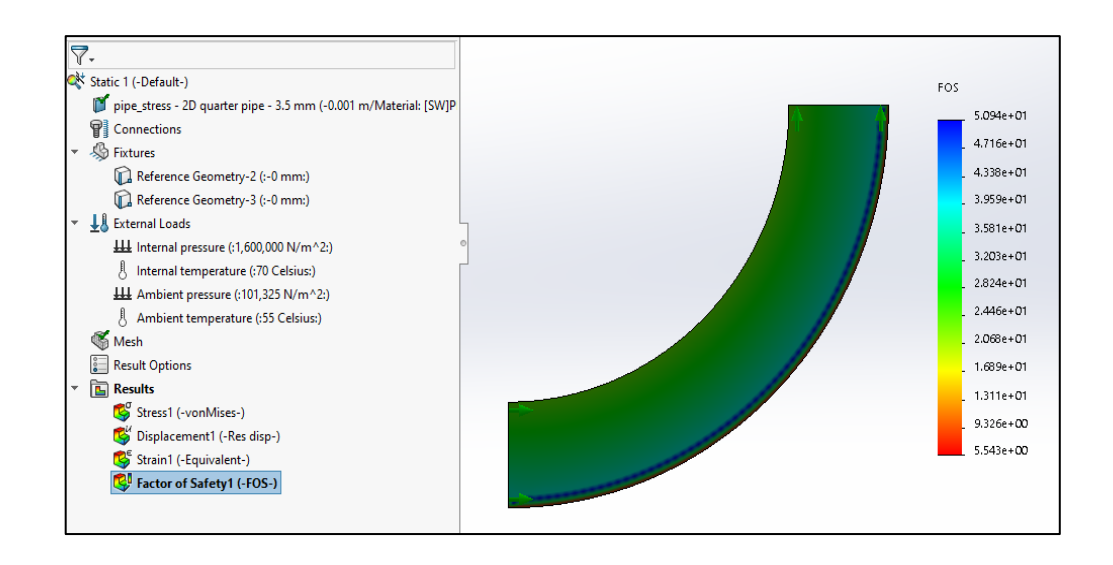


Figure 3.14 Factor of safety plot for the chosen material thickness

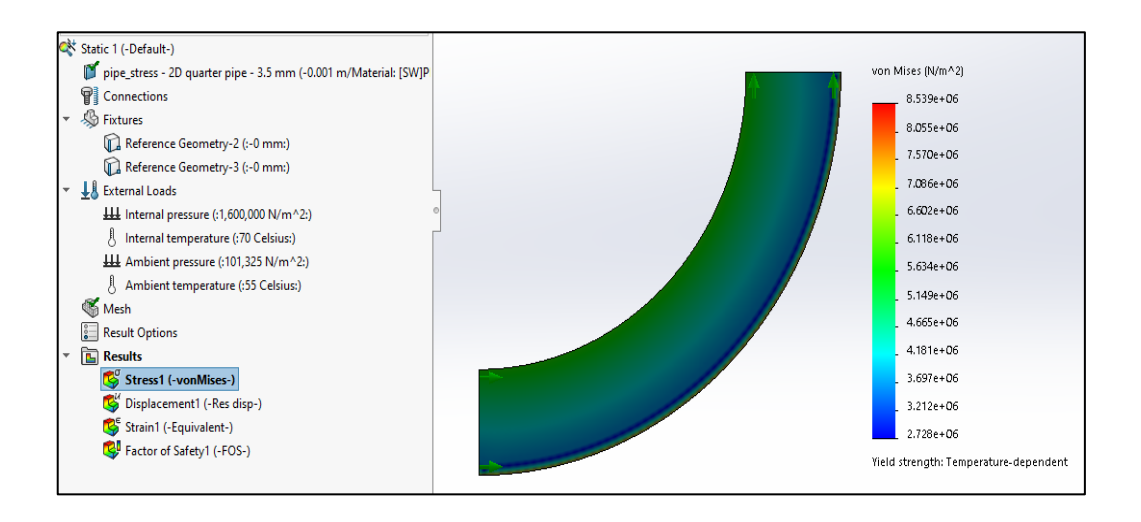


Figure 3.15 Stress plot for the chosen material thickness

3.5 Accounting for anisotropic effects

It is written in [32] that "The mechanical properties in the machine direction are the upper limits of the material, and the properties in the transverse direction can be considered as approximating to the lower limits (with the exception of welds). If, therefore, the maximum load acting in the transverse direction is about equal to or greater than about half the static strength in the machine direction, it is necessary to consider anisotropy when designing a product." Analytical information on these effects are shown in figure 3.16 where the modulus of elasticity graph is from [32] and figure 3.17 where a set of mechanical property ratios are given from [31].

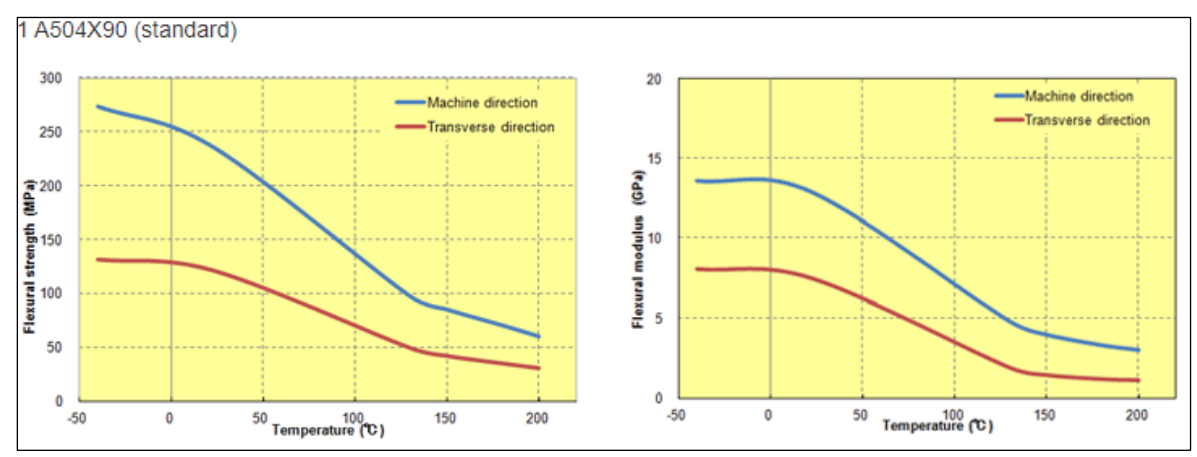


Figure 3.16 Effects of anisotropy - TORAY plastics

	Dt/Df (%)				
Material	Flexural Strength	Flexural Modulus	Tensile Strength	Tensile Elongation	
40% Glass- Reinforced Fortron® PPS	50	60	55	65	

Figure 3.17 Effects of anisotropy - FORTRON plastics

As a validation of the wall thickness of 3,5 mm, the worst-case scenario for these effects are chosen to cover the possibility that every critical stress in the design acts in the weaker transverse direction. A limit for the ratio of transverse to longitudinal direction was chosen as 0,5, which is a rough estimate taken from TORAY and FORTRON datasheets. An analysis of this issue was done by assuming that the part is half as strong as it was designed to be. It can be seen in figure 3.14 that the minimum safety factor of the result is 5,5 and this would be enough to compensate for a %50 decrease in yield strength.

This worst-case assumption is very extreme in the sense that the minimum safety factor in the result is almost a point hotspot (which may be a result of computation inaccuracy), and the general colour of the simulation indicates that the safety factor is around 30. Furthermore, in the actual product this ratio will never be as small as 0,5. In fact, it will be significantly higher since it is not possible to achieve this condition where all critical stresses act on the transverse direction.

3.6 Conclusions

In this analysis, the goal of justifying the material type and thickness have been achieved. It was shown with the Solidworks stress analysis tool that the chosen material thickness is enough to withstand the worst conditions in the determined operating ranges of temperature and pressure. The problem iv in section 2.3 is solved. The industrial standards, such as points i, ii, iii in section 2.2.1 were satisfied.

4. CONSTRUCTION OF THE SECOND REVISION

4.1 Justification of choices

In this section, the reasons for the chosen features in the second design will be addressed and information about the manufacturing possibilities and constructions of individual elements will be presented.

i. The measurement should be done at a narrow section of the flow. This is advised by the hardware division at the company on the basis that it will increase its sensitivity to low flow rates. The volumetric flow rate is

$$Q = A. v (4.1)$$

where Q – volumetric flow rate, m^3/h ,

A – cross sectional area of the pipe (normal to flow direction), m^2 ,

v - velocity, m/s

The area of the cross-section is

$$A = \frac{\pi d^2}{4},\tag{4.2}$$

Where d – diameter of the pipe, m

so, the velocity and the diameter have an exponential relation in order to compensate for the constant flow rate (equation 4.3). As diameter decreases, the flow rate increases exponentially.

$$v = \frac{4Q}{\pi d^2} \tag{4.3}$$

Furthermore, other than clamp-on meters seen on the internet, a device that did not have this feature was not found. Regarding the mechanical design, it was concluded that the pipe between the transducers should be less than the standard pipe diameter.

- ii. The distance between the transducers should be as much as possible, to decrease electronic measurement errors. This distance can be maximized by knowing what is constrained and subtracting it from the total length. The length of the whole enclosure is 110 mm by standard. The length of threaded parts at the two ends of the pipe (set by the employer) and the material thickness of the enclosure are the constants that can be subtracted from the total length.
- iii. It was advised by the electronics division that it would be best if the transducers were facing each other, instead of vertical mounting and directing their signals via reflectors. In addition to the benefits of coaxial transducers that are mentioned in the review in item 2.1.3, another basis for this idea is to minimize the uncertainty of measurement by decreasing the amount of travel medium of the signal that is not being measured. These distances inside the device that are included in the calculation but do not contribute to the actual measurement may have turbulent properties which add uncertainty to the transmitted sound signal. The increase in the length of the path of the signal that is outside the measured portion, when reflectors are used is illustrated in figure 4.1.

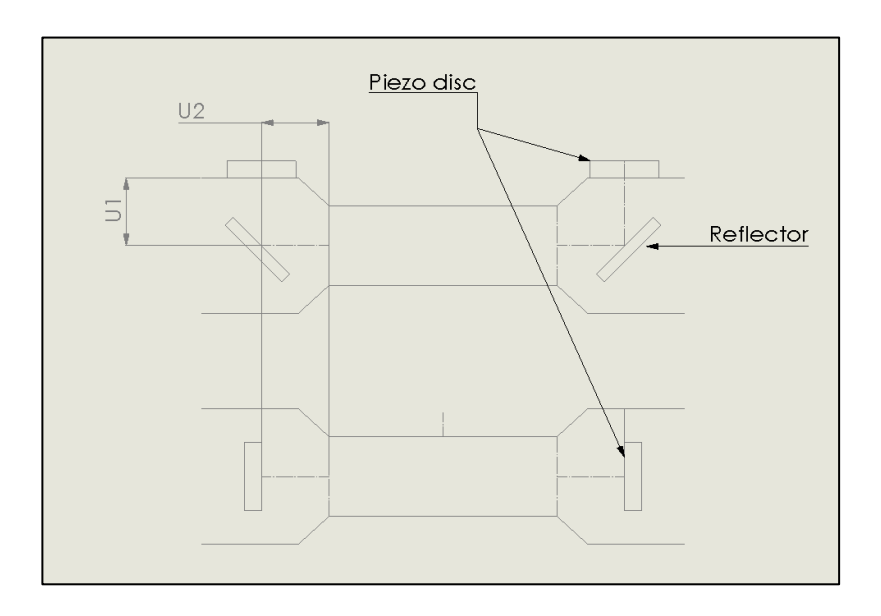


Figure 4.1 Comparison of U-type (above) and coaxial (below) transducers

It can be seen that if the pipe and transducer dimensions are the same, the unmeasured distance of the first setup with the reflectors is a total of 2(U1+U2) whereas in the second setup without the reflectors this value is only 2(U2).

iv. Combining points i and iii, the diameter of the reduced portion of the pipe should be as small as possible, but not smaller than the diameter of the piezo disc. It was learned from correspondences with piezo ceramic disc manufacturers and measuring the diameters of discs used in other products in the industry (Multical 21) that the size of typical discs used in flow metering applications can be as small as 8 mm. The hole size was chosen to be 10 mm in order to leave room for modification of the size of the disc in the future without changing the enclosure dimensions.

According to these criteria, a second revision was constructed. The cross section taken from the pipe section of the 3D model is given in figure 4.2.

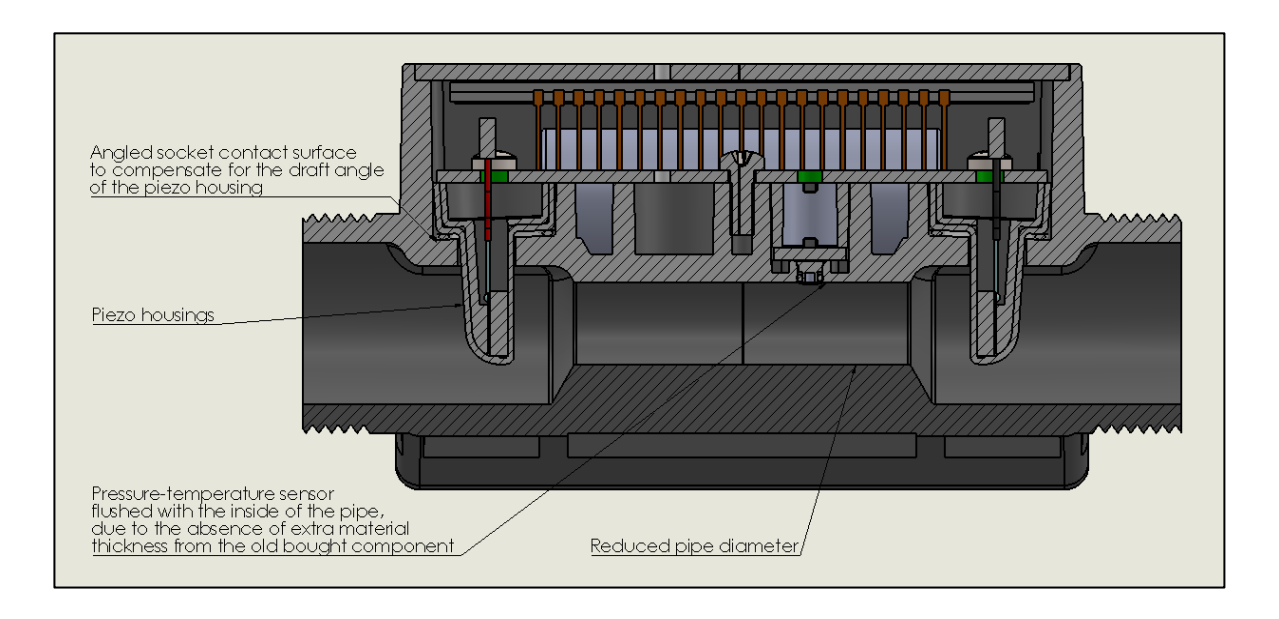


Figure 4.2 Second revision assembly cross-section

The alternative construction that was built had two separate reflector brackets that are fixed from the ends of the pipe separately to make a U-type meter. These reflectors would be three-part assemblies with two symmetric injection moulded parts and a reflector plate that is fixed in the middle. The reflector would be an ellipse that looks like a circle from the vertical point of view and when looked at from the flow direction of the fluid. The piezo discs would be fixed from the inside of the meter. The cross section of the mentioned assembly inside the pipe and the piezo disc socket can be seen in figure 4.3. The 3-part bracket assembly is also shown with and without one of the parts. This idea was discarded because the coaxial arrangement was preferred for previously stated reasons. Hence, the construction does not have any details like how the brackets are fixed inside the pipe, or how the moulded parts and the reflector are assembled together.

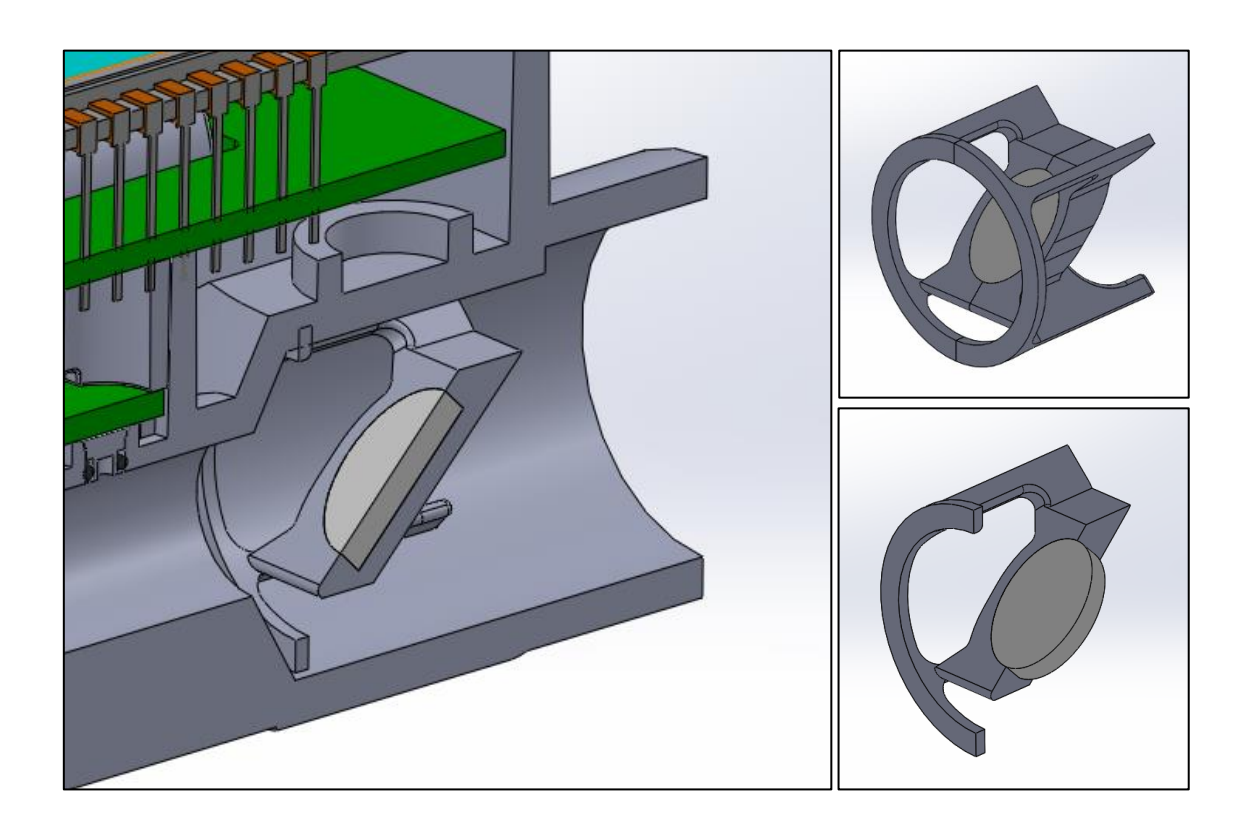


Figure 4.3 Discontinued alternative solution

4.2 Components of the second revision

4.2.1 Main enclosure bottom part

Figure 4.4 shows the modified enclosure bottom part with features that satisfy the design revisions. It has a wall thickness that deviates around 3,5 mm.

The design was also done by taking into consideration mould separating possibilities. It can be seen in figures 4.5 and 4.6 that it is possible for a two-part mould to separate and no surfaces are left out, with a total draft angle of 2 degrees (1 degree on each side). The splitting line is the border between red and green colours. An additional separation direction is along the longitudinal axis of the pipe and outwards from both sides to obtain the inner geometry of the pipe. The initial design was manufactured the same way, and samples were received without significant manufacturing defects. 5 holes for screw thread metal inserts are placed so that the one in the middle is pressing down on the middle two sockets and the other four are pressing down on the transducer assemblies. These four ports for metal inserts are placed as close to the transducer sockets as possible to reduce the amount of bending of the PCB that is caused by the vertical load from the transducer assembly. The steel inserts are not modelled because

it is enough to show their positions, thread pitch and depth in the technical drawings for the manufacturer.

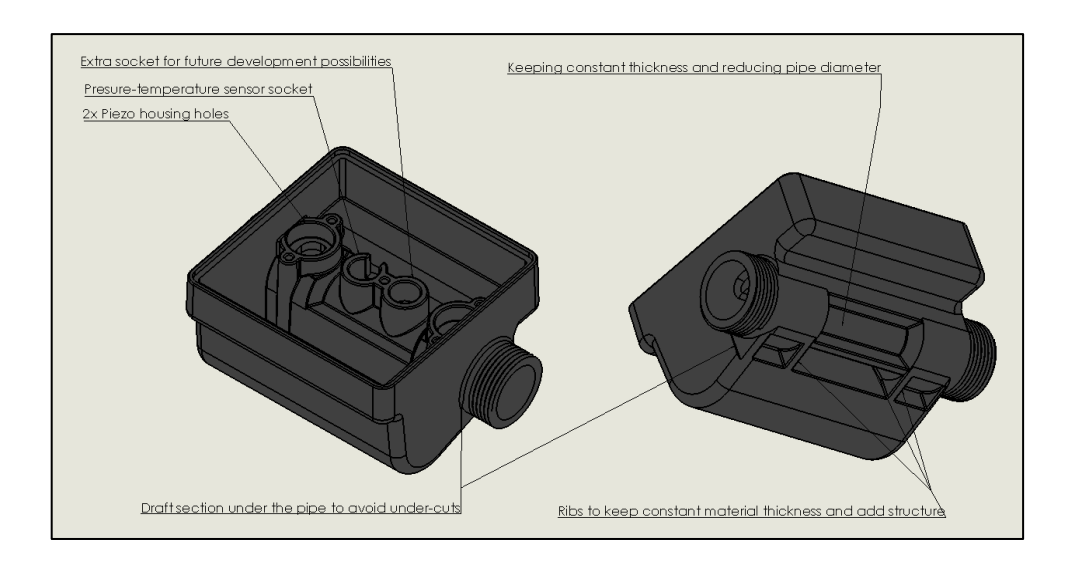


Figure 4.4 Second revision – enclosure bottom part features

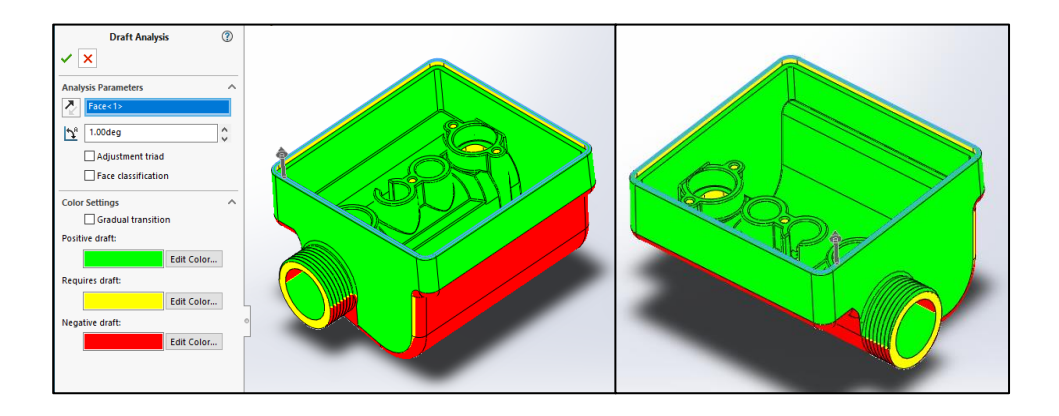


Figure 4.5 Second revision enclosure top side drafts

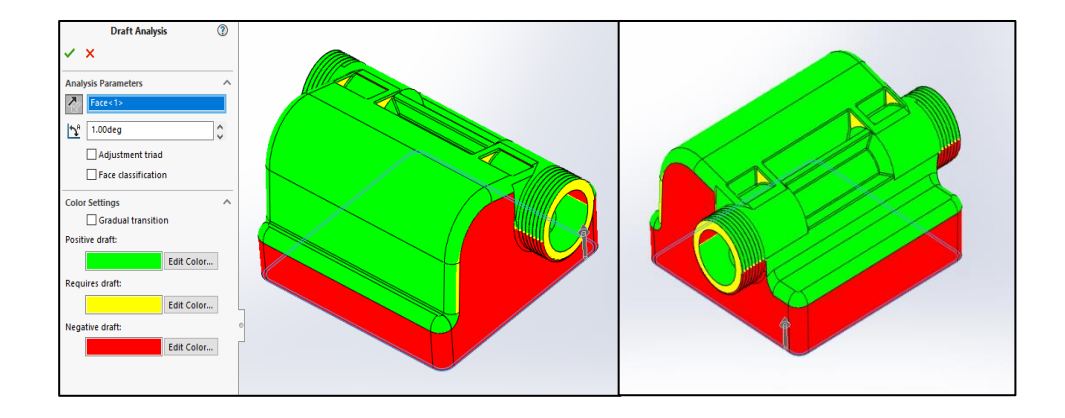


Figure 4.6 Second revision encosure bottom side drafts

4.2.2 Enclosure lid

The lid of the enclosure was determined by the employer to be a glass plate which will be cut using a .dxf type file that is exported from Solidworks. Reasons for changing the material and fixing method is to eliminate the need for screws and make the device more streamlined by assembling it with glue. A silk screen printing will be made so that it is not see-through except where the display is. It will then be possible to laser-engrave device specifications on the lid as required by the OIML standard.

4.2.3 Transducer assembly

The purpose of the piezo housing is to fix the piezo discs inside the pipe so that they are oriented to face directly at each other and protect the discs from direct contact with the fluid. Figure 4.7 shows the three components of the assembly.

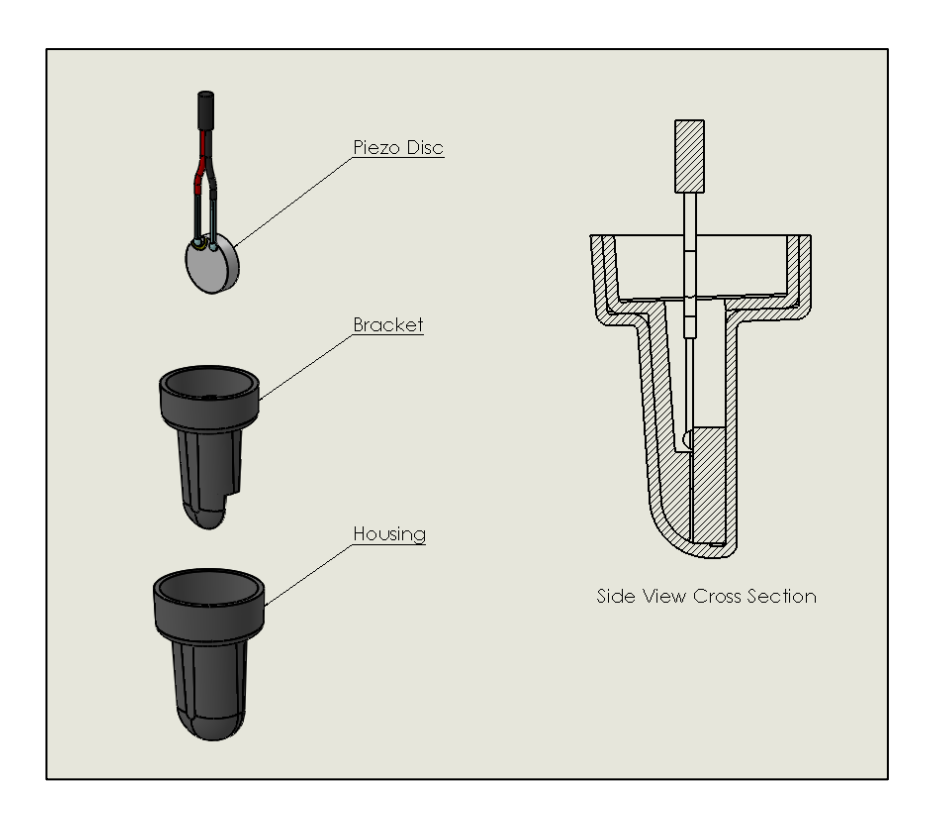


Figure 4.7 Second revision transducer assembly

The bracket and housing materials are also made from PPS-GF40 because of the low humidity absorption properties of the material. Making these parts from the same material should also reduce manufacturing costs compared to making them from completely different plastics. Mould designs that allow different material injections for different cavities are possible with special injection gate mechanisms, but this was assumed to be an extra design process for the manufacturer that costs time and

material. In addition to the benefits of the physical properties of PPS-GF40, it is easier for the manufacturer to include these smaller parts into the same mould as the main enclosure.

Due to the necessity of a draft angle on all plastic injection parts, complete vertical orientation of the piezo disc inside the pipe was not possible by simply mounting the transducer assembly on a horizontal surface. To compensate for this angle difference, the surface of the main enclosure where the transducers are mounted on are also slanted with the same draft angle. The surface of the piezo housing that has complete contact with the PCB was also designed to have an angle according to the mould splitting direction in order to enable complete contact with the PCB bottom surface. This can be seen in figure 4.2 where the contact surface of the transducer housing has an angle, but the piezo disc is completely vertical. This draft angle is also the main reason for the existence of the bracket, which is used as a wedge on the back side of the piezo disc to ensure that its front face is always in contact with the vertical inner face of the housing. Without this bracket, a solution to inserting a perfect cylinder (piezo disc) inside a drafted wall and keeping complete contact with all the faces was not found. The bracket also allows room for the solder points of wires and the wires themselves for the piezo discs. After the assembly of these three parts, the transducer assembly will be potted with epoxy. Finally, it can be seen from figures 4.8 and 4.9 that both the housing and the bracket can be manufactured as injection moulded plastics.

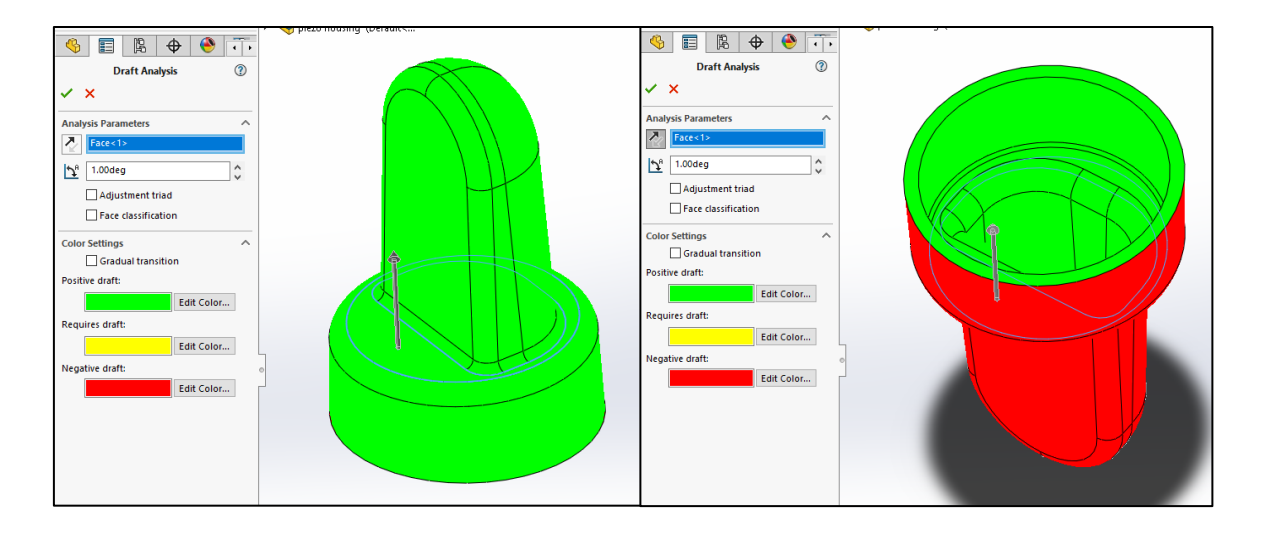


Figure 4.8 Second revision transducer assembly housing draft analysis

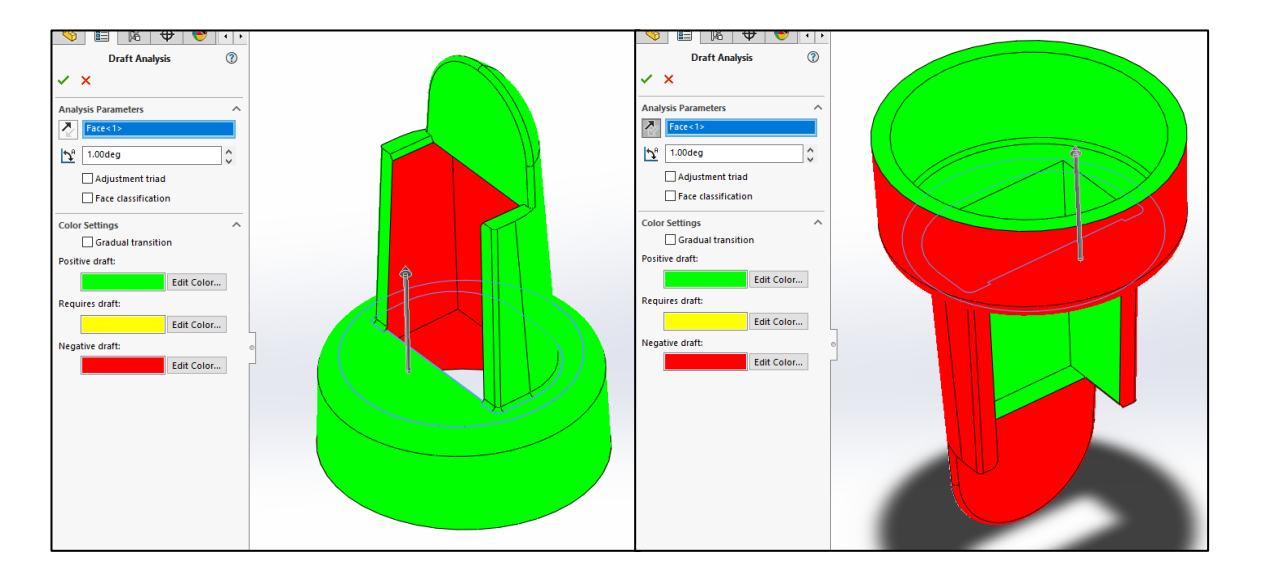


Figure 4.9 Second revision transducer assembly bracket draft analysis

4.2.4 PCB

The break-off PCB that was used for the pressure sensor, as well as the NFC tag were included in the main PCB as flexible extensions in order to simplify the assembly of the

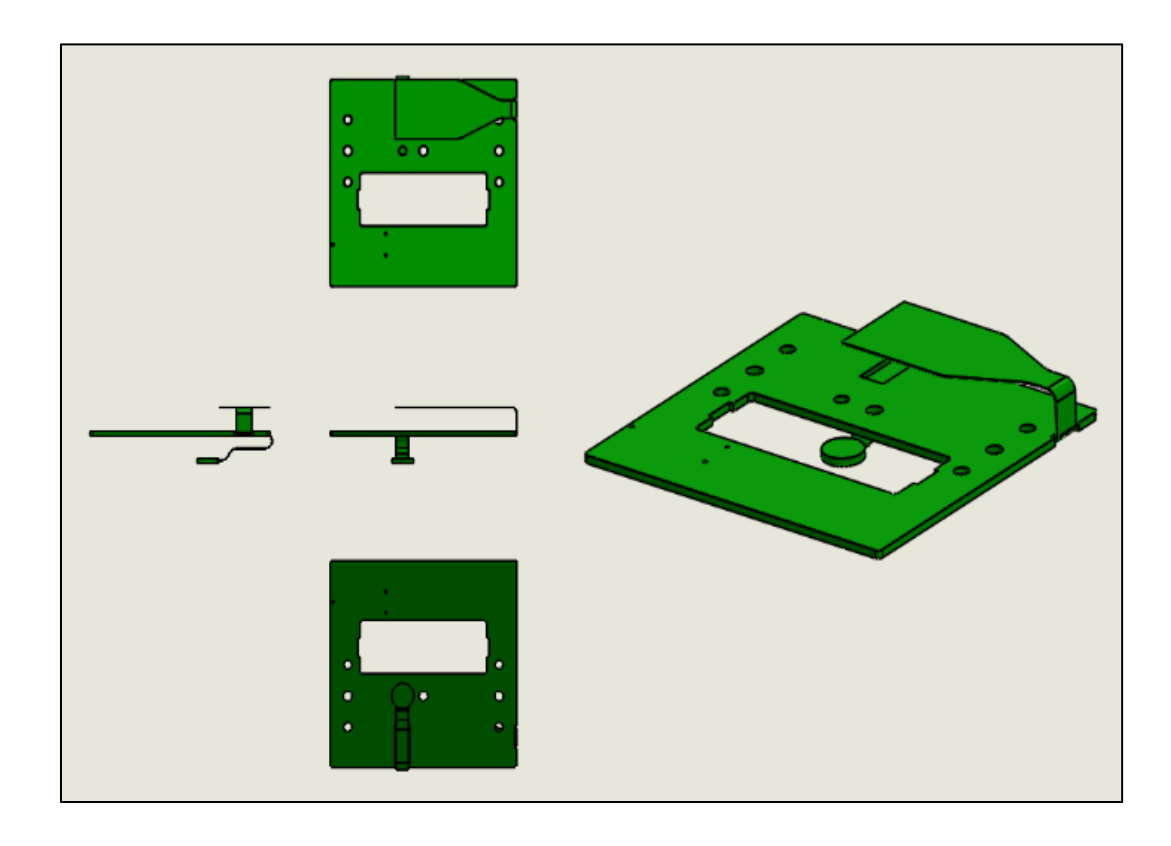


Figure 4.10 Several views of the PCB

product and eliminate extra components. These components are the NFC tag, the connector for the NFC tag, extra piece of PCB for the sensor and pins and headers for

the break-off PCB. This flexible extension possibility is known in the industry as rigidflex PCB. The output from the constructor for this part is a .dxf type file that has the drawing of the flattened PCB and lines where the thickness changes from 1,6 (main PCB thickness) and 0,2 mm (flexible part thickness). In order to make this output possible, the CAD model of the constructed PCB was designed with 3 bodies and converted to sheet metal so that it can be flattened for manufacturing. Several views of the PCB are shown in figure 4.10.

4.2.5 Fixing part for the extension PCB

This part was constructed so that the PCB can directly press down on the pressure sensor extension to fix it in place. There are no sealing elements like o-rings, but it will be potted with epoxy through the hole on the PCB that is made for this purpose (figure 4.11). It is made so that it has structure, but also has 6 openings on top and bottom so that epoxy can flow through and contact the inner wall of the socket.

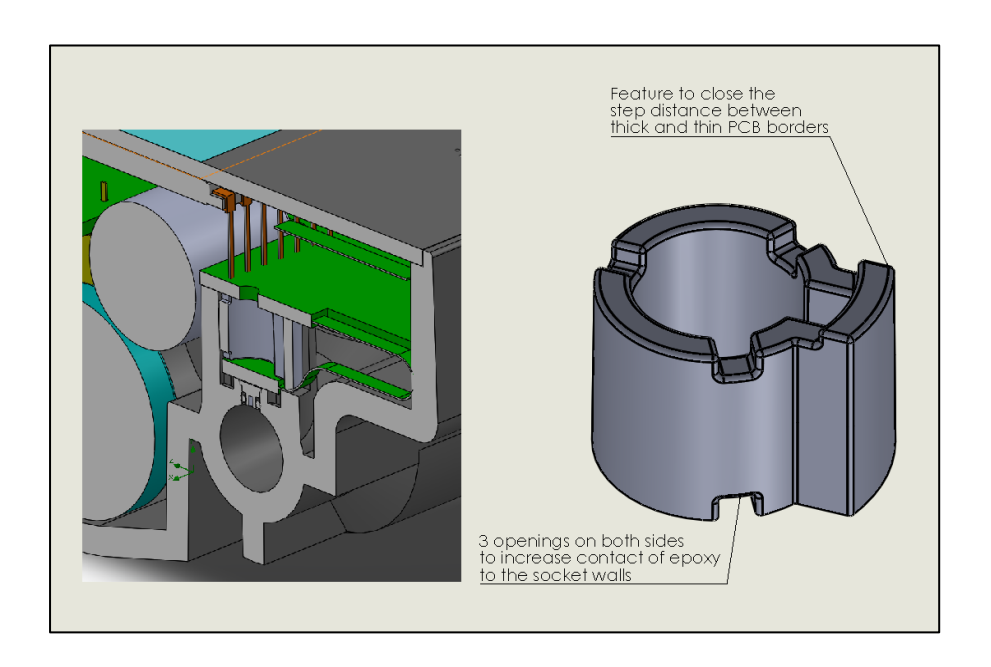


Figure 4.11 Second revision – part to press down on the extension PCB

4.3 Assembly

The device has the same battery group, but the display has been changed to BDT-M1008 and the screws that hold the PCB were changed to M3 screws. Overall dimensions of the second design are given in figure 4.12 and an exploded view is shown in figure 4.13.

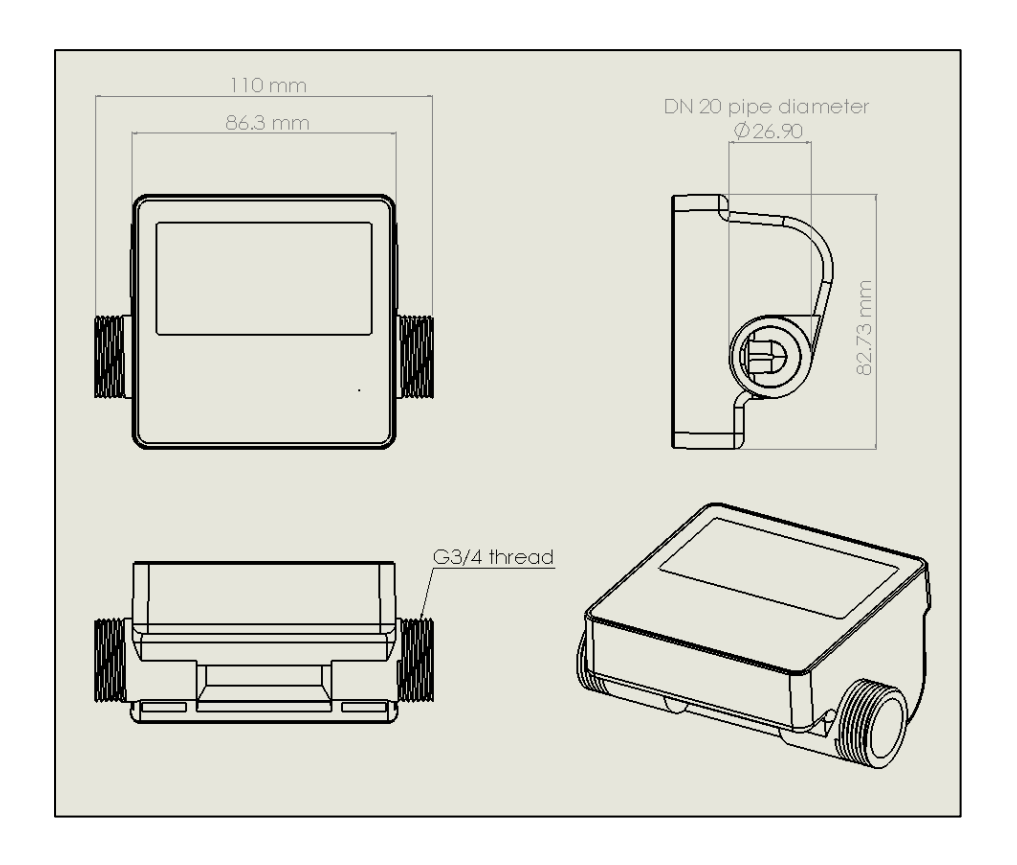


Figure 4.12 Second revision assembly – general dimensions

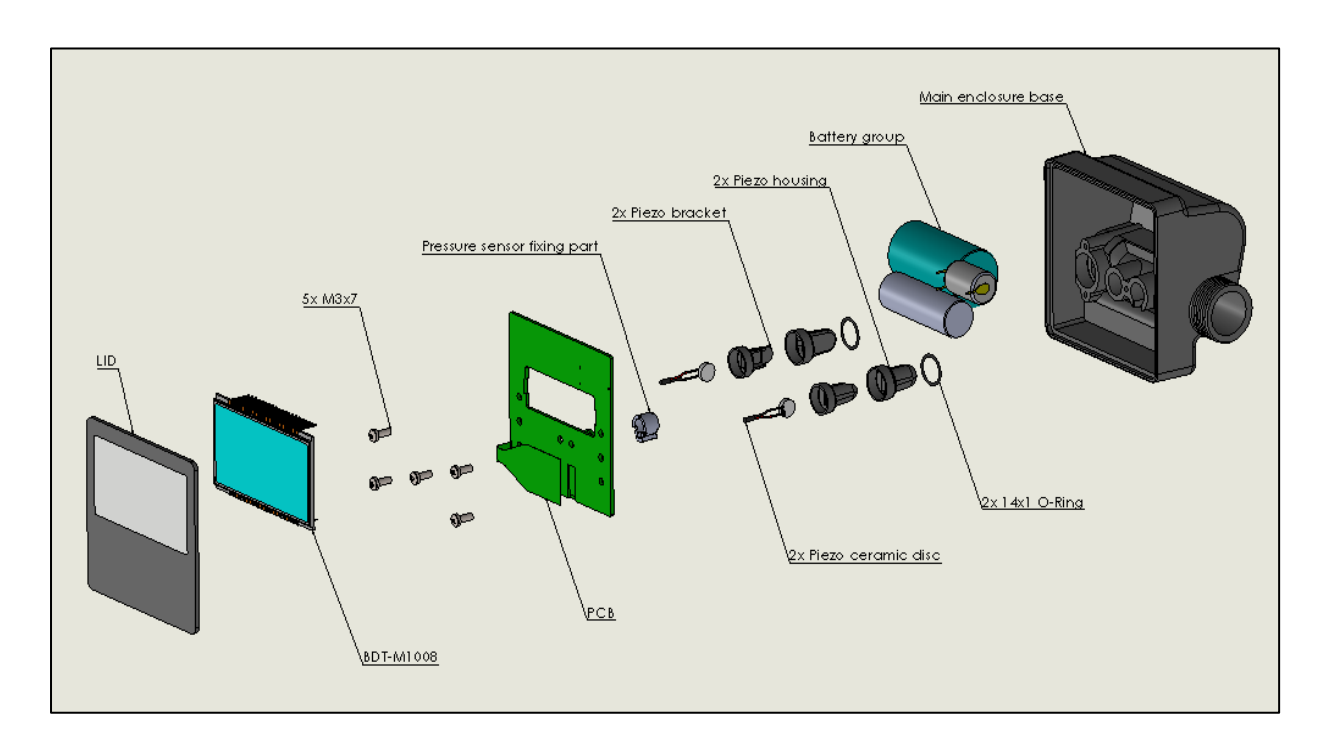


Figure 4.13 Second revision assembly - exploded view

4.4 Conclusions

The construction and the details of the components of a new design have been presented in this chapter, for a product that satisfies the second and third goals that

are given in section 2.4. Solutions to points i, ii, iii and v of the specified problems with the initial design in section 2.3, have been achieved.

The bought spool piece was eliminated to reduce cost and provide a new arrangement solution that has benefits such as better alignment of the signal and reduced uncertainties. Furthermore, a reduced pipe diameter in the measured section of the flow enables accuracy of measurement in lower flow rates and better contact of the pressure sensor to the flow which should improve accuracy.

5. FLOW SIMULATIONS

5.1 Definitions and motivation

Equation 2.5 works with the assumption that the flow field inside the pipe is uniform. The term uniform flow field means that the flow velocity is constant i.e independent of all space coordinates throughout the entire flow field [36] (figure 5.1).

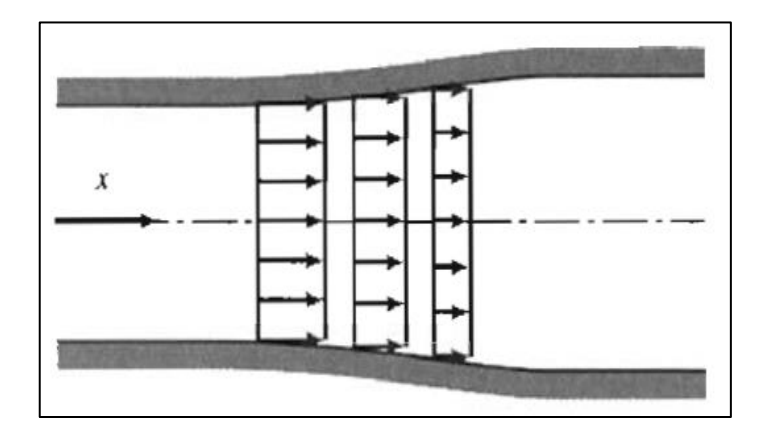


Figure 5.1 Uniform flow. Image taken from [36]

In practice, the points that are near the walls of the pipe move slower than the particles that are near the axis due to the viscosity of the fluid. This is called the no-slip condition, which means the particles that are on the walls do not travel at all. This leads to a flow profile where the middle section of the pipe has higher velocities (figure 5.2).

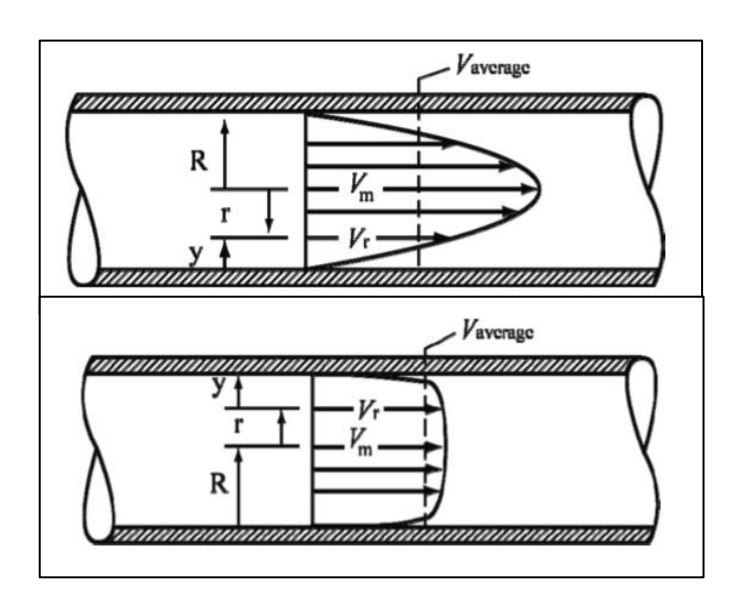


Figure 5.2 Laminar and turbulent flow profiles (image taken from [37])

This flow profile can be described mathematically depending on whether the flow is laminar or turbulent. These descriptions are called theoretical flow profiles [38, 1, 6, 15].

The theoretical velocity profile equation (equation 5.1) describes the distribution of velocity in the flow [11, 39, 13, 1].

If the flow is
$$v = v_m \left(1 - \frac{r^2}{Re^2}\right)$$
 (5.1) If the flow is
$$v = v_m \left(1 - \frac{r}{Re^2}\right)^n$$

where v_m – maximum velocity in the flow, m/s,

r – distance of that point to the flow axis (effective radius), m,

Re – unitless Reynolds number

n – empirical unitless variable dependent on the Reynolds number

It was seen from [14, 1] that the accuracy of ultrasonic flowmeters is affected by the velocity profile and correction factors can be applied to the measurement based on the value of the Reynolds number. For example, in [1] the correction factors are derived by comparing the results of transit time equation assuming uniform flow, to the derivation of the same equation using velocity profiles that depend on the Reynolds number. The resulting correction factor is given with the relation

$$O = k_t O_0 (5.2)$$

where Q – real flow rate, m^3/h ,

 Q_0 – reading flow rate, m³/h,

 k_t – correction factor

For laminar flows, k_t is a constant 0,75. For turbulent flows it depends on the Re number. The relation between the Reynolds number and the correction factor is given in figure 5.3.

In the same publication, the relative error between theoretical calculations and experimental results are 0,976 % for laminar flow and 0,25% for turbulent flow. These are small errors and it shows that the calculated correction factor is very close to practical applications.

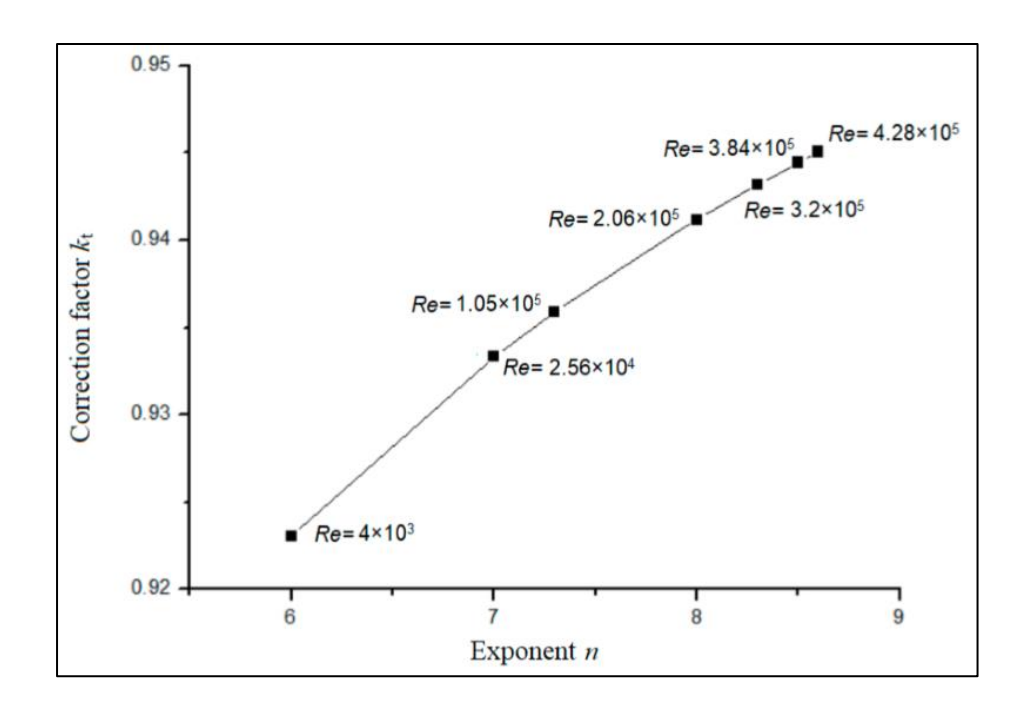


Figure 5.3 Effect of Re to the correction factor. Image taken from [1]

5.1.1 Relation between flow regimes and Re number

The flow of water in a pipe is characterized as laminar flow, transitional flow and turbulent flow [38, 36, 40, 41]. Laminar flow is when all particle trajectories are straight lines that are parallel to the flow direction and turbulent flow describes the state of flow when the particle trajectories have chaotic components. This means that the particle trajectories have components that are randomly fluctuating (5.4). Transitional flow is the flow regime that is between laminar and turbulent.

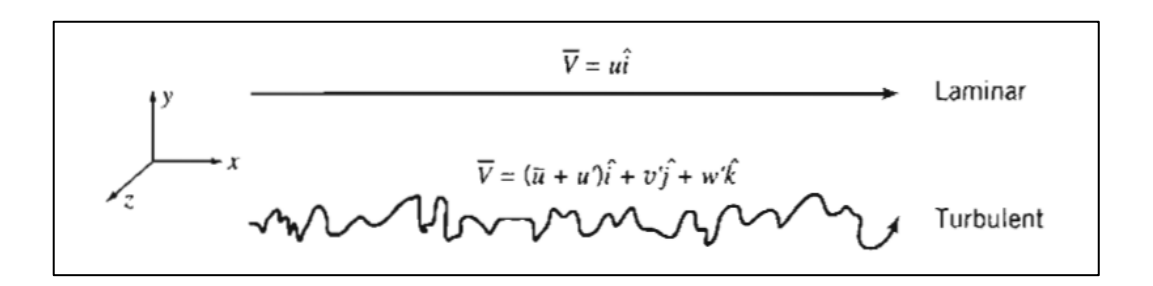


Figure 5.4 Laminar and turbulent flow particle trajectories (image taken from [36])

These movement behaviours of particles in the flow are a result of the viscosity of the fluid and are identified by computing the Re number of the flow. The Reynolds number is a unitless value that is calculated with equation 5.3.

$$Re = \frac{vd}{v_k} \tag{5.3}$$

where v – average velocity of the fluid, m/s,

d - diameter of the pipe, m,

 v_k – kinematic viscosity of the fluid, m²/s

Kinematic viscosity is a property of the fluid that depends on the density and dynamic viscosity as shown in equation 5.4.

$$v_k = \frac{\mu}{\rho} \tag{5.4}$$

where μ - dynamic viscosity, Ns/m²,

 ρ - density of the fluid, kg/m³,

Using equation 5.4, Equation 5.3 can also be written in the form of equation 5.5.

$$R_e = \frac{vd\rho}{\mu} \tag{5.5}$$

The viscosity of water changes significantly depending on the temperature of the fluid. It can be seen in table 5.1 that the dynamic viscosity is $0,404.10^{-3}$ [Ns/m²] at the maximum working temperature and $1,787.10^3$ [Ns/m²] at 0 °C.

Although there are small deviations in literature about what ranges of the Reynolds number correspond to which characteristic, it is generally written that in practice the flow inside a pipe is laminar when Re is less than 2300; transitional when it is between 2300 and 4000; turbulent for values greater than 4000 [39].

As shown in equation 5.5 and table 5.1, the Reynolds number depends on the average velocity of the fluid, the cross-sectional diameter of the pipe and the temperature of the fluid (which determines the viscosity). The aim of increasing the accuracy of the design can be achieved by applying the corresponding correction factors to the measurement, depending on the state of the fluid passing through the device at that instant. The assumption was that the device can sense the current physical states of the fluid and correct itself automatically.

Table 5.1 Dynamic and kinematic viscosity according to temperature (taken from [42])

Temperature - t - (°C)	Dynamic Viscosity - μ - (N s/m2) x 10-3	Kinematic Viscosity -v - (m2/s) x 10-6	
0	1.787	1.787	
5	1.519	1.519	
10	1.307	1.307	
20	1.002	1.004	
30	0.798	0.801	
40	0.653	0.658	
50	0.547	0.553	
60	0.467	0.475	
70	0.404	0.413	
80	0.355	0.365	
90	0.315	0.326	
100	0.282	0.294	

5.2 Simulations

The flow simulation environment in Solidworks (formerly called FloXpress and Flow Simulation in later versions) makes mesh calculations for fluids that are flowing around or through (called external or internal flow respectively) a 3D model and gives predictions about the physical properties of that fluid during the flow at chosen points, surfaces or volumes. The results depend on the model geometry and the input parameters that describe the properties of the fluid that is entering or exiting the system and the material of the solid model parts. For the scope of this thesis, the simulations were set up and carried out by implementing the instructions at the help facility of Solidworks.

This chapter documents the work on flow simulation in three parts. Item 5.2.1 provides an explanation to how the program is set up. An analysis of laminar and turbulent flow is carried out to observe the effect of flow rate and temperature to the velocity profile.

In Item 5.2.2, a set of *Re* numbers are simulated for a range of volume flow and temperature with the parametric simulation facility, in order to provide information to the employer, which will help in increasing the accuracy of the device.

Item 5.2.3 is the documentation of a parametric simulation in order to show how the pressure drop changes with respect to changing total pressure and volumetric flow rate and constant temperature. Developers in the company who will design the software and electronics for the device will use this information to program and calibrate the device.

5.2.1 Initial simulation and velocity profile analysis

There are several ways of how to set up a simulation. "Flow Simulation" add-in is activated in the assembly model file. The project wizard can be chosen by pressing "Wizard" in the upper left corner of the simulation window, and the program guides the user by presenting selection windows for necessary settings for a new project. Another way is to simply choose "New" from the upper left corner of the simulation window, which creates a new project and parameters can be manually defined after that. The settings can also be changed after using the wizard.

The ends of the pipe must be shut off with solid parts to create the internal volume that the fluid will be defined in. These can be manually constructed or automatically generated by the "Create Lids" button inside the simulation environment. This feature enables the user to simply choose the surfaces where the lids are supposed to be and a selection for the thickness of the caps. The cap thickness was left as default thickness value of the program, which was less than 1 mm (figure 5.5).

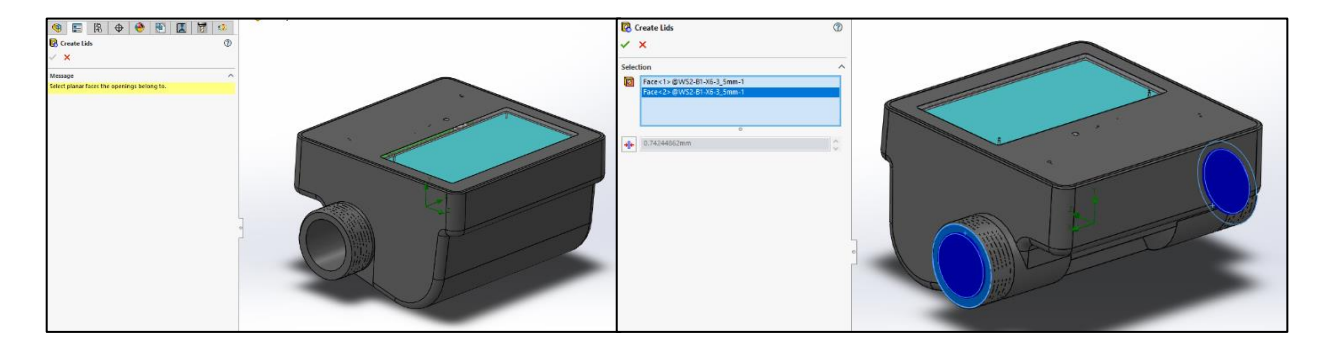


Figure 5.5 Creating lids for the flow simulation

The model must also be prepared by extruding features to cover up surfaces that do not have full contact with other parts. In this model, these were the surfaces between

the transducer o-rings and the enclosure. Without these extrusions that create interference in the assembly model, the program did not recognize the closed volume of the pipe as a separate subdomain.

Internal volumes can be selected individually by right-clicking "Fluid Subdomains" from the project tree and inserting a new selection (figure 5.6).

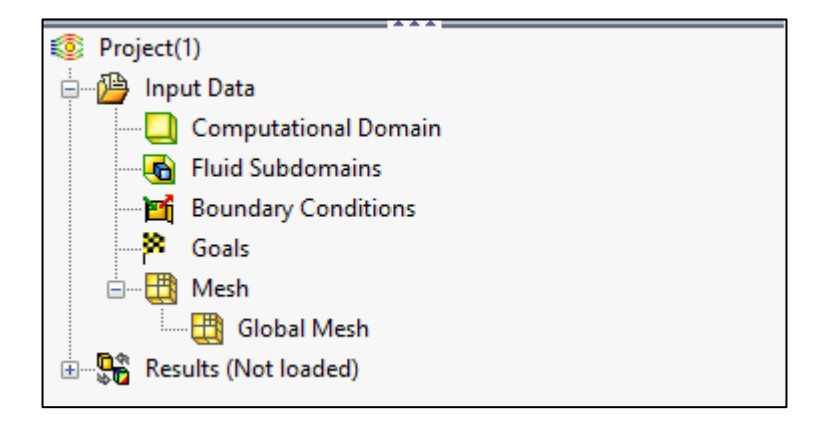


Figure 5.6 Project tree in the flow simulation environment

From there, the type of fluid, the flow parameters, thermodynamic properties, turbulence properties and flow characteristics of the fluid can also be specified (figure 5.7). In this selection, water was chosen as the liquid type and other parameters were left as default. Changing the values of the temperature and pressure at this stage did not seem to have a significant effect on the result. For example, it was seen that the resulting maximum and minimum temperatures were the same when simulation parameters were changed in the fluid sub-domain selection.

The physical properties of the fluid are determined by setting boundary conditions on the model. These describe the inlet or outlet flow amounts (flux, flow or velocity), pressure openings and walls. The flow can be described by having one pressure opening and one flow opening.

Defining these conditions is enough to run the simulation because other settings like material selection and wall properties are automatically set to default by the program. The results are visualized by using several plotting tools of the Flow Simulation environment.

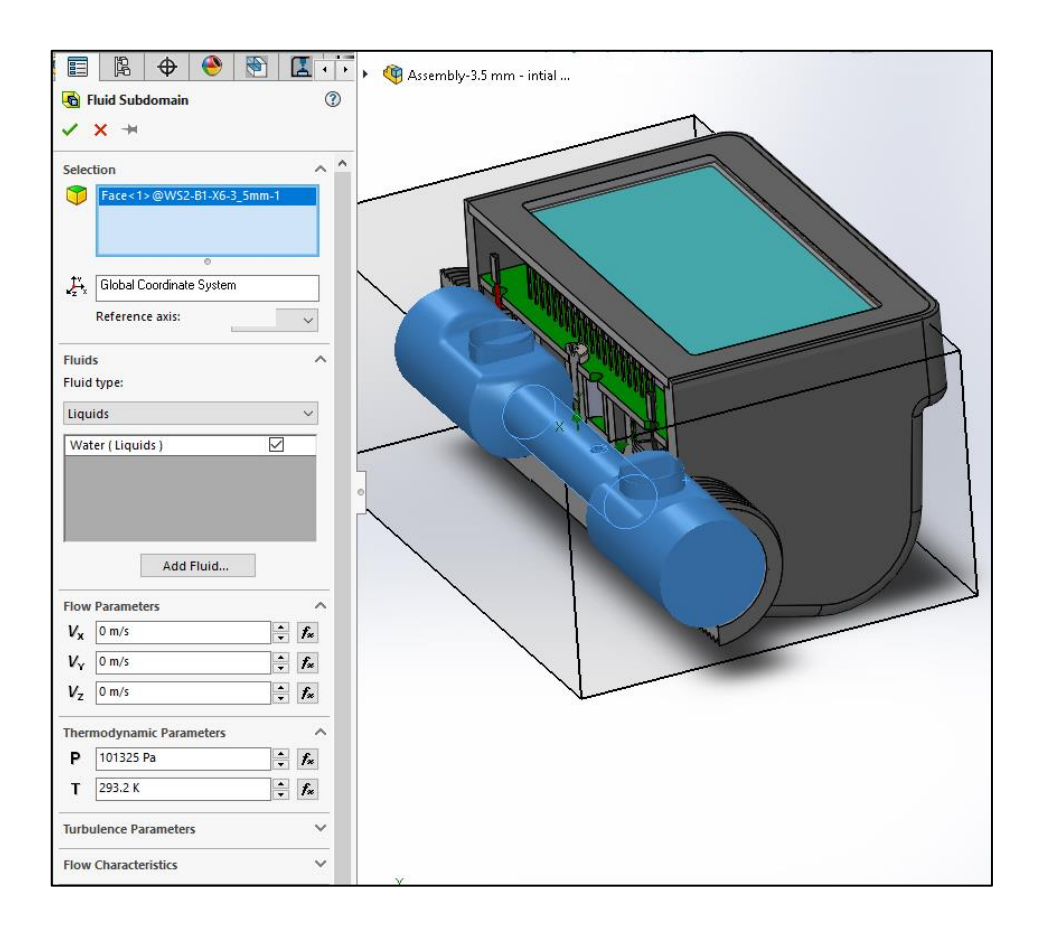


Figure 5.7 Specification of the fluid sub-domain

The boundary conditions for this simulation were set by right-clicking the "Boundary Conditions" selection and inserting two separate boundary conditions. The first is the pressure boundary (figure 5.8). This boundary condition defines the pressure and temperature of the liquid. This was set as a total pressure on one end of the pipe (the inside surface of the lid) and the temperature is set to the desired fluid temperature in the "Thermodynamic Parameters" selection. Other settings were left as default (figure 5.8). The volumetric flow rate was defined as outlet volume flow (figure 5.9).

The last step is to go over the general settings of the "Input Data" (figure 5.6) to specify the solid materials and the computational domain of the simulation. The computational domain is the specification of which part of the model will be included in the simulation. The general settings are accessed by the "General Settings" button in the Flow Simulation menu or right clicking 'Input Data' and selecting it from there.

In the "Analysis type" setting, the "Heat conduction in solids" check box was activated in order to include the material properties of the enclosure (figure 5.10) to the calculation.

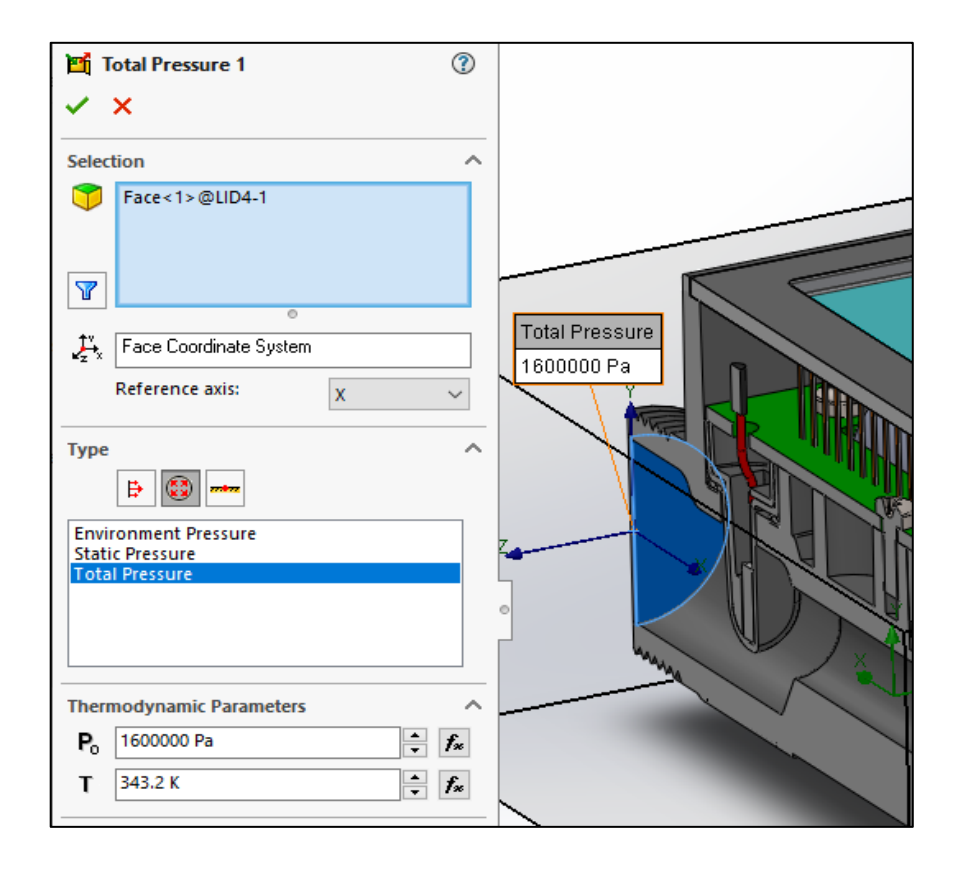


Figure 5.8 Defining the pressure boundary condition

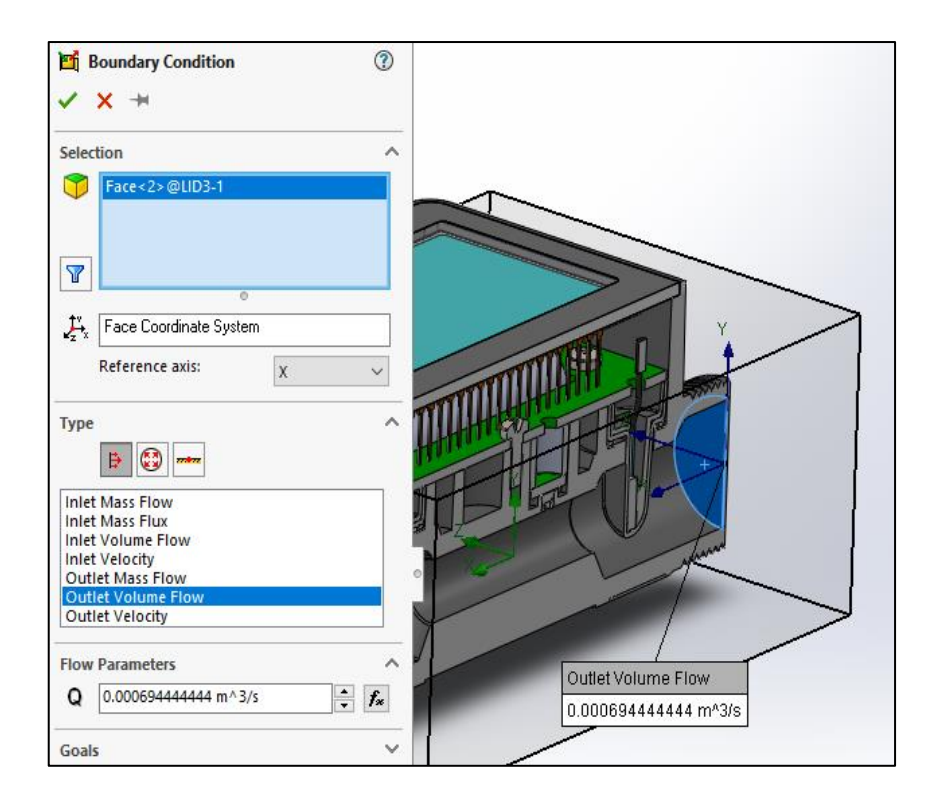


Figure 5.9 Defining the outlet volume flow boundary condition

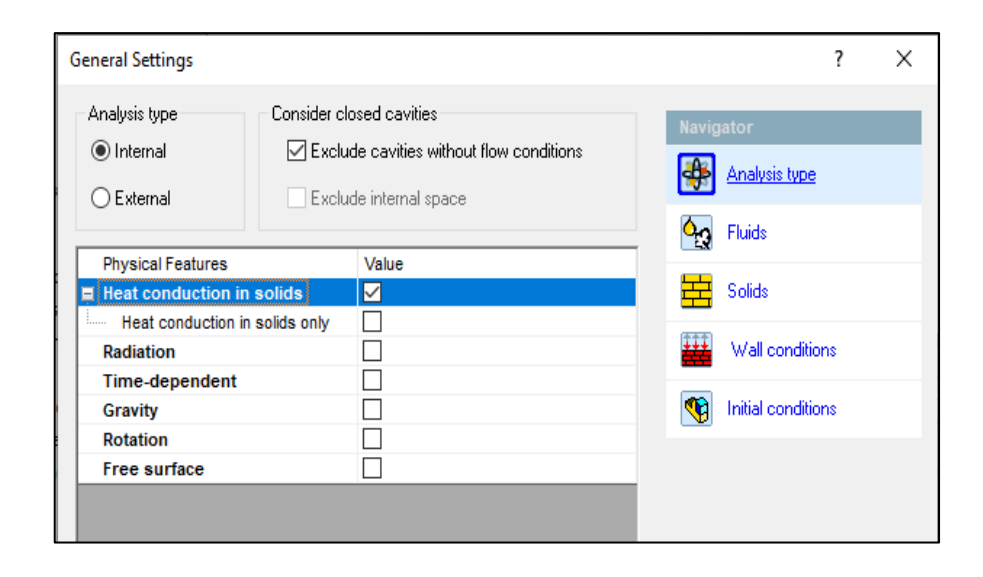


Figure 5.10 General settings - Analysis type

By default, the computational domain only appears around the where the fluid sub domain is previously defined (figure 5.11).

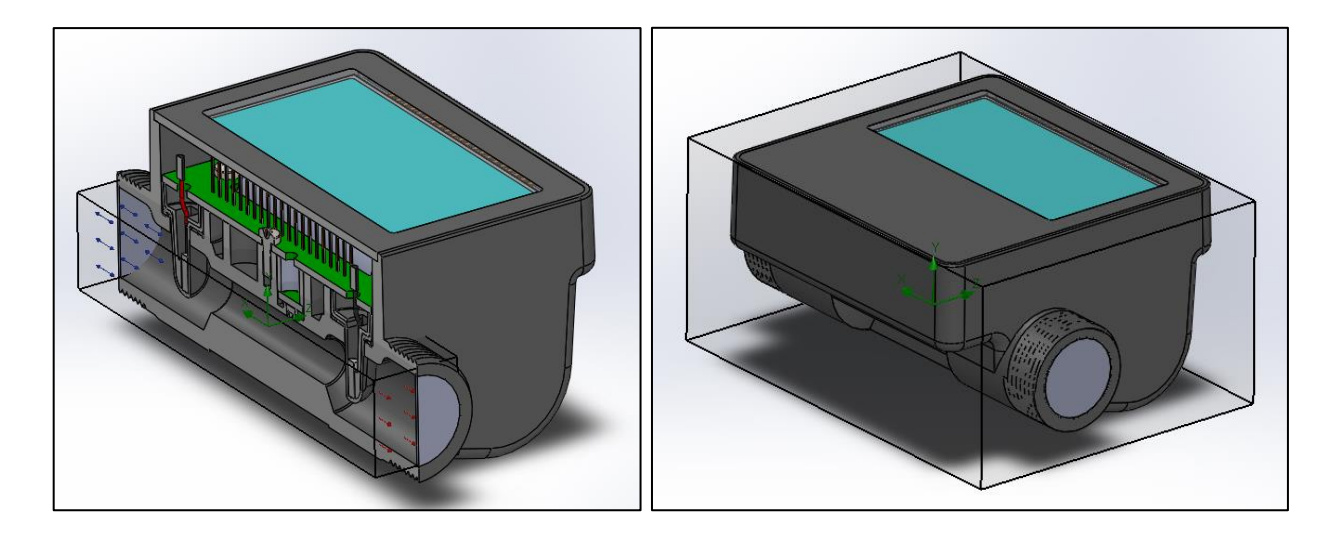
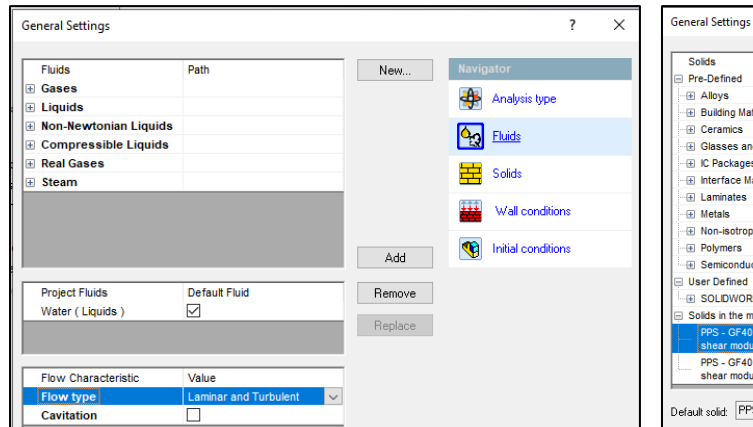


Figure 5.11 Computational domains. The first image is shown in cross section view to make the computational domain more visible. The first image is default; the second is with the selection of 'Heat conduction in solids' option in general settings

The type of liquid is defined as water in the "Fluids" setting (figure 5.12). Possible effects of the chemical substances in domestic water use were neglected for simplicity. Other settings like "Flow type" and "Cavitation" were left as default.

The material PPS-GF40, that was defined in chapter 3 is chosen from the "Solids" selection (figure 5.13). This will add accuracy to the representation of heat transfer between the fluid and its surroundings, since the custom physical properties of the

material include heat related properties like thermal expansion coefficient, thermal conductivity and specific heat. For the same reason, the outer wall thermal condition selection was changed from "adiabatic" to room temperature in the "Wall conditions" setting (figure 5.14). The initial conditions were left as default (figure 5.15).



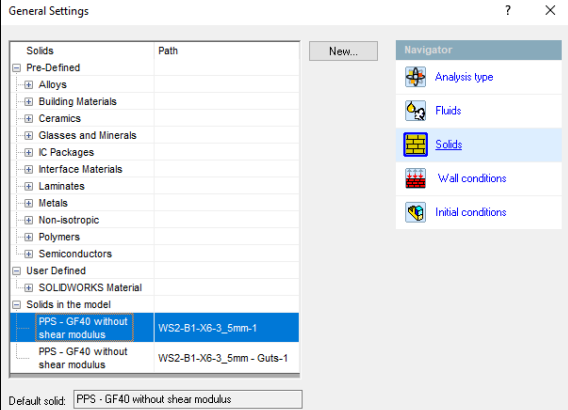


Figure 5.12 General settings- Fluids

Figure 5.13 General setting - Solids



Figure 5.14 General settings- Wall conditions

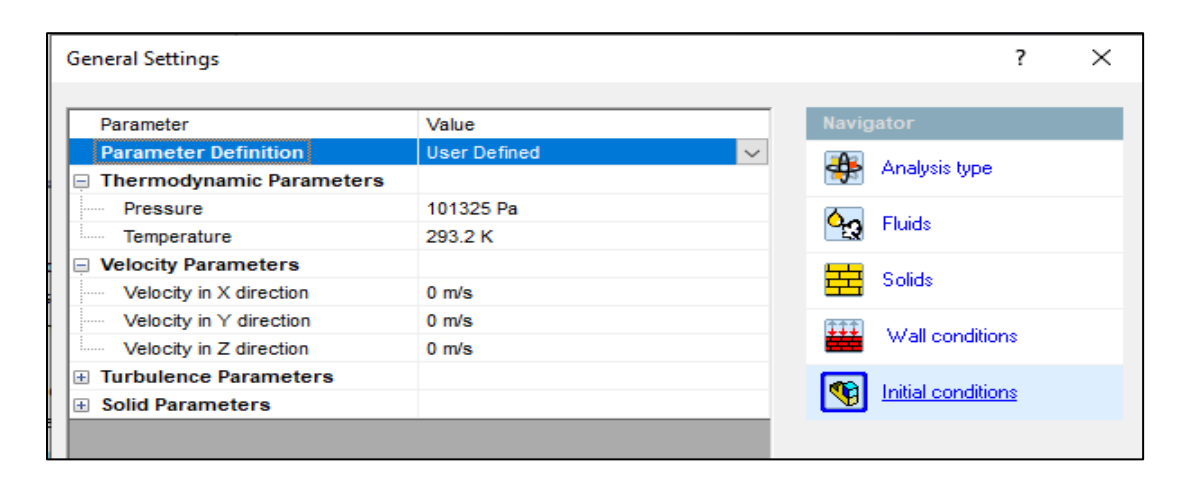


Figure 5.15 General settings- Initial conditions

Calculation of laminar velocity:

Equation 5.5 shows that in order to achieve lower Reynolds numbers, the average velocity must decrease, and the dynamic viscosity should increase. From table 5.1, 5 °C was chosen as a low temperature that has high viscosity. For this temperature, the necessary inflow rate to make the Reynolds number 2300 can be calculated, because the velocity and inflow rate are related.

Plugging equation 4.3 into equation 5.5 and solving for *Q*:

$$Q = \frac{\pi d^2}{4} \cdot \frac{R_e \mu}{d\rho} = \frac{R_e \mu \pi d}{4\rho}$$

$$Q = \frac{2300.1,519.10^{-3} \cdot \pi \cdot 1 \cdot 10^{-2}}{4.1000} \left[\frac{\binom{Ns}{m^2} \cdot m}{kg} \right]$$

$$= 2,872.10^{-5} \frac{m^3}{s} = 0,103 \frac{m^3}{h}$$
(5.6)

There should be laminar flow for volumetric flow rates lower than this value at 5 $^{\circ}$ C. Therefore, a flow rate of 0,1 m³/h was chosen. According to [4], water consumption in recent purifiers installed in many homes is between 0,06 and 0,12 m³/h, so the chosen value corresponds to an upper limit of practical situations.

The second simulation is made with values that should make the flow as turbulent as possible in order to provide contrast, so that the change in results can be clearly observed. The flow rate was set as $2.5 \text{ m}^3/\text{h}$ and the temperature of the fluid was set as $70 \, ^{\circ}\text{C}$ in the second simulation, which are limit values of the operating range.

Results of the initial simulations for velocity profile:

Two plots are made for each simulation by right clicking and inserting "Cut Plot" from the results section of the project tree. One is on a perpendicular plane that coincides with the axis of the pipe and is parallel to the direction of flow and "turbulence length [m]" is chosen from the drop-down menu as the plot value. Contours are selected as visual preference. The other is on a plane that coincides with the middle point of the pipe and is perpendicular to the flow. In the second plot, velocity in the direction of the

flow (the x axis in this case) is chosen and only contours are enabled for visual preference.

The exported results of the first plots for turbulence length are shown in figure 5.16. It can be seen that the amount of turbulence is more in the simulation that has higher temperatures and flow rate. The second plots for fluid velocity that is parallel to the pipe axis are given in figure 5.17.

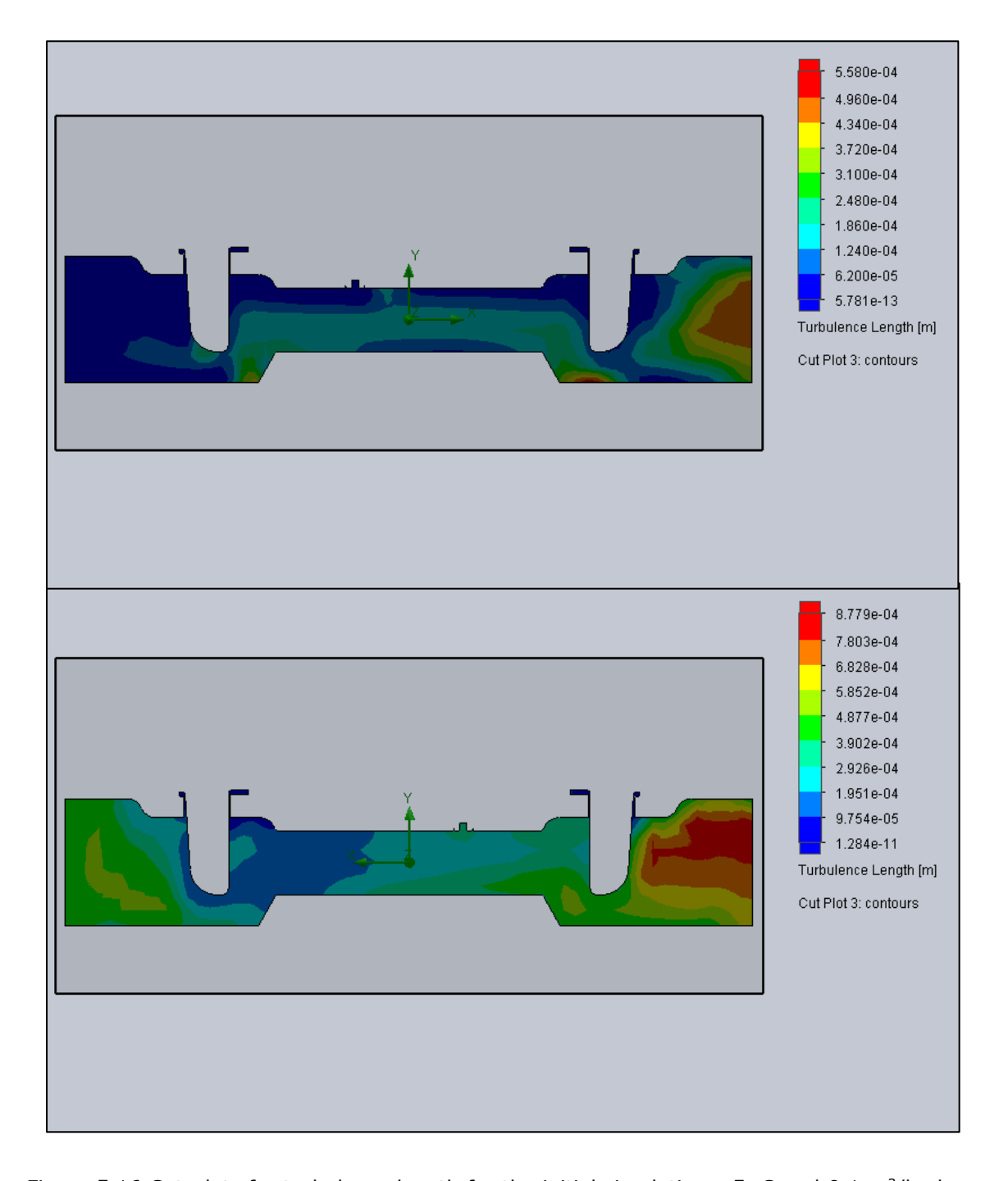


Figure 5.16 Cut-plots for turbulence length for the initial simulations. 5 $^{\circ}$ C and 0,1 3 /h above and 70 $^{\circ}$ C and 2,5 3 /h

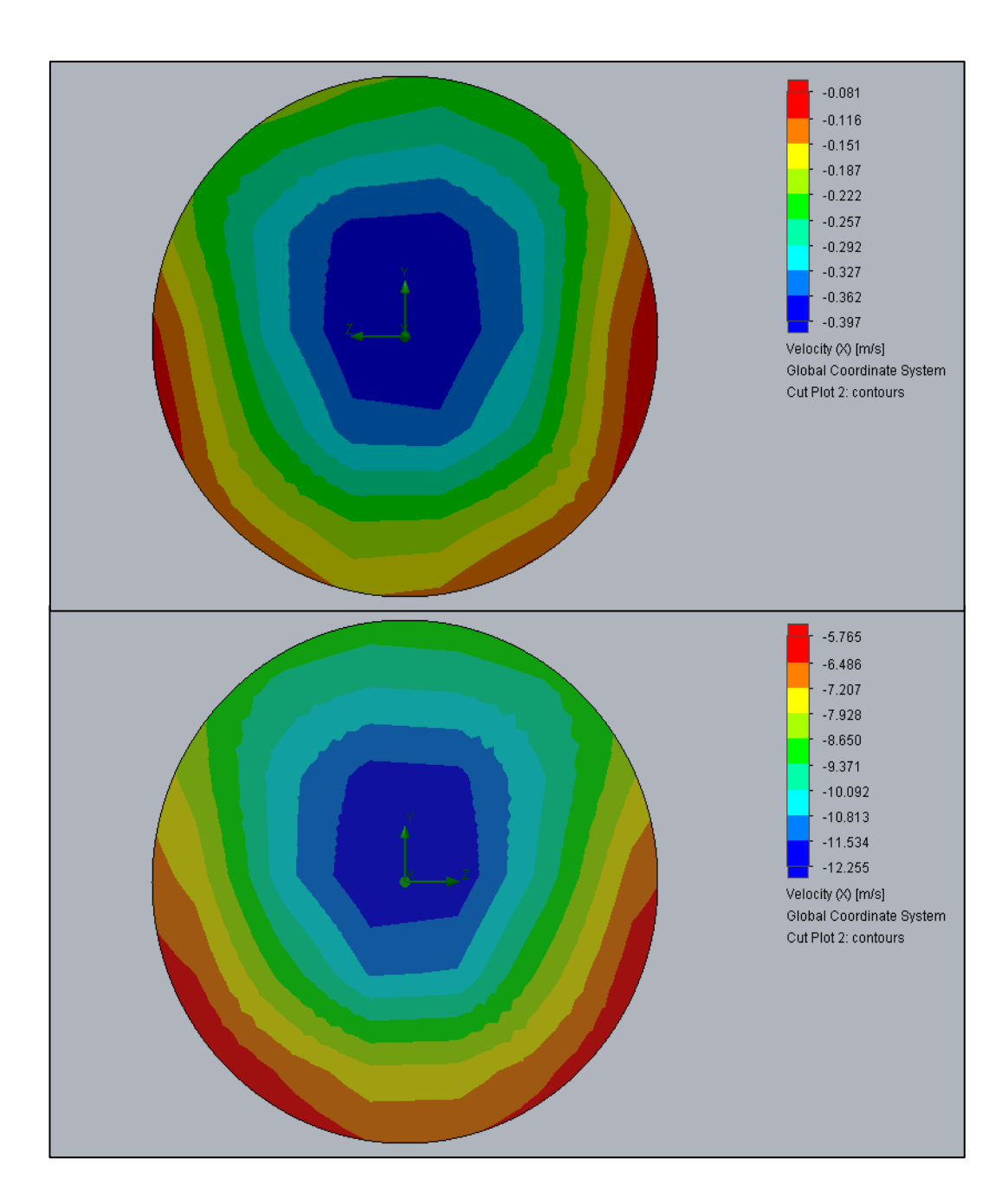


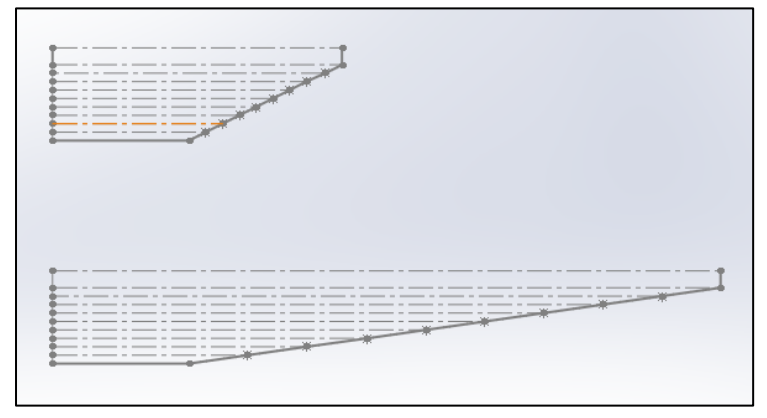
Figure 5.17 Cut-plots for fluid velocity inside the 10 mm diameter pipe section. 5 $^{\circ}$ C and 0,1 $^{\circ}$ A above and 70 $^{\circ}$ C and 2,5 $^{\circ}$ A

The interpretation of the velocity plots shown in figure 5.17 were done with Microsoft Excel in order to validate that these velocities show characteristics that are compatible with typical velocity profiles of laminar and turbulent flow. The distributions of the contours are similar in figure 5.17 between the two plots but the ratio of maximum and minimum values of the velocities are different. In order to roughly visualize the velocity profiles, the 10 values in the legends of both simulation results were entered to an Excel file and the minimum values were normalized according to the minimum length to achieve a comparative scale (figure 5.18). These values were then entered into a sketch

as line lengths. The parallel distance between the lines are equal. The vertical line that creates the middle section is also equal. The ends of the lines were connected with a spline which was revolved around an axis as a surface (figure 5.19).

Low flow rate	High flow rate	High flow rate normalized	
81	5765.00	80.99825	0.01409
116	6486.00	91.1283	
151	7207.00	101.25835	
187	7928.00	111.3884	
222	8650.00	121.5325	
257	9371.00	131.66255	
292	10092.00	141.7926	
327	10813.00	151.92265	
362	11534.00	162.0527	
397	12255.00	172.18275	

Figure 5.18 Normalizing minimum values for obtaining a scale between two simulation results. The number 0,01405 on the top right is the factor that all high flow rate values are multiplied with. It is 81/5765 (minimum values of both sets)



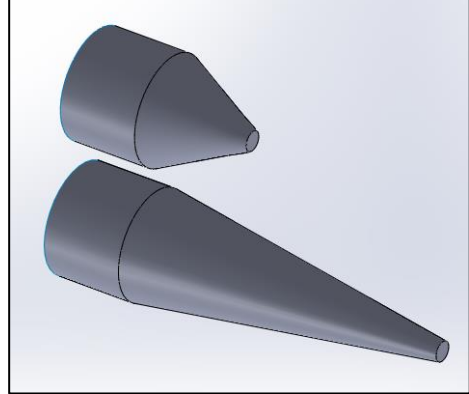


Figure 5.19 Visualization of the high temperature and flow rate flow (above) and low temperature and flow rate (below)

Although this is a rather low-resolution representation of the velocity profiles, the low flow rate simulation produced a shape that is gradually elongated compared to the blunt shape of the turbulent high flow rate result. These shapes comply with the characteristic flow profiles of laminar and turbulent flow in figure 5.2.

It was concluded that the simulations produce meaningful results with this set-up configuration. Laminar and turbulent flow were observed with predicted flow rates.

5.2.2 Parametric calculation of the Reynolds number for a range of variables

A parametric study is made in the flow simulation environment for 10 values of volumetric flow rates, ranging from 0 to 2,5 m 3 /h and 10 values for temperature, ranging from 5 $^{\circ}$ C to 70 $^{\circ}$ C. As a result, a set of 100 Re numbers are obtained for each flow rate-temperature configuration.

A tool that simply gives the Reynolds number at a specified geometry was not found. The solution is to calculate it using Goals (figure 5.6). Goals are defined before running the simulation and are used to extract desired data from global results or from specified geometry in the simulation model. These geometries can be points, surfaces or volumes. For example, average temperature in a volume, minimum pressure on a surface, velocity at a point etc. They can also be equation goals. Equation goals are manually defined equations that use other determined goals as input variables.

The approach is to obtain the dependencies of the Reynolds number at a cross-section of the pipe and use these values in an equation goal that computes it. These variables are the average velocity of the fluid, the dynamic viscosity and the density. A goal for kinematic viscosity was not found in the parameter list of Solidworks, so dynamic viscosity and density were used instead.

In order to obtain these values from a cross-section of the pipe, a surface needs to be defined. This is done by constructing a thin plate component that has a perpendicular surface that intersects the middle point of the pipe (figure 5.20).

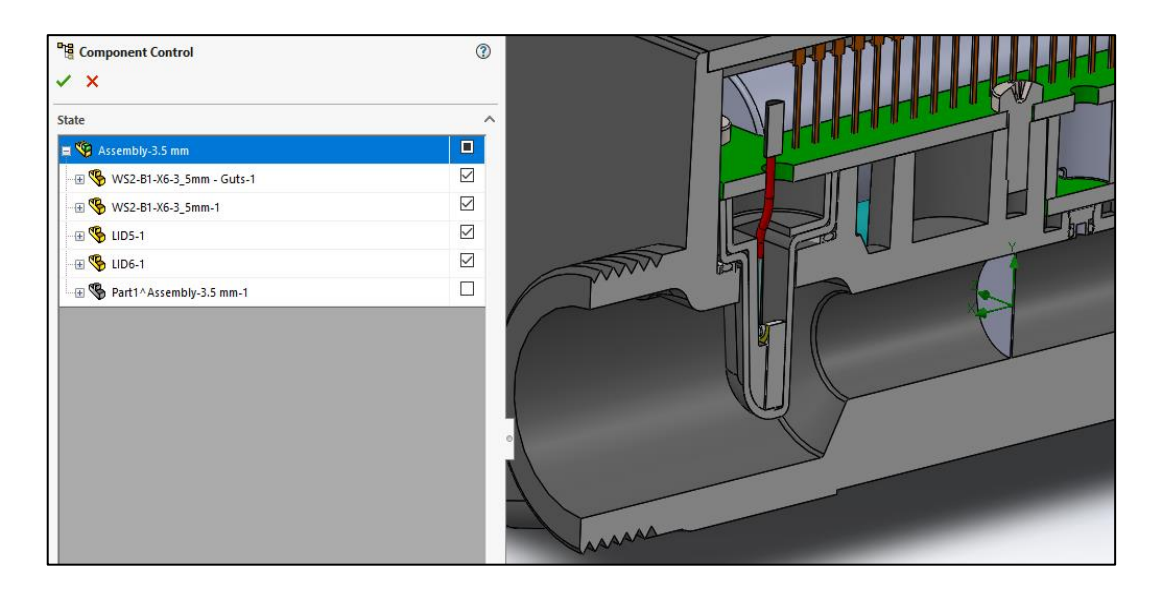


Figure 5.20 Disabling the surface plate from the simulation

However, this part is only used for its surface and would obstruct the flow in the simulation. Therefore, it needs to be excluded from the simulation by right clicking "Input Data" and selecting "Component Control" and disabling it from the component list in the assembly (figure 5.20).

Goals are inserted by right clicking "Goals" in the Input data window, choosing the face and choosing the value to be obtained from the drop-down Parameter list (figure 5.21). The Equation Goal to calculate the Reynolds number can be seen in figure 5.22. The variables can be inserted by simply clicking on the defined goal in the Goals list. The diameter of the pipe was manually entered into the equation as 0,01 m.

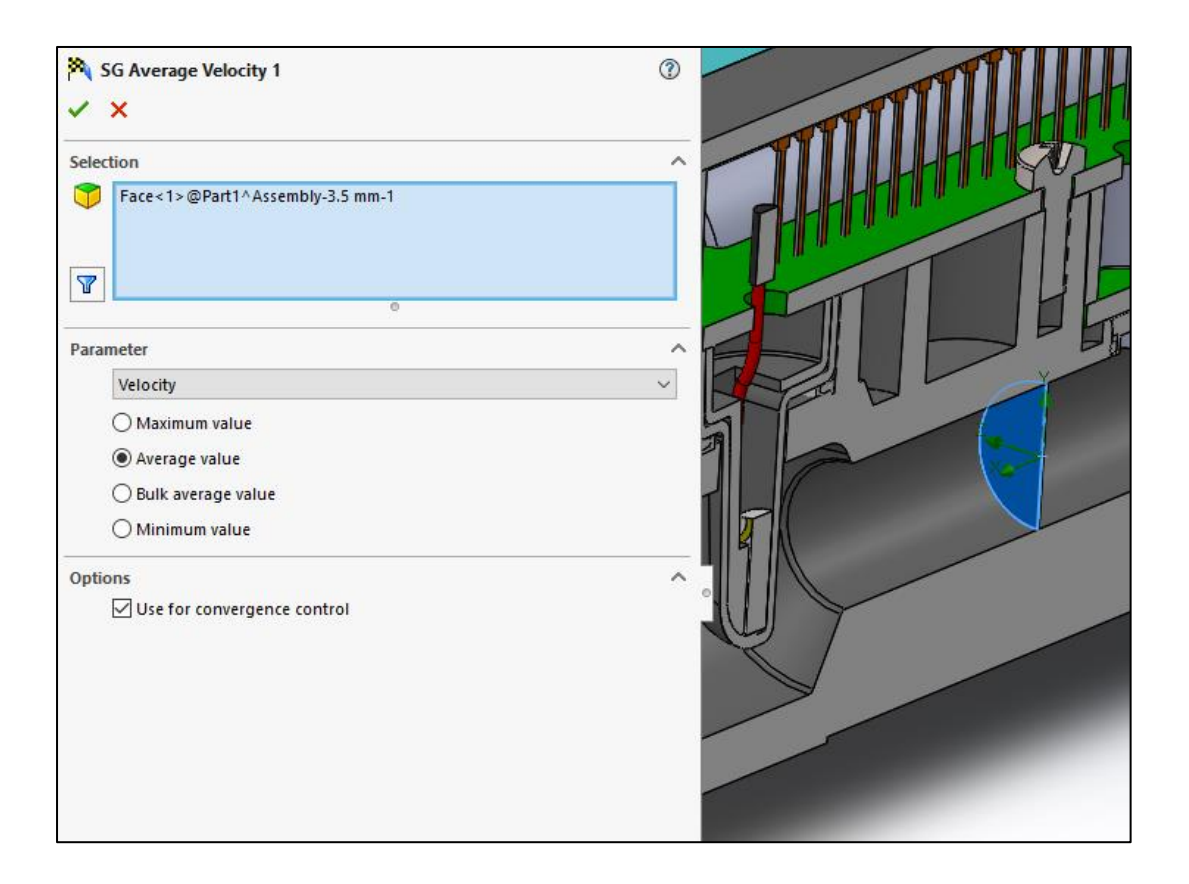


Figure 5.21 Setting a surface goal for average velocity

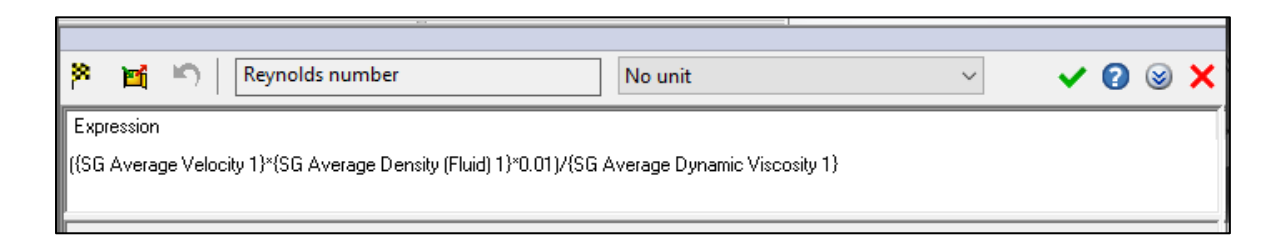


Figure 5.22 Setting an equation goal for the Reynolds number

The next step is to create a parametric study that creates a range of input variables in order to generate a set of results. This is done by right-clicking the project name and inserting a new Parametric Study. A "What-If Analysis" window appears at the bottom of the screen where input parameters can be defined (figure 5.23). As input variables, temperature and volumetric flow rate are chosen and are assigned 10 values each by setting the Variation Type (double-click on the cell) as "Range with Number". In this selection, a minimum and maximum value and desired number of evenly spaced values in between are specified.

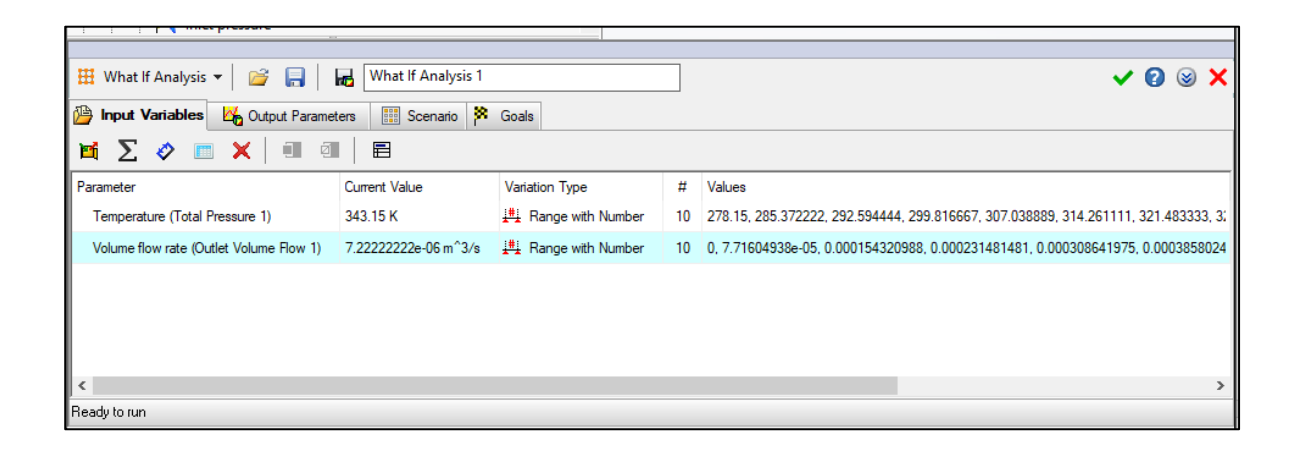


Figure 5.23 Input variables for parametric study

In the "Output Parameters" tab, the desired result is entered by the "Add Goal" button as the pre-defined equation goal for the Reynolds number (figure 5.24). The parametric study can then be started by running it from the "Scenario" tab (figure 5.25).

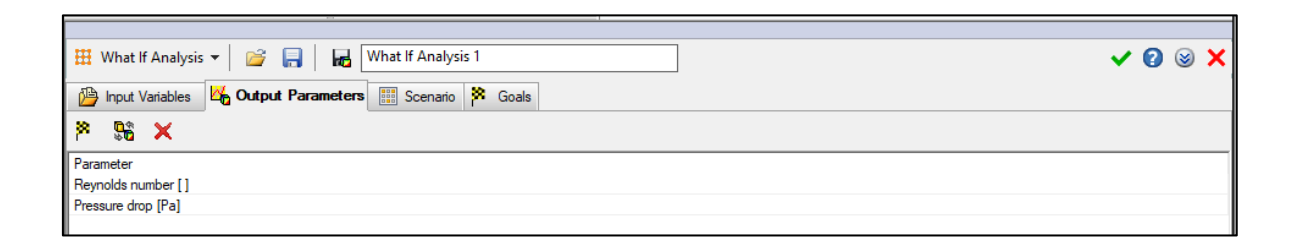


Figure 5.24 Output variables for parametric study

After the simulation is completed for all the design points, the results are exported to an Excel file ("Export to Excel" button in the Scenario tab), where they are organized manually in order to create a 3-D plot of how the Reynolds number changes with respect to varying temperature and flow rate. The plot and the organized values can be seen in figure 5.26.

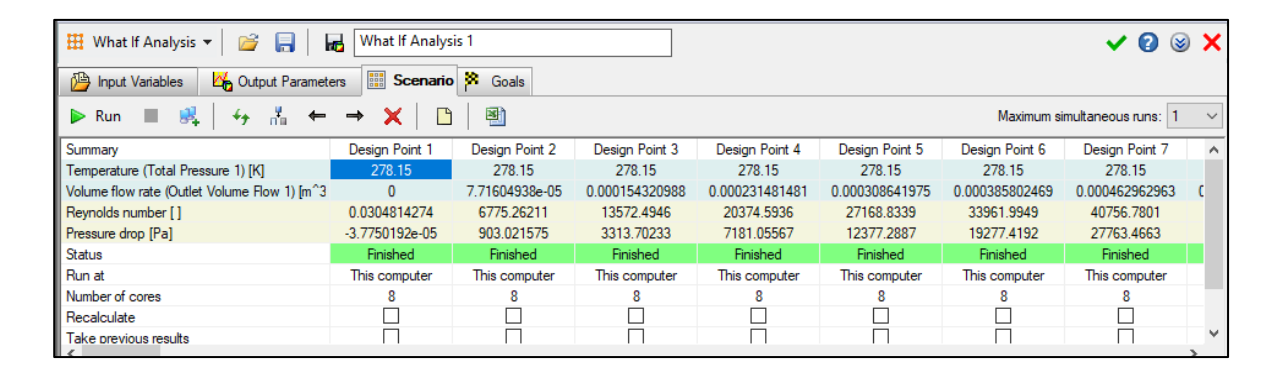


Figure 5.25 Running the parametric study from the scenario tab

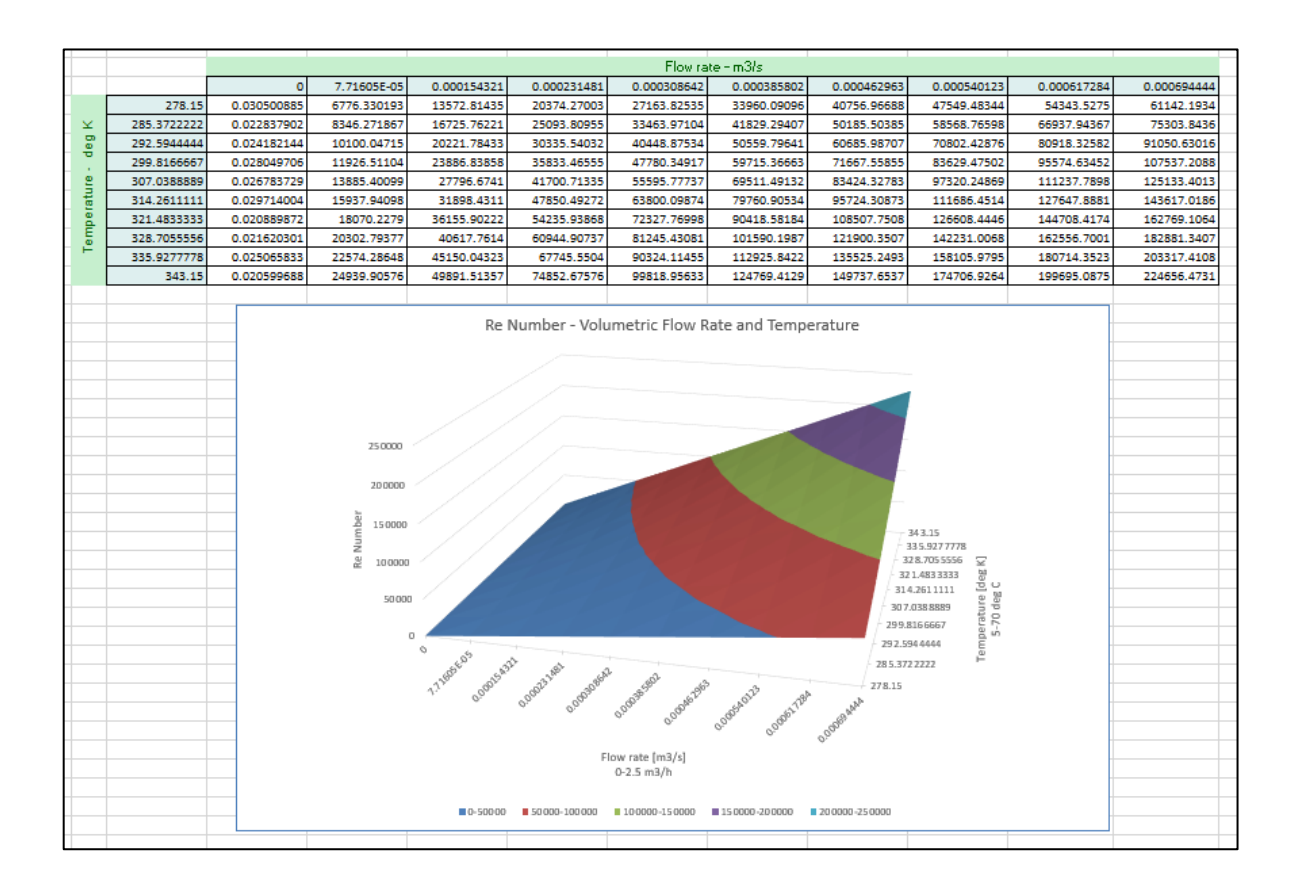


Figure 5.26 Visualization of results for the Re number

This approach and an output of Solidworks simulation of how the Reynolds number changes with respect to temperature and the volumetric flow rate was presented to the developers in the company. The feedback was, this information and visual is exactly what is needed to contribute to improving the accuracy and the Solidworks simulation results are beneficial for validating the behaviour of the Reynolds number in various conditions. The equations of the physical conditions and their corresponding correction factors would be hard coded in the device, but Solidworks would be used for having reference values that would be more accurate since it is taking the entire enclosure and the heat transfer properties of the material into the calculation as well.

As a validation that the simulation is calculating what it is supposed to, three arbitrary design points were picked out from the simulation and the Re number for these points were calculated with an online tool [43]. It can be seen in figure 5.27 that the calculated values are almost the same.

278.15 00231481 09135087 000.6003	0.000462963 6.18484068	0.000694444 9.27896719
00231481 09135087	0.000462963 6.18484068	0.000694444 9.27896719
09135087	6.18484068	9.27896719
000.6003	993,555435	981.527931
01518168	0.000736646	0.000447962
374.5936	83418.3531	203311.006
		203311
		374.5936 83418.3531 20375 83418

Figure 5.27 Comparison of results with another calculation tool

The dynamic viscosity values at these points were compared with the values that the online tool generates for water at these temperatures [44], to check if the program is updating the viscosity value of the water consistently (figure 5.28).

	Design point 4	Design point 47	Design point 90
Temperature [K]	278.15	307.038889	335.927778
Average dynamic viscosity [Pa*s] - Solidworks	0.001518168	0.000736646	0.000447962
Average dynamic viscosity [Pa*s] - EngineeringToolbox	0.0015215	0.0007358	0.0004464

Figure 5.28 Validation of results of dynamic viscosity

5.2.3 Pressure drop depending on total pressure and volume flow

A requirement of the OIML standard is that the loss of pressure inside the device is rated according to the maximum pressure loss that can happen. This information was also requested from the software developers at the company for calibration purposes depending on the pressure and temperature information. The pressure drop simulations were done the same way as the calculation of the Reynolds number. An equation goal was set that subtracts the inlet pressure from the outlet pressure. A discrete input value for temperature was defined to see what happens when the temperature is constant. The ranges of pressure and volume flow were chosen as values that are generally used in residential water consumption. The pressure is between 0 and 5 bar (500000 MPa)

and the volume flow rate is between 0 and $0.15~\text{m}^3/\text{h}$. The temperature was chosen as 20 °C. figure 5.29 shows the input variable definition and Figure 5.30 shows the visualized result in Excel.

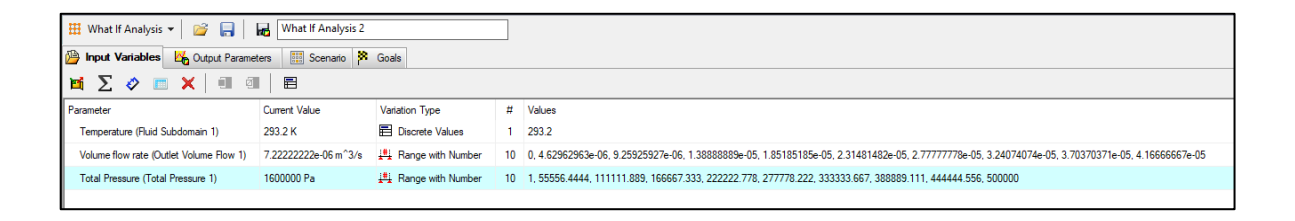


Figure 5.29 Visualization of results for the Re number

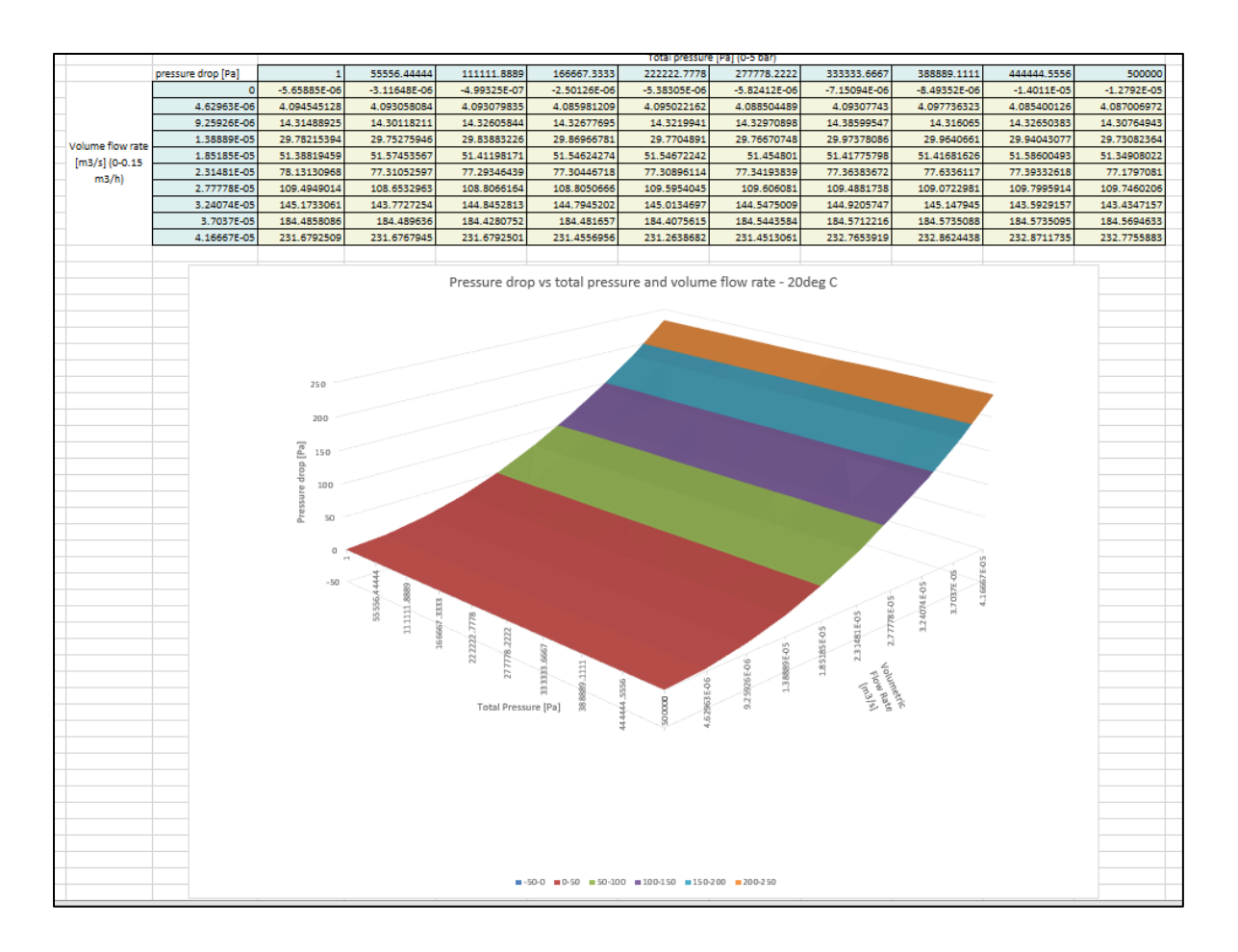


Figure 5.30 Results of the parametric study for pressure drop according to total pressure and volume flow rate for regular conditions

This result was presented to the company as was requested.

A pressure drop simulation for varying temperature and volume flow rate was also made to observe the pressure drop for the full range that the device is supposed to operate in. Because the variation in total pressure does not affect the result (figure 5.30), the

parametric study was done under a constant maximum pressure of 1,6MPa (PN16 pressure rating), temperature ranging from 0 to 70 °C (T70 temperature class) and volume flow rate from 0 to 2.5 m³/h (OIML standard flow rating). The results can be seen in figure 5.31. According to the OIML standard, the pressure drop can not exceed the value of 0.063 MPa. This is barely satisfied in the results, but it is the maximum pressure drop rating that can be achieved. Studies to achieve lower pressure drop ratings were not in the scope of this thesis, but Solidworks flow simulation environment was used to visualize these maximum conditions of the operating range.

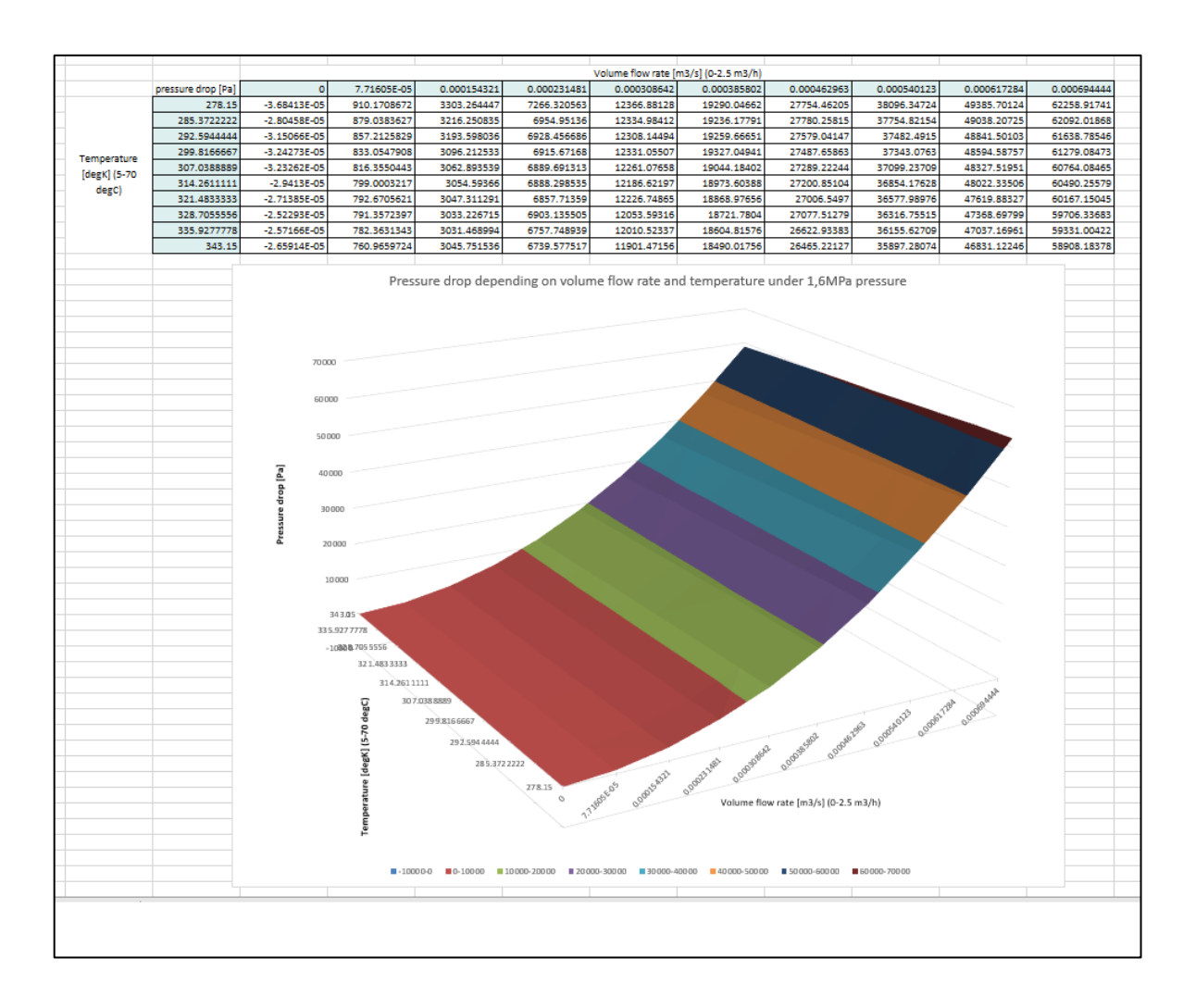


Figure 5.31 Results of the parametric study for pressure drop according to total pressure and volume flow rate for regular conditions

5.3 Conclusions

In this chapter, the works done in the Fluid Simulation environment in Solidworks were documented. The Fluid simulation environment was studied, and an initial simulation was done to verify that the chosen set-up was calculating values that agree with

characteristic flow regimes. The goal of increasing accuracy has been addressed by creating parametric calculations of the Reynolds number and pressure drop. The information on the Reynolds number will contribute to assigning correction factors to the measurement depending on the physical state of the fluid and pressure drop calculations will provide information to aid in programming and calibration of the device. The pressure drop simulations will also be used to assess the conformity of the device to the standards in the future.

6. SUMMARY

In conclusion, a transit-time ultrasonic water flow meter for residential use, with coaxial transducers has been constructed and optimized in Solidworks to satisfy the requirements of the employer, the industrial standard for water meters and requests of other engineering divisions in the company. The initial construction was revised to have dimensions and features that help improve the measurement accuracy and expand the measurement range of the device to lower flow rates.

In the beginning, a model of an initial construction of an ultrasonic water meter has been presented along with problems with the manufactured prototype that need to be addressed. These problems were, the expensiveness of the product and dimensional problems that arise from using a bought spool piece and bought transducers; the absence of engineering practices to document the mechanical performance of the device in determined operating conditions; the need for improvement of the accuracy of the measurement.

In order to tackle the goals and solve the determined problems from a constructor's point of view, research has been done on the governing principles of transit-time ultrasonic flow metering and the construction possibilities of transducer arrangements. Observations and reverse engineering on competing products in the industry are shown. Recent and non-recent but ground-breaking academic studies that were found, which focus on increasing the measurement accuracy have been presented. Out of this research, it was seen that there is a relation between the flow properties of the fluid and the measurement accuracy, and this relation can be utilized in real-time correction of the measurement.

A minimum allowable wall thickness for the enclosure that can withstand the worst conditions inside the operating range was determined with FEA simulations in Solidworks. The minimum safety factor of the construction was documented. The anisotropic property of the chosen material was analysed. It was concluded that the chosen material thickness is enough to overcome the physical loads despite these effects. This study provided a more in-depth understanding of the used material and a reference for further possible modifications of the material thickness for the employer.

A second revision of the enclosure and the assembly was constructed that addresses all of the identified problems in the review. Cost reduction was obtained by eliminating bought components and designing custom transducer assemblies that are cheaper to produce. These transducers have a different positioning that allows better alignment of the ultrasonic signal and decreases the amount of uncertainties in measurement due to their position and orientations. Furthermore, the diameter of the pipe was modified to allow better measurement of lower flow rates and better positioning of sensors which is a mechanical design contribution to the measurement capabilities of the device.

It was found from research that the Reynolds number of the flow inside the pipe directly affects the measurement accuracy. Errors in the measurement due to variations in flow regimes can be mitigated by applying correction factors to the measurement depending on the Reynolds number, which is calculated by the physical properties of the fluid. The learning process of using the Flow simulation tool and observations on the simulated effects of the Reynolds number to the flow characteristics were reported. A parametric study of the Reynolds number results was made, that depends on the temperature and the volumetric flow rate of the fluid. The calculation and visualization of the results were directly beneficial to the other divisions in the company that are dealing with the programming and electronics design of the product. The device will measure the temperature and volumetric flow rate for a real-time adaptive solution. Based on these values, it will associate a corresponding Reynolds number with a correction factor to the measurement. Finally, a pressure drop simulation was done to show the dependence of this value to varying total pressure, temperature and flow rate. This result is valuable to the programming process of the device and shows that the Fluid simulation environment can be used to document the pressure drop characteristics of the device. This will contribute to a more robust development of the device during the certification process according to industrial standards.

KOKKUVÕTE

Kokkuvõtteks, transiidi ajatehnoloogial põhinevad ultraheli vee vooluhulgamõõturid koduseks kasutamiseks koos koaksiaalmuunduritega on disainitud ja optimeeritud SolidWorks-is selleks, et vastata tööandja nõuetele, veearvestite tööstusstandardile ning firma muude tehniliste üksuste soovidele. Esialgne konstruktsioon oli üle vaadatud selleks, et mõõtmed ja funktsioonid aitaksid täiustada mõõtmistäpsust ja laiendada seadme mõõtmisvahemikku vooluhulkade alandamiseks.

Alguses ultraheli veearvesti konstruktsiooni esialgne mudel oli esitatud koos valmistatud prototüübi probleemidega, mis tuleb lahendada. Need probleemid olid järgnevad: toote kallidus ja mõõtmete probleemid, mis tulenevad ostetud torupoole ning ostetud muundurite kasutamisest; tehniliste meetodite puudumine selleks, et dokumenteerida seadme mehaanilist toimimist määratud töötingimustes; mõõtmistäpsuse täiustamise vajadus.

Eesmärkide saavutamiseks ja määratud probleemide lahendamiseks disaineri seisukohast, viidi läbi uuring ultraheli transiidi aja vooluhulgamõõtmise juhtivate põhimõtete suhtes ja muunduri konfiguratsiooni disainivõimaluste kohta. Vaatlused ja pöördprojekteerimine konkureerivate toodete kohta tööstuses on näidatud. Äsjased ja mitte-äsjased, aga murrangulised akadeemilised uurimused, mis leiti ja mis keskenduvad mõõtmistäpsuse suurendamisele, on esitatud. Sellest uuringust oli näha, et on olemas suhe vedeliku voolu omaduste ja mõõtmistäpsuse vahel, ning seda suhet saab kasutada reaalajas mõõtmise korrigeerimisel.

Minimaalne lubatud seinapaksus korpuse jaoks, mis võib taluda halvimaid tingimusi töövahemiku piires, määrati FEA simulatsioonide abiga Solidworks-is. Konstruktsiooni minimaalne ohutegur oli dokumenteeritud. Valitud materjali anisotroopne omadus oli analüüseeritud. Jõuti järeldusele, et valitud materjali paksus on piisav selleks, et füüsilistest koormustest üle saada hoolimata nendest mõjudest. See uuring võimaldas põhjalikumat arusaamist kasutatud materjalist ja andis viidet materjali paksuse edasistele võimalikutele modifikatsioonidele tööandja jaoks.

Korpuse ja sõlme teine versioon oli disainitud, mis lahendab kõiki tuvastatud probleeme ülevaates. Kulude vähenemine oli saavutatud kõrvaldades ostetud komponente ja disainides kohandatud muunduri sõlmesid, mis on odavam toota. Nendel muunduritel on erinev positsiooneerimine, mis võimaldab ultrahelisignaali paremat joondamist ja vähendab määramatuste hulka mõõtmisel tänu oma positsioonile ja orientatsioonidele.

Lisaks muudeti toru läbimõõtu selleks, et võimaldada madalamate vooluhulkade paremat mõõtmist ja andurite paremat positsioneerimist, mis on mehhaaniline disainipanus seadme mõõtmisvõimalustesse.

Uuringust selgus, et voolu Reynoldsi arv toru sees mõjutab otseselt mõõtmistäpsust. Vigu mõõtmisel varieerumise tõttu voolurežiimides saab leevendada rakendades parandustegureid mõõtmisele sõltuvalt Reynoldsi arvust, mis on arvutatud vedeliku füüsikaliste omaduste alusel. Flow simulatsioonivahendi kasutamise õppeprotsess ja tähelepanekud Reynoldsi arvu simuleeritud mõjude kohta voolu omadustele olid teatatud. Reynoldsi arvu tulemuste parameetrilist uuringu tehti, mis sõltub temperatuurist ja vedeliku mahuvoolukiirusest. Tulemuste arvutamine visualiseerimine olid otseselt kasulikud teistele üksustele firmas, mis tegelevad toote programmeerimise ja elektroonikadisainiga. Seade mõõdab temperatuuri ja mahuvoolukiirust reaalajas adaptiivse lahenduse jaoks. Tuginedes nende väärtustel, see seostab vastava Reynoldsi arvu parandusteguriga mõõtmisel. Lõpuks rõhulangu simulatsiooni tehti selleks, et näidata selle väärtuse sõltuvust varieeruvast kogurõhust, temperatuurist ja voolukiirusest. Käesolev tulemus on väärtuslik seadme programmeerimisprotsessile ja näitab, et Fluid simuleerimiskeskkonda saab kasutada seadme rõhulangu omaduste dokumenteerimiseks. See aitab kaasa seadme jõulisemale arengule sertifitseerimisprotsessi jooksul vastavalt tööstusstandarditele.

LIST OF REFERENCES

- 1) Effects of Velocity Profiles on Measuring Accuracy of Transit Time Ultrasonic Flowmeter Hui Zhang, Chuwen Guo, Jie Lin
- Review on Transit time Ultrasonic Flowmeter Gurindapalli Rajita, Nirupama Mandal
- **3)** Analysis of calibration and verification indirect methods of ultrasonic flowmeters Sergey Gerasimov, Vladimir Glushnev, Nikolay Serov
- **4)** An implementation of ultrasonic water meter using dToF measurement Chul-Ho-Lee, Hye-Kyung Jeon, Youn-Sik Hong
- **5)** A novel mathematical model for transit-time ultrasonic flow measurement Lei Kang, Andrew feeney, Will Somerset, Riliang Su, David Lines, Sivaram Nishal Ramadas, Steve Dixon
- **6)** Optimisation of an Ultrasonic Flow Meter Based on Experimental and Numerical Investigation of Flow and Ultrasound Propagation Neil Colin Temperley
- **7)** A design and implementation of low-power ultrasonic water meter Youn-Sik Hong, Chul-Ho Lee
- 8) Ultrasonic Flowmeters R. Siev, L.D. Dinapoli, B.G Liptak, J. Yoder
- **9)** Fundamentals of Industrial Instrumentation and Process Control William C. Dunn
- **10)** Ultrasonic flowmeters: Half-century progress report, 1955-2005 L.C. Lynnworth, Yi Liu
- **11)** Measurement of transitional flow in pipes using ultrasonic flowmeters Liu Zheng-Gang, Du Guang-Sheng, shao Zhu-Feng, He Qian-Ran, Zhou Chun-Li
- **12)** Reducing additional error caused by the time-difference method in transit time UFMs Behroz Yazdanshenasshad, Mir Saeed Safizadeh
- **13)** Ultrasonic transit-time flowmeters modelled with theoretical velocity profiles: methodology Pamela Moore, Gregor J. Brown, Brian P. Stimpson
- **14)** Numerical simulation of transit-time ultrasonic flowmeters: uncertainties due to flow profile and fluid turbulence b. Iooss, C. Lhuillier, H. Jeanneau
- **15)** Estimation of the flow profile correction factor of a transit-time flow measurement in a nuclear power plant Jae Cheon Jung, Poong Hyun Seong
- **16)** Calibration of an ultrasonic flow meter for hot water Karsten Tawackolian, Oliver Buker, Jankees Hogendoorn, Thomas Lederer

- **17)** Study of errors in ultrasonic heat meter measurements caused by impurities of water based on ultrasonic attenuation Shi Shuo, Liu Zhenggang, Sun Jian-ting, Zhang Min, Du Guang-sheng, Li Dong
- 18) Minimizing zero-flow error in transit-time ultrasonic flow meters Douwe van Willigen, Paul van Neer, Jack Massaad, Martin Verweij, Nicolaas de Jong, Michiel Pertijs
- **19)** 3D Isosceles Triangular Ultrasonic Path of Transit-Time Ultrasonic Flowmeter: Theoretical Design and CFD Simulations Guoyu Chenc, Guixiong Liu, Bingeng Zhu, Wensheng Tan
- **20)** https://www.kamstrup.com/en-en/water-solutions/smart-water-meters/multical-21
- **21)** Ultrasonic Transducer Positioning System for Clamp-on Flowmeter Applications Anett Bailleu
- **22)** The uncertainties induced by internal pipe wall roughness on the measurement of clamp-on ultrasonic flow meters Xiaotang Gu, Frederic Cegla
- 23) Studies on the transducers of clamp-on transit-time ultrasonic flow meter
 Jianping Han, Hao Liu, Yuanyuan Zhou, Rumei Zhang, Changji Li
- **24)** Fluid Flow Velocity Measurement Using Dual-Ultrasonic Transducer by Means of Simultaneously Transit Time Method K. Amri, L.F. Wiramata, Suprijanto, D. Kurniadi
- **25)** An intelligent flow measurement technique using ultrasonic flow meter with optimized neural network Santhosh Kv, Binoy Krishna Roy
- **26)** Designing Successful Products with Plastics Fundamentals of Plastic Part design Mark T. MacLean-Blevins
- **27)** Guide to Ultrasonic Plastics Assembly Design guide by DUKANE Intelligent Assembly Solutions
- **28)** Designing with Fortron Polyphenylene Sulfide Ticona Plastics Design Manual FN-10
- **29)** Engineering Design with Polymers and Composites James C. Gerdeen, Harold W. Lord, Ronald A. L. Rorrer
- **30)** https://forum.solidworks.com/thread/81114
- **31)** FORTRON 1140L4 / PPS / Glass Reinforced Ticona Engineering Polymers datasheet
- **32)** https://www.toray.jp/plastics/en/torelina/technical/tec_005.html
- **33)** PLASTUM Trading s.r.o Material Datasheet for PPS-GF40
- **34)** Machine Design A CAD APPROACH Andrew D. Dimarogonas

- **35)** https://forum.solidworks.com/thread/65142
- **36)** Introduction to Fluid Mechanics 6th Edition Robert W. Fox, Alan T. McDonald, Philip J. Pritchard
- **37)** Fundamentals of multipath ultrasonic flow meters for liquid measurement Dave Seiler
- **38)** Theoretical Fluid Mechanics Laminar Flow Velocity Profile James C.Y. Guo, Professor and P.E. Civil Engineering, U. of Colorado at Denver
- **39)** cen72367_ch08.qxd 11/4/04 7:13 PM Page 321
- **40)** An Introduction to Computational Fluid Dynamics The Finite Volume Method 2nd Edition H. K. Versteeg, W. Malalasekera
- **41)** Fluid Mechanics Fundamentals and Applications 3rd Edition Yunus A. Cengel, John M. Cimbala
- **42)** https://www.engineersedge.com/physics/water__density_viscosity_spec ific_weight_13146.htm
- **43)** https://www.engineeringtoolbox.com/reynolds-number-d_237.html
- **44)** https://www.engineeringtoolbox.com/water-dynamic-kinematic-viscosity-d 596.html